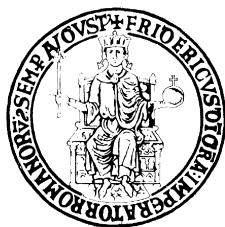


UNIVERSITÀ DEGLI STUDI DI NAPOLI
FEDERICO II



DIPARTIMENTO DI FARMACIA

DOTTORATO DI RICERCA IN SCIENZA DEL FARMACO
XXVI CICLO

**Design and Synthesis of New Urotensin-II
Derivatives**

Coordinatore:
Chiar.ma Prof.ssa
MARIA VALERIA D'AURIA

Tutor:
Chiar.mo Prof.
PAOLO GRIECO

Candidato:
FRANCESCO MERLINO

*to Valentina,
for being so strong
and for loving me*

Contents

Abbreviation	5
1. Urotensin-II and the Urotensinergic system	8
1.1. The features of Urotensin-II	9
1.2. Urotensin-II receptor (UT)	10
1.3. Functional relationships between U-II and somatostatin	12
1.4. Patho-physiological role of U-II	14
2. Structure-activity relationship studies (SARs)	17
2.1. Background to Urotensin-II	18
2.2. Peptidic urotensin analogues	21
2.3. Non-peptidic urotensin analogues	28
3. Design of new urotensin analogues	34
3.1 Leads optimization of P5U and Urantide	35
3.1.1 Trp-constrained analogues of P5U and Urantide	35
3.1.2 Tyr ⁹ -selective uncoded amino acids incorporation	37
3.2 N-methylation of Urotensin-II	39
3.2.1 Mono- and multiple-N-methylated series	41
3.3 Aza-sulfuryl peptides mimics of urotensin-II	43
4. Synthetic strategies	46
4.1 General method for peptide synthesis	47
4.2 N-methylation on solid phase	48
4.3 Synthesis of protected aza-sulfuryl tripeptides	50
4.4 Aza-sulfuryl peptide synthesis	55
4.5 Analysis and purification of aza-sulfuryl peptides	57
5. Results and discussion	59
5.1 Trp-constrained analogues: results and discussion	60
5.1.1 Biological data	60
5.1.2 NMR analysis	61

5.1.3 Discussion	62
5.2 Tyr ⁹ -modified series	65
5.2.1 Biological data	65
5.2.2 Peptide stability	69
5.2.3 NMR analysis	70
5.2.4 Discussion	72
5.3 N-methylation: biological data and discussion	75
5.4 Aza-sulfuryl peptides: biological data	79
5.5 Future perspectives	81
6. Conclusions	83
7. Experimental section	87
7.1 Materials and general procedures	88
7.2 Binding experiments	89
7.3 Intracellular calcium assay	90
7.4 Serum peptide stability	91
7.5 Organ bath experiments	91
8. Characterization	94
9. Acknowledgements	108
10. References	109

Abbreviations

Abbreviations used for amino acids and designation of peptides follow the rules of the IUPAC-IUB Commission of Biochemical Nomenclature in *J. Biol. Chem.* **1972**, 247, 977-983. Amino acid symbols denote L-configuration unless indicated otherwise.

The following additional abbreviations are used:

3D	Three-dimensional
Aic	2-Aminoindan-2-carboxylic acid
Alloc	Allyloxycarbonyl group
Bip	Biphenylalanine
BTPP	<i>tert</i> -Butylimino-tri(pyrrolidino)-phosphorane
Btz	Benzothiazolylalanine
Cha	Cyclohexylalanine
Cin	(4-Cl)-(<i>trans</i>)-cinnamoyl
Cpa	4-Chlorophenylalanine
CNS	Central Nervous System
Dab	2,4-Diaminobutyric acid
DBU	1,8-Diazabicycloundec-7-ene
DCM	Dichloromethane
DIC	N,N'-Diisopropylcarbodiimide
DIEA	N,N-Diisopropylethylamine
DMAP	4-Dimethylaminopyridine
DMF	Dimethylformamide
DMSO	Dimethyl sulfoxide
DQF-COSY	Double Quantum Filtered Correlated Spectroscopy
ESI	Electrospray ionization
Fpa	4-Fluorophenylalanine
HATU	2-(7-Aza-1H-benzotriazole-1-yl)-1,1,3,3-tetramethyluronium hexafluorophosphate
HBTU	2-(1H-Benzotriazole-1-yl)-1,1,3,3-tetramethyluronium hexafluorophosphate
HOAt	1-Hydroxy-7-azabenzotriazole

HOBt	1-Hydroxybenzotriazole
HPLC	High-Performance Liquid Chromatography
HTS	High-throughput screening
hU-II	Human Urotensin-II
IBC	Isobutylchloroformate
LC	Liquid Chromatography
MeCN	Acetonitrile
MS	Mass Spectrometry
Nal	Naphthylalanine
NBS	2-Nitrobenzenesulfonyl
NDMBA	1,3-Dimethylbarbituric acid
NMM	4-Methylmorpholine
NMP	N-Methyl-2-pyrrolidone
NMR	Nuclear Magnetic Resonance
NOE	Nuclear Overhauser Effect
NOESY	Nuclear Overhauser Enhancement Spectroscopy
Pal	3-Pyridylalanine
Pen	Penicillamine
Phg	Phenylglycine
Orn	Ornithine
RP-HPLC	Reversed-Phase High-Performance Liquid Chromatography
SAR	Structure-activity relationship
SDS	Sodium-dodecyl-sulfate
SMC	Smooth Muscle Cell
TFA	Trifluoroacetic acid
THF	Tetrahydrofuran
Tic	Tetrahydro-isoquinoline-3-carboxylic acid
TIS	Triisopropylsilane
Tle	<i>tert</i> -Leucine
TOCSY	Total Correlated Spectroscopy
Tpi	1,2,3,4-tetrahydro- β' -carboline-3-carboxylic acid

U-II	Urotensin-II peptide
URP	Urotensin Related Peptide
UT	Urotensin receptor

1 Urotensin-II and the Urotensinergic System

1.1 The features of Urotensin-II

Urotensin II (U-II) belongs to a series of regulatory neuropeptides first isolated from the urophysis of the teleost fish *Gillichthys mirabilis* by the groups of Karl Lederis and Howard Bern in the 1960s. This cyclic dodecapeptide, H-Ala-Gly-Thr-Ala-Asp-c[Cys-Phe-Trp-Lys-Tyr-Cys]-Val-OH, was originally characterized on the basis of its interesting smooth muscle contracting and hypertensive effects. It has been long considered that U-II was exclusively produced by the fish urophysis [1]. However, the identification of U-II from frog brain [2] demonstrated that the cDNA encoding prepro-U-II existed in several species. In fact, Urotensin-II isoforms are present in several species of vertebrates. Moreover, the gene is expressed not only in the caudal portion of the spinal cord but also in brain neurones, from frogs to humans [3]. Although the amino acid sequence in the N-terminus of urotensin peptides diverges across species, the cyclic hexapeptide sequence, c[Cys-Phe-Trp-Lys-Tyr-Cys], is conserved in all isoforms (Figure 1.1).

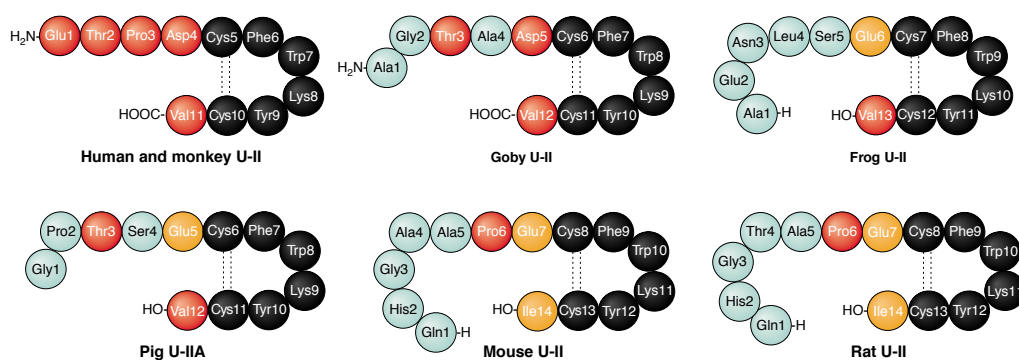


Figure 1.1. U-II isoforms are present in several non-mammalian (snails, fish and frogs) and mammalian (human, monkey, pig, rat and mouse) species. Although the amino terminus of U-II diverges across species, all isoforms share a conserved, cyclic hexapeptide, core sequence motif of Cys-Phe-Trp-Lys-Tyr-Cys (black residues).

The length of the isoforms of the Urotensin-II peptide is variable across species and ranges from 17 amino acid residues in mice to 11 in humans, depending on proteolytic cleavages of precursors. Although the N-terminus region of U-II is highly variable among animal species

[4], the C-terminal amino acids, organized in a disulphide-linked cyclic array, c[Cys-Phe-Trp-Lys-Tyr-Cys], are stringently conserved from species to species, suggesting their important role in the peptide's biological activity [5]. In addition, the goby isoform of U-II exhibits some structural similarities with **somatostatin-14**, H-Ala-Gly-c[Cys-Lys-Asn-Phe-Phe-Trp-Lys-Thr-Phe-Thr-Ser-Cys]-OH, both containing the presence of a disulphide-linked cyclic core at their C-terminus portion with the biologically active domain Phe-Trp-Lys [6].

The **human U-II (*hU-II*)** is a cyclic undecapeptide, H-Glu-Thr-Pro-Asp-c[Cys-Phe-Trp-Lys-Tyr-Cys]-Val-OH, recognized as the natural ligand of an orphan G-protein coupled receptor, first characterized in rat, which possess a receptor with high affinity for U-II, GPR14 [7]. Subsequently, a human G-protein coupled receptor showing 75% similarity to the orphan rat receptor was cloned and renamed **UT receptor** by IUPHAR [8] (Figure 1.2).

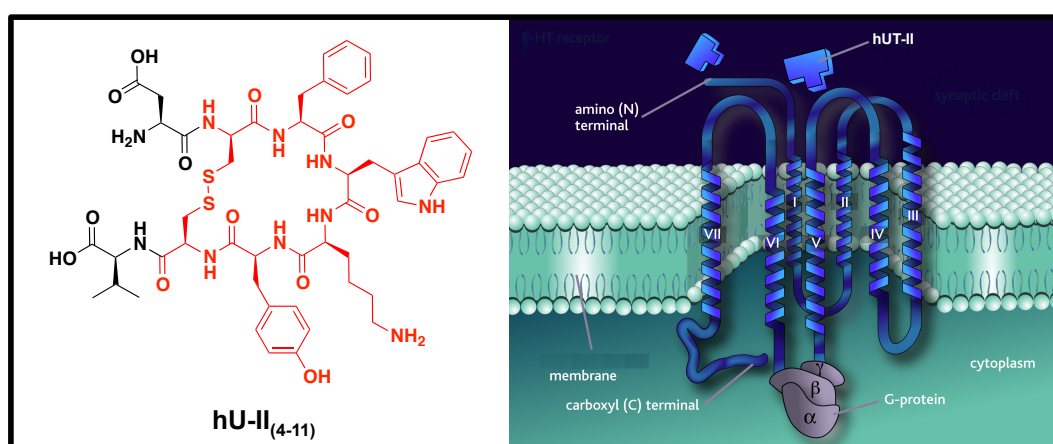


Figure 1.2. The *hU-II*(4-11) is the minimal sequence needed for maintaining biological activity. The exocyclic portion of this peptide (red) is responsible of interaction with its G-protein coupled receptor, named UT receptor.

1.2 Urotensin-II receptor (UT)

Investigation of the role of the UT receptor has shown that it is widely distributed in the CNS and in different peripheral tissues including cardiovascular system [9], kidney, bladder and adrenal gland [10]. This extensive expression has also suggested implication in multiple pathophysiological effects mediated by the *hU-II*/UT receptor, such as cardiovascular

disorders (heart failure, cardiac remodelling, atherosclerosis), smooth muscle cell proliferation, renal disease, diabetes [11], and tumor growth. The UT receptor is especially expressed in vascular smooth muscle, endothelium and myocardium, and plays a key role in the regulation of the cardiovascular homeostasis. Furthermore, this receptor has structural homology to members of the somatostatin receptor family and may be activated by somatostatin-14 and cortistatin at micromolar doses [7]. The gene coding for the UT receptor has been located on chromosome 17q25.3 [12].

The *hU*-II peptide binds with high affinity to the UT receptor, resulting in intracellular calcium mobilization via phospholipase C-dependent increase in inositol phosphate (Figure 1.3).

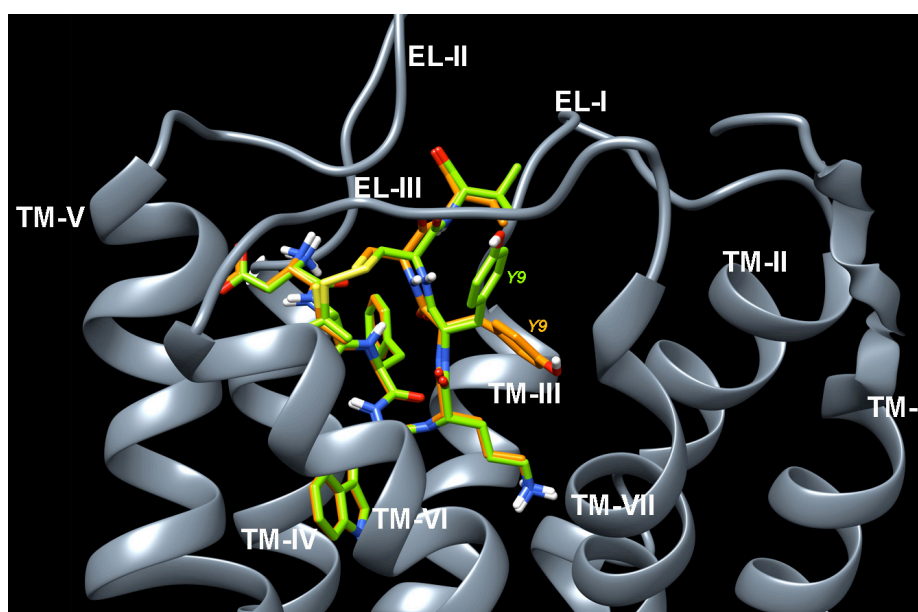


Figure 1.3. *hUT* receptor model complexed with *hU*-II. Receptor backbones are represented in gray and labeled.

In isolated rat thoracic aorta fragments *hU*-II induces contraction mediated by two distinct tonic and phasic components. The vasoconstrictor activity of *hU*-II is also observed in primate arteries, in which it causes a concentration-dependent contraction of isolated arterial rings with an EC_{50} value <1 nM, meaning a >10 -fold potency than endothelin-1. Moreover, the *in*

vivo effects of hU-II may depend on species, blood vessel type, U-II concentration, administration route, tissue and species. Contradictory, the peptide has also elicited vasodilatory effects on the small arteries of rats and on the resistance arteries of humans, probably due to the release of endothelium-derived hyperpolarising factor and nitric oxide [13]. In a healthy human, U-II behaves as a chronic regulator of vascular tone rather than influencing tissues in a phasic manner [14]. U-II binds to its receptor in a 'pseudo-irreversible' manner. Its slow dissociation from the UT receptor leads to prolonged activation of the receptor and a functionally silent system [15]. This state of homeostasis is altered since pathogenesis of several cardiovascular disorders provokes an upregulation of UT receptor and U-II resulting in vasoconstriction.

1.3 Functional relationships between U-II and somatostatin

Somatostatin was originally discovered around 40 years ago as an inhibitor of growth hormone release from the pituitary gland [6,16], and was later shown to play an important role in the regulation and release of insulin, as well as a variety of other hormones and enzymes. In addition to expression in nervous, neuroendocrine, and gastrointestinal cells, somatostatin is expressed in cancer cells [17]. Most neuroendocrine tumors display strong overexpression of somatostatin receptors. Currently five somatostatin receptor subtypes are known (sst1-5), and the subtype receptor sst2 is mainly expressed in tumor, whereas the density of these receptors is highly variable in non-tumor tissues.

Somatostatin-14 is structurally similar to U-II (Figure 1.4) and, originally, U-II was suspected to be a somatostatin analog because of the peptide sequences analogies and the sharing of some biological properties (particularly in the context of the metabolic syndrome, diabetes, and cardiovascular disease). However, the functional correlation between hU-II and somatostatin has been discerned, including their roles in cancer cells. U-II may act on tumor cells as an autocrine/paracrine factor affecting cancer cell growth [18] and U-II mRNA has

been detected in tumor cell lines of neural origin; U-II stimulates significantly proliferation of human adrenocortical carcinoma SW-13 and human renal cell carcinoma VMRC-RCW cell lines [19]. In 2011, Grieco et al. [20] performed bio-pharmacological studies to assess the role of U-II in human carcinogenesis. In particular, they evaluated UT receptor expression in *in vivo* samples collected from patients affected by prostate adenocarcinoma, and found that the UT receptor was highly expressed in well-differentiated human prostate cancer and moderately expressed in prostate hyperplasia. Moreover, the UT receptor is also expressed in colon cancer cells; recent studies have demonstrated that urotensin agonists and antagonists could modulate colon cancer cell growth, motility and invasion [21].

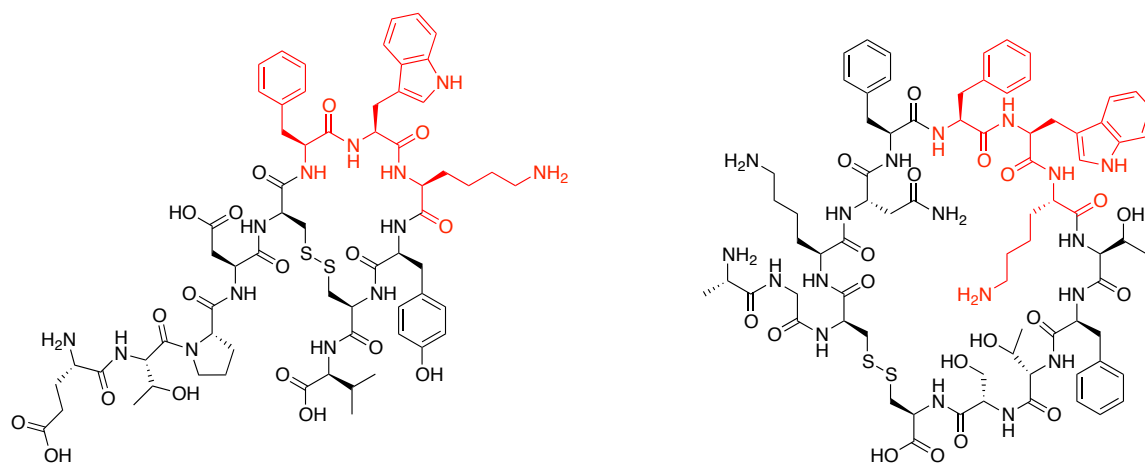


Figure 1.4. Representation of human U-II (*hU-II*) and somatostatin-14 peptides. The common sequence Phe-Trp-Lys shared between these two peptides is in red.

The characterization of cDNA encoding carp pro-U-II has shown that the U-II and somatostatin-14 precursors share a common structural organization, because the active peptides are both located at the C-terminal portion of the precursors [22]. After the UT receptor was identified as a member of somatostatin receptor family, some somatostatin-like peptides containing a disulphide bridge, such as human melanin-concentrating hormone, somatostatin-14, cortistatin-14 and octreotide, were screened on the UT receptor to compare their biological activities with that of endogenous U-II [23]. These comparisons have

established that U-II is the only endogenous ligand with high-affinity for the somatostatin-like receptor named the UT receptor.

1.4 Patho-physiological role of U-II

U-II binds to the the Gq protein urotensin-II receptor (UT) which has been identified in several tissues, such as cardiac myocytes, vascular smooth muscle cells (SMC), endothelial cells, spinal cord, central nervous system (CNS), and kidneys. On the other hand, U-II is expressed in blood vessels from the heart, pancreas, kidney, placenta, thyroid, adrenal gland, and umbilical cord. Thus, both U-II and the UT receptor seem to be ubiquitously expressed in human tissues [24] (Figure 1.5).

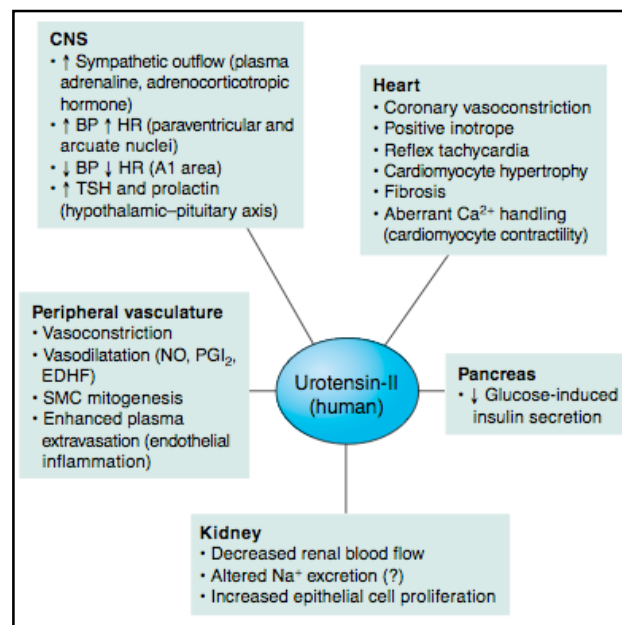


Figure 1.5. U-II has diverse biological actions in mammals and might influence several major organ systems in humans. However, U-II seems to be primarily involved in the cardiorenal system where evidences indicates that blood pressure might be regulated by direct effects on heart, kidney, and peripheral vasculature and by indirect central mechanisms and secondary endocrine actions. Abbreviations: A1, area of the medulla; BP, blood pressure; EDHF, endothelial-derived hyperpolarization factor; HR, heart rate; NO, nitric oxide; PGI_2 , prostacyclin; SMC, smooth muscle cell; TSH, thyroid-stimulating hormone.

U-II is generally considered to be the most potent endogenous vasoconstrictor discovered to date [10]. Stimulation of UT can trigger the release of nitric oxide (NO), prostacyclin,

prostaglandin E2, and endothelium-derived hyperpolarizing factors to balance contractile effects on SMCs [13]. In a healthy human, U-II modulates vascular tone as a chronic regulator and its “pseudo-irreversible” binding properties and slow dissociation rate from the UT receptor leads to prolonged activation of UT and to a functionally silent system [24,25]. In patients with cardiovascular diseases, this homeostasis is disturbed with evidences of upregulation of UT and U-II in atherosclerotic lesions resulting in vasoconstriction (Figure 1.6).

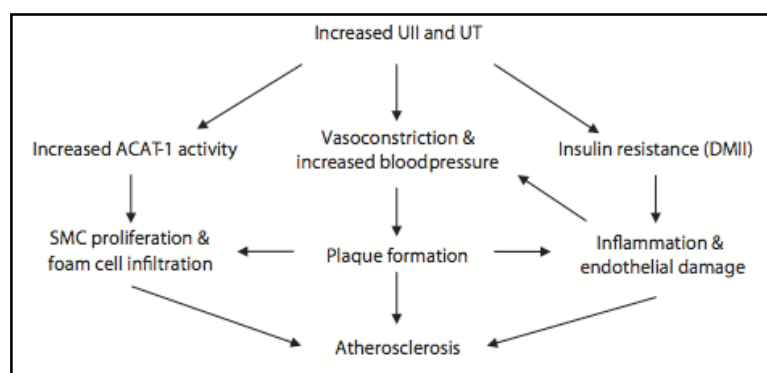


Figure 1.6. Schematic view of consequences related to elevated levels of U-II and UT receptor. U-II is known to inhibit insulin release and may contribute to the development of metabolic syndrome. The resulting inflammation and endothelial damage leads to kidney injury, which increases blood pressure. Cardiovascular disease is also provoked by the formation of atherosclerotic plaques.

The high-fat diet associated with a Western lifestyle can contribute to the upregulation of U-II and UT receptor expression. U-II is known to inhibit insulin release and may be implicated in the development of metabolic syndrome. Both U-II and UT receptor are present in the human pancreas and seem to inhibit directly β -cell function, thus inhibiting insulin release evoking type II diabetes mellitus [26]. Elevated U-II plasma concentrations in metabolic syndrome may be a result of damaged endothelial cells resulting in kidney injury and, thus, increased blood pressure. Indeed, the kidney plays an important role in regulating cardiovascular homeostasis, influencing both cardiac preload and afterload volume, and vasomotor tone. U-II

and possibly urotensin-related protein bind UT in renal tubule cells leading to decreased urine flow. In addition, U-II acting at the glomerulus decreases directly glomerular filtration rate. These effects impair normal cardiovascular homeostasis, increasing blood pressure, and promoting cardiovascular disease (Figure 1.7).

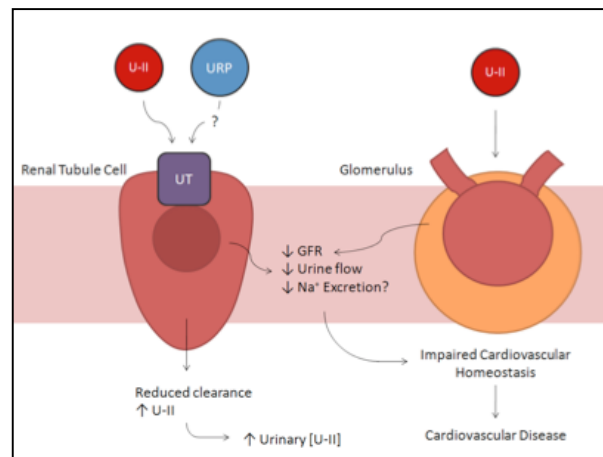


Figure 1.7. Urotensin-II and possibly urotensin-related peptide (**URP**) binding to UT receptor in renal tubule cells promote decreased urine flow. U-II acting at the glomerulus directly decreases glomerular filtration rate. These effects impair normal cardiovascular homeostasis, increasing blood pressure, and promoting cardiovascular disease.

In conclusion, elevated plasma levels of U-II have been found in patients with heart failure, congestive heart failure, carotid atherosclerosis, renal failure, renal dysfunction, portal hypertension-cirrhosis, diabetes mellitus, and essential hypertension. Moreover, the use of UT antagonists to treat cardiovascular diseases has revealed improvements in hemodynamics and cardiovascular remodeling, suggesting that U-II is involved in the development of diseases [26].

2 Structure-Activity Relationship Studies (SARs)

2.1 Background to Urotensin-II

As mentioned above, the human U-II peptide is involved in several pathophysiological pathways related to the cardiovascular system. The interaction of U-II with the UT receptor has been observed to regulate the contractility and growth of cardiac and peripheral vascular vessels facilitating identification of selective ligands. Selective compounds are intriguing, because modulation of the U-II system offers great potential for therapeutic strategies in the treatment of cardiovascular diseases. To define the roles of U-II and its receptor in cardiovascular homeostasis and pathophysiology, as well as in the aetiology of related disorders, the design of suitable tools of peptide or nonpeptide nature would be of significant utility [27]. New molecules may assist in determining these roles by serving as selective UT receptor antagonists.

With the aim to investigate the role played by the exocyclic region of the peptide in receptor interactions, a series of modifications on *h*U-II have been performed to elucidate the relations between structure and biological activity. One of the first studies involved synthesis of a series of abridged *h*U-II peptides, because truncation studies can detect the minimal sequence for biological activity. The effect of sequential deletion of exocyclic residues from the N- and C-termini of the *h*U-II sequence did not appear to be significant for the calcium-mobilizing potency and efficacy; however, removal of any residue within the cyclic region reduced or total abolished biological activity. The shortest, fully potent sequence of U-II was the octapeptide U-II(4-11), H-Asp-c[Cys-Phe-Trp-Lys-Tyr-Cys]Val-OH, which exhibited potency at the human UT receptor similar to somatostatin-14.

The importance of a free amino group at the N-terminal of the octapeptide U-II(4-11) was evaluated in 2002 by modification using a succinoyl derivative [28]. Introduction of additional carboxylate residues by substitution of Asp⁴ showed similar results. Furthermore, the replacement of this amino acid with the corresponding Asn gave a fully potent analog in all three assays, suggesting that a negative charge in the side chain was not required for

activity. These results were confirmed subsequently by the discovery of a second endogenous peptide named **URP** (urotenisin related peptide, H-Ala-c[Cys-Phe-Trp-Lys-Tyr-Cys]-Val-OH). The Nle⁴ analog lacked potency indicating that the -CH₂COX carbonyl group present in both the Asp and Asn side chains is important probably because of its possibility to act as an acceptor for hydrogen-bond with the UT receptor. The side chain can also contain an aromatic ring substituted with polar groups such as -OH and -NO₂, which is of great interest in the development of antagonists based on the previously identified somatostatin antagonist octapeptides.

The cyclic structure is essential for hU-II. McMaster *et al.* in 1986 [29] reported a lack of biological activity for the corresponding 'ring-opened' analogue. In 2002, Grieco *et al.* [30] considered the replacement of the disulphide bridge by a side chain-to-side chain lactam bridge in accordance with observations on active analogs of several biologically relevant peptides, such as the conotoxins, endothelin-1 and somatostatin. Starting from the minimum active fragment U-II(4-11), introduction of a lactam bridge led to peptides that maintained bioactivity, albeit with reduced potency, suggesting that the size of the lactam bridge was a crucial parameter. Peptide analogues synthesized in this study were characterized by rings that ranged from 20 to 24 atoms; the smallest peptide sequence having the same length as the native peptide containing the disulphide bridge did not show any biological activity. In contrast, the analogue corresponding to the larger ring, containing Orn and Asp as residues in the 22 atom lactam bridge, behaved as a full agonist with approximately 100-fold less potency than hU-II. Replacement of the Cys-Cys cyclic motif could thus be well tolerated by an appropriately longer lactam bridge with partial loss of activity, probably due to the different orientation of the key amino acid side chains. Subsequently, Foister *et al.* in 2006 [31] made a cyclic 'cysteine-free' hexapeptide derivative of U-II, in which Tyr⁹ was replaced with a β -naphthylalanine residue, c[Ala-Phe-Trp-Lys-(2')Nal-Ala], and found it bound at the human UT receptor with higher affinity than the corresponding disulphide-bridged truncated

hexapeptide U-II(5-10). Modifications of the Cys⁵-Cys¹⁰ disulfide bridge, such as the macrocyclic lactam and the penicillamine-derived disulphide moiety, have also been pursued to chemically stabilize and restrict the conformational flexibility of the biologically active cyclic hexapeptide core sequence. Replacement of Cys⁵ with penicillamine resulted in a potent agonist, [Pen⁵]hU-II(4-11), subsequently renamed **P5U** [30], which was later studied by NMR spectroscopy in DMSO [32]. An alanine scan of truncated goby U-II peptide demonstrated that the Trp, Lys and Tyr residues were crucial for biological activity [33]. The sequence **Trp-Lys-Tyr** within Urotensin-II peptide is essential for binding and activation of the receptor. The hydrophobic side chains of Trp⁷ and Tyr⁹ and the positive charge of Lys⁸ represent key pharmacophoric elements. Moreover, NMR studies performed by Flohr *et al.* in 2002 [34] revealed the importance of the distances between these pharmacophoric points. Accordingly, the first NMR studies applied to the receptor-unbound hU-II in water were used to provide a putative agonist pharmacophore. Flohr *et al.* studied D-isomer substitution of the amino acids in the hexacyclic part of hU-II. This led to dramatic decrease of the agonist activity, suggesting the importance of the configuration of the side chains of these amino acids and their spatial orientation for interaction with the UT receptor. Stereoinversion of the L-Trp residue gave a D-Trp analog, which did not exhibit a significant change of EC₅₀ value relative to the endogenous ligand. The role of Lys⁸ was also investigated by replacement with lipophilic amino acids and hydrophilic non-basic amino acids that produced inactive peptides [35], indicating that the positive charge of the primary aliphatic amine is essential for biological activity. Reducing the distance of the primary aliphatic amine from the peptide backbone led to a progressive decrease of both potency and efficacy. [**Orn**⁸]U-II caused weak contractions of rat aorta strips corresponding to about 20% of the U-II maximal effect at micromolar concentrations. In position 9 the phenol hydroxyl group of tyrosine was replaced with -OCH₃, -NO₂, -CH₃, -F, -H, and -NH₂ without improvement in potency or efficacy at the

rat UT receptor. The 3-iodo-Tyr analog exhibited 6-fold greater UT receptor agonism than the natural peptide.

The introduction of non-natural amino acids into the U-II sequence has also been pursued to alter potency and efficacy at the UT receptor [33]. Replacement of the Tyr residue with the bulkier (2-naphthyl)-L-alanine [(2')Nal] in the goby U-II sequence gave an analog with similar agonist potency in the functional assay and a 6-fold improvement in binding affinity, presumably due to enhanced hydrophobic interactions at the tyrosine-binding pocket. In contrast, replacement of Tyr with a Bip [(2-biphenyl)-L-alanine] residue did not give an equal result, confirming that larger side chain groups are not well accommodated.

2.2 Peptidic urotensin analogues

The potential therapeutic applications of urotensin-II system have driven structure-activity relationship (SAR) studies to discover new agonists and antagonists, and to elucidate features responsible for the function of the *h*U-II hormone. Early observations of shared sequence homologies between *h*U-II and somatostatin, gave rise to analogues such as **PRL-2903** {H-Fpa-c[Cys-Pal-DTrp-Lys-Tle-Cys]-(2')Nal-NH₂}, which blocked *h*U-II-induced rat aorta ring contractions at micromolar concentrations, albeit with low species selectivity [37]. Another peptide somatostatin analogue, **SB-710411** {H-Cpa-c[DCys-Pal-DTrp-Lys-Val-Cys]-Cpa-NH₂} exhibited moderate affinity for UT receptor and inhibited U-II induced contractions in rat isolated thoracic aorta in a surmountable manner [37].

A cyclo-somatostatin octapeptide analogue that shares structural similarity with SB-710411, the peptide neuromedin B receptor antagonist **BIM-23127** {D(2')Nal-c[Cys-Tyr-DTrp-Orn-Val-Cys]-(2')Nal-NH₂} [38] was investigated for functional activity at recombinant and native UT receptors [39]. Increasing concentrations of BIM-23127 antagonized competitively *h*U-II-induced intracellular calcium mobilization in HEK293 cell lines expressing human and rat UT receptor. Moreover, BIM-23127 showed about a 0.5 log unit lower affinity in

competition binding experiments to human and rat UT receptors, suppressing significantly the maximum contractile response to *h*U-II. In isolated rat aorta, BIM-23127 exhibited non-competitive antagonism of U-II and inhibited competitively calcium mobilization in human embryonic kidney 293 cells. A related neuromedin B receptor antagonist, **BIM-23042** {D-(2')Nal-c[Cys-Tyr-DTrp-Lys-Val-Cys]-(2')Nal-NH₂} displayed different functional activities at several UT receptor orthologs. It behaved as a full agonist at the human and monkey UT receptors, as partial agonist at the mouse UT receptor, and as a competitive antagonist at rat UT receptor [39].

Among the most potent compounds, [**Orn**⁸]**U-II** was introduced by Camarda *et al.* in 2002 [40], characterized *in vitro* as a novel peptide ligand for the UT receptor, and behaved as a full agonist in the calcium functional assay in HEK293 human and rat UT cells, inducing similar maximal effects as U-II. However, the potency of [**Orn**⁸]**U-II** at both receptors was 3-fold lower than U-II. In contrast, different results were obtained in the rat aorta bioassay, in which the compound behaved as a competitive antagonist, showing only in highest concentrations (10 μM) a weak residual agonist activity (25% compared to the maximal effect of U-II). The variance between results obtained in the cell and tissue assays could be interpreted assuming that [**Orn**⁸]*h*U-II is a partial agonist.

In 2002 Grieco *et al.* [30] generated a novel peptide UT receptor agonist by introduction of β,β-dimethyl-substituted cysteine (penicillamine) at the disulphide bridge of *h*UT-II(4-11). The resulting analogue **P5U** {[**Pen**⁵]*h*U-II(4-11)} was rigid, potent and exhibited a 3-fold higher affinity for the UT receptor than the endogenous ligand in competition with iodinated radioligand. In functional experiments on the rat aorta, P5U was 20-fold more potent than *h*U-II and 10-fold more potent than *h*U-II(4-11), being the most potent U-II analogue in the rat thoracic aorta bioassay described so far. Interestingly, conformational analysis by ¹H nuclear magnetic resonance (NMR) spectroscopy combined with molecular modelling on this peptide also indicated further details about structure-activity relationships since the putative

pharmacophoric Trp-Lys-Tyr sequence of the cyclic portion of P5U maintains the same spatial orientation as in the native peptide. Initial structural studies on U-II by NMR spectroscopy revealed no classical secondary structure for the preferred conformer of the peptide in DMSO and water; however, *h*U-II and some analogues folded into a defined secondary structure in the membrane mimetic environment of SDS solution. Analogues retaining high affinity for the UT receptor, such as P5U, all possessed a type II' β -hairpin conformation regardless of their agonist or antagonist activity, indicating that such backbone conformation is necessary for UT recognition [41] (Figure 2.1).

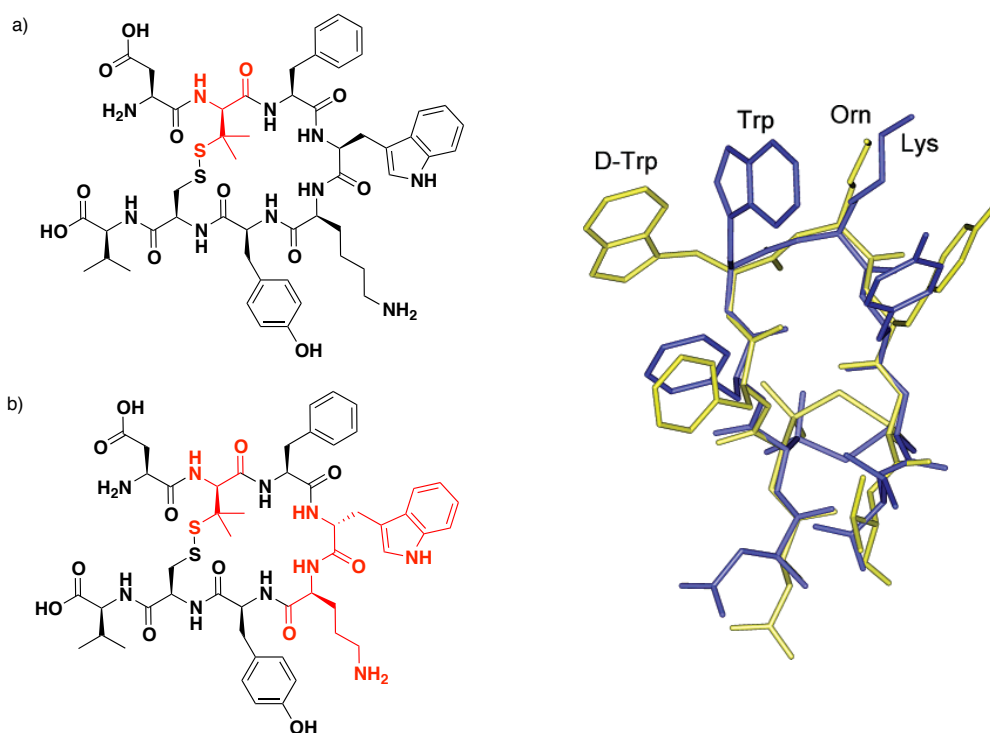


Figure 2.1. P5U (a) and urantide (b) peptides represent the most potent agonist and antagonist, respectively, to date. The uncoded amino acids which differ from *h*U-II(4-11) sequence are in red. On the right, superimposition of representative structures of P5U (blue) and urantide (yellow).

The chemical modification induced by penicillamine influences mainly the proximal Phe⁶ position and leaves the conformation unaffected about the Trp, Lys and Tyr residue. The enhanced pharmacological properties observed in the case of P5U can be assigned to this

conformational restriction revealing the importance of the exploration of specific orientations in the three-dimensional space by which amino acid side chains can interact with the receptor. Subsequent attempts were challenged to develop more potent and selective UT receptor antagonists, because antagonist peptides such as SB-710411 and [Orn⁸]U-II, BIM-23127 exhibited weak potency at the UT receptor with concomitant antagonist activities at different receptor types, as well as partial agonist activity at UT, Patacchini *et al.* in 2003 [42] described the pharmacological activities of two compounds: [Pen⁵, Orn⁸]hU-II(4-11) and [Pen⁵, DTrp⁷, Orn⁸]hU-II(4-11), named **urantide** (Urotensin-II antagonist peptide). Both peptides derived from the hU-II(4-11) fragment, previously reported as the minimal active sequence of hU-II, included replacement of Cys⁵ by penicillamine (β,β-dimethylcysteine) to enhance conformational rigidity and stabilize the putative bioactive conformation. In functional experiments both peptides showed no agonist effect in the range 0.1 nM to 10 μM. Urantide exhibited no agonist effects even when administered at a single concentration. In contrast, [Pen⁵, Orn⁸]hU-II(4-11) exhibited a desensitization that affected UT receptor-mediated responses in this preparation. As the most potent UT receptor antagonist yet to be reported, urantide has high affinity for human and rat UT receptors. Conformational studies on urantide performed in 2005 by Grieco *et al.* [41] showed that the distance between Trp⁷ and Tyr⁹ side chains was greater than that observed in the peptide agonist P5U because of the inversion of L-Trp⁷ into the corresponding D-isomer in urantide. Urantide is a relatively potent UT receptor antagonist exhibiting about 50- to 100-fold greater potency than any other compounds tested in the rat-isolated aorta. In spite of its potent UT receptor antagonist activity in the rat aorta bioassay, urantide showed residual agonist activity in a human recombinant cell calcium mobilization assay [43]. In order to develop a selective antagonist, chemical modifications led to **UFP-803** {[Pen⁵, DTrp⁷, Dab⁸]U-II(4-11)}, which is closely related [44], but exhibits less residual agonist activity than urantide. In the rat aorta bioassay,

UFP-803 competitively antagonizes U-II contractile action behaving as a selective UT receptor antagonist.

In 2003 a report from Sugo *et al.* [45] demonstrated the existence of a paralogue of U-II named U-II related peptide (URP, H-Ala-c[Cys-Phe-Trp-Lys-Tyr-Cys]-Val-OH), a novel peptide first isolated from the extract of rat brain and subsequently observed as the endogenous ligand for the UT receptor in rat, mouse and possibly in human. URP exhibits high binding affinity for the human UT receptor in transfected cell lines and high contractile potency in the rat aortic ring assay, suggesting that some physiological effects could be not completely attributed to U-II. In spite of the structural homology between U-II and URP, and their concurrent expression in several human tissues, recent studies have reported different actions for these two peptides such as cell proliferation [46] and distinctive myocardial contractile activities [47]. Therefore, the identification of more selective ligands should be helpful for clarifying the roles of U-II and URP in the urotensinergic system.

In order to evaluate the correct orientation of amino acid side chains belonging to the cyclic region of URP in the activity of the peptide, each amino acid has been replaced with the corresponding stereoisomer in a D-amino acid scan analysis [48]. Substitution of D-isomers within the cyclic region residues Phe³, Lys⁵ and Tyr⁶ reduced binding affinity and contractile activity, confirming the primary role of this portion in receptor recognition. In contrast, the [DTrp⁴]URP analogue retained important binding affinity, suggesting a relative tolerance in the interaction with the receptor by stereoinversion at the 4-position. With reduced efficacy, [DTrp⁴]URP appeared to behave as a partial agonist with moderate potency and a full antagonist with low potency, indicating that substitution at the Trp residue in U-II and URP sequence could lead to antagonists. Subsequently, Chatenet *et al.* in 2012 [49] replaced the indole moiety of Trp in URP to obtain promising antagonists. For example, **urocontrin**, {[Bip⁴]URP} was a novel antagonist with the selective ability to specifically reduce the maximal efficacy of *h*U-II but not URP-associated vasoconstriction in a rat aorta assay. Based

on this atypical behavior, a recent study by Chatenet et al. (2012) [50] identified urocontrin A ([Pep⁴]URP), which exhibited no agonistic activity, and behaved as an allosteric modulator of the urotensinergic system. Urocontrin A reduced the efficacy of *h*U-II but not URP-induced vasoconstriction. By acting at a purported allosteric binding site, urocontrin A is suggested to modify UT receptor topography in a way that prevents interaction with the *h*U-II(1-11) N-terminal region leading to reduced efficacy. On the other hand, such conformational alteration of the UT receptor has no effect upon URP-mediated action (Figure 2.2).

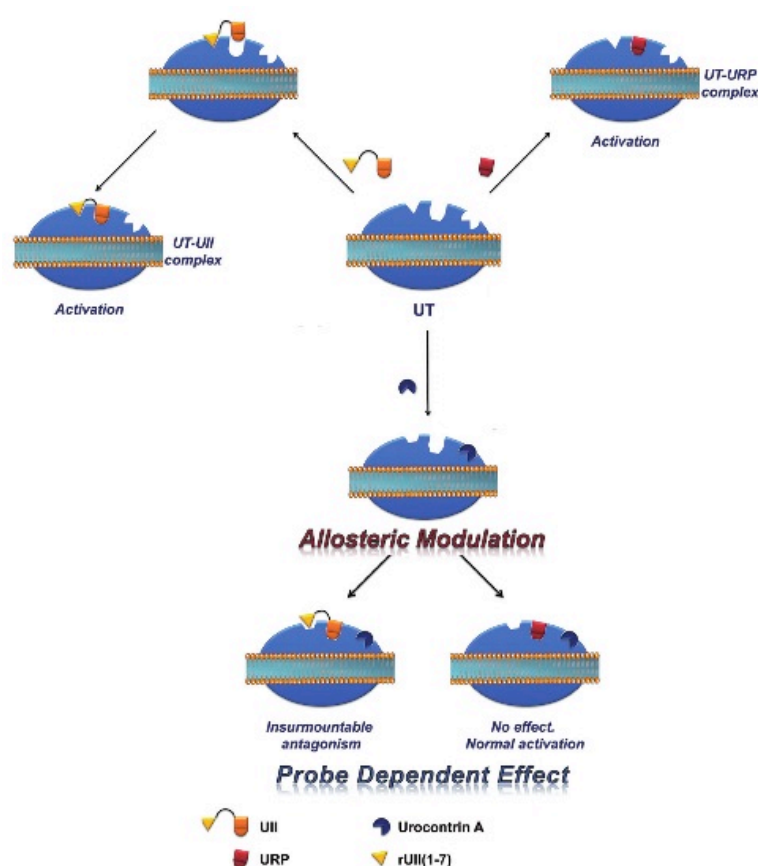


Figure 2.2. Allosteric modulation mechanism proposed for urocontrin A.

Antagonist peptides, such as urantide, [Orn⁸]U-II, UFP-803, BIM-23042 and SB-710411, all exhibit contradictory actions in selected assay systems. For example, they have shown antagonist properties in rat-isolated aorta, and partial agonist action by mobilization of intracellular calcium in specific recombinant UT receptor HEK/CHO cell systems. Similar

observations of residual agonist activity made by Kenakin in 2002 [51] and Camarda *et al.* in 2002 [40] have led to the proposal of ‘assay-dependent’ agonism- and antagonism-activity from different amounts of UT receptor expression and signal transduction-coupling efficiency. For example, activity may change depending on the receptor density and the efficiency of receptor couplings. For this reason, identification of a novel and selective antagonist was achieved by examining ligand-evoked UT receptor agonism under conditions of both low and high receptor density and efficient coupling and amplification. In 2006 Behm *et al.* [52] described **GSK248451** {H-(4-Cl)-(trans)-cinnamoyl-c[DCys-Pal-DTrp-Orn-Val-Cys]-His-NH₂} [53], which is a potent UT receptor antagonist in all native mammalian isolated tissues retaining an extremely low level of relative intrinsic activity in recombinant HEK cells (4-5 fold less than observed for urantide). Furthermore, GSK248451 became a suitable tool compound for further investigations concerning the role of U-II in the aetiology of mammalian cardiometabolic diseases, because it represents a selective UT receptor antagonist that blocks the systemic vasopressor actions of exogenous U-II.

Name	Peptide Sequence
PRL-2903	H-Fpa-c[Cys-Pal-DTrp-Lys-Tle-Cys]-(2')Nal-NH ₂
SB-710411	H-Cpa-c[DCys-Pal-DTrp-Lys-Val-Cys]-Cpa-NH ₂
BIM-23127	H-D(2')Nal-c[Cys-Tyr-DTrp-Orn-Val-Cys]-(2')Nal-NH ₂
BIM-23042	H-D(2')Nal-c[Cys-Tyr-DTrp-Lys-Val-Cys]-(2')Nal-NH ₂
[Orn ⁸]U-II	H-Glu-Thr-Pro-Asp-c[Cys-Phe-Trp-Orn-Tyr-Cys]-Val-OH
P5U	H- Asp-c[Pen-Phe-Trp-Orn-Tyr-Cys]-Val-OH
urantide	H- Asp-c[Pen-Phe-DTrp-Orn-Tyr-Cys]-Val-OH
UFP-803	H- Asp-c[Pen-Phe-DTrp-Dab-Tyr-Cys]-Val-OH
URP	H-Ala-c[Cys-Phe-Trp-Lys-Tys-Cys]-Val-OH
urocontrin	H-Ala-c[Cys-Phe-Bip-Lys-Tys-Cys]-Val-OH
GSK248451	H-Cin-c[DCys-Pal-DTrp-Orn-Val-Cys]-His-NH ₂

Table 2.1. Peptidic urotensin analogues.

2.3 Non-peptidic urotensin analogues

The use of peptides as drugs in a therapeutic approach is often problematic, because of their poor oral and tissue absorption, and their low stability due to rapid proteolytic cleavage by enzymes. The pharmacokinetic limits of peptides may be overcome by the development of non-peptide molecules, which mimic the sequence and specific secondary structure responsible for the parent peptide's biological activity. In the challenge to design nonpeptide ligands, mimicry of the conformation and shape of the peptide backbone may be achieved using organic molecules as scaffolds onto which substituents may be attached possessing hydrophobic, steric and electronic properties to generate and optimize the affinity and selectivity of potentially active compounds. Non-peptide agonists and antagonists of the human UT receptor could be important tools for determining the role of U-II and its derivatives in the urotensin system, and have been developed in several studies. Specifically, the design and synthesis of selective receptor antagonists may clarify the roles of human U-II as a multifunctional peptide in mammalian patho-physiological functions. Stable non-peptide antagonists could be administered *in vivo* to provide alternative pharmacological strategies for treating different diseases.

Many approaches to discover non-peptide ligands of GPCRs have employed high-throughput screening (HTS) combined with knowledge of the 3D structure adopted by the natural ligand. Virtual screening based on the pharmacophore model and key residues of U-II was performed using the Aventis compound database in 2002 by Flohr *et al.* [34], who identified functional antagonists of U-II. Screening was performed based on two agonist pharmacophore models: associated respectively with the human U-II peptide and Ac-[Cys-Phe-DTrp-Lys-Tyr-Cys]-NH₂. From 500 compounds that matched the U-II pharmacophore, the most notable compound, **S7616** {1-(3-carbamimidoyl-benzyl)-4-methyl-1H-indole-2-carboxylic acid (naphthalene-1-ylmethyl)amide} exhibited an IC₅₀ of 400 nM (Figure 2.3).

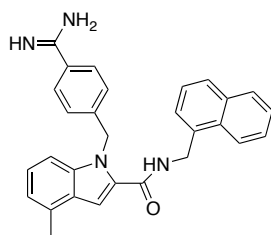


Figure 2.3. Molecular structure of S7616.

The phenyl ring of the indole and the naphthalenemethylamine side chain are localized onto the two aromatic features of the pharmacophore. The basic benzamidine group in S6716 was shown to form a charged interaction with Asp¹³⁰ within TM3 of the human UT receptor. The basic amino group was considered crucial for designing antagonists. Croston *et al.* [54] in 2002 employed a functional mammalian cell-based R-SAT assay for high-throughput screening to identify small molecule UT receptor agonists. In this assay the UT receptor was multiplexed with vectors for the expression of additional receptor targets, such as the muscarinic M3 receptor and some orphan GPCRs to increase the number of drug-target interactions tested without altering the response and sensitivity characteristics of potential ligands. From screening a library of 180000 small diverse organic molecules, **AC-7954** {3-(4-chlorophenyl)-3-(2-(dimethylamino)ethyl)isochroman-1-one} was identified as a novel non-peptide agonist with a potency of 300nM at the human UT receptor (Figure 2.4).

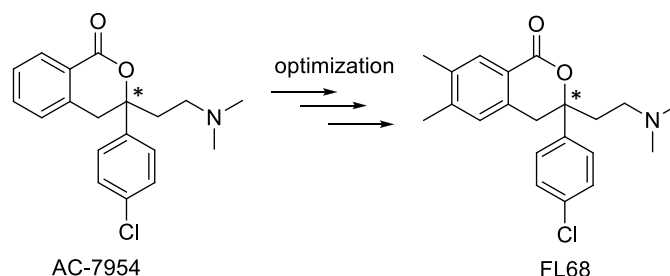


Figure 2.4. Structures of AC-7954 and its optimized derivative FL68.

This low molecular weight bicyclic isochromane activated selectively the UT receptor and possessed druglike lipophilicity, a basic amino function ($pK_a=8.7$), and limited conformation flexibility. Resolution of the racemic mixture and testing of both enantiomers in R-SAT revealed (+)-AC-7954 to be a more potent agonist at the stereoselective UT receptor, as clarified later by docking studies [32].

As the first non-peptide agonist AC-7954 was employed as a lead compound to develop more potent non-peptide ligands for the human UT receptor [55]. In accordance with this study, the isochromanone core was kept intact, and bulkier amino groups and hydrophobic aromatic ring substituents were investigated on AC-7954 to provide knowledge about the interaction between U-II and the UT receptor. Beneficial effects were obtained when substituents were introduced on the aromatic part of the isochromanone ring system; however, sterically demanding amino groups diminished activity. The 6,7-dimethyl derivative of AC-7954 exhibited the best potency in the series and on resolution of the racemate, the (+)-enantiomer **FL-68** (Figure 2.4) was active at the UT receptor without activity at the closely related somatostatin receptors.

Although the isochromanone-based agonists so far described were interesting for their druglikeness properties and their high selectivity for the UT receptor, in 2005, Lehmann *et al.* [56] found a path to obtain active molecules by breaking the C3-C4 bond of the isochromanone scaffold. Employing different linkers between the two aromatic rings, a series of ether, ester, amide, sulfonamide, carbamate, and urea derivatives was prepared, and furnished molecules retaining activity and efficacy comparable to AC-7954, except for the ether and sulfonamide analogs probably due to the absence of conformational effects induced by the pharmacophoric carbonyl group. Biphenylamide (+)-**FL-104** was shown to be considerably more active than its enantiomer and identified as one of the most potent non-peptide agonists known ($pEC_{50}=7.49 \pm 0.03$, Figure 2.5).

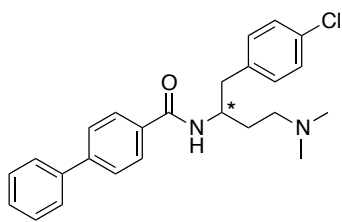


Figure 2.5. Structure of FL-104.

Palosuran (ACT-058362, Figure 2.6) is a specific and potent inhibitor of the human UT receptor reported in 2004 by Clozel *et al.* [57], who have used it as a pharmacological tool in determining the physiological and pathological roles of endogenous U-II in kidney disease.

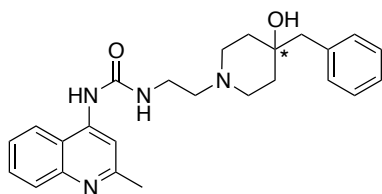


Figure 2.6. Structure of palosuran (ACT-058362).

The **4-ureido-quinoline** core in the structure of palosuran may be a promising template for antagonists as indicated in several patent applications. 4-Ureido-quinoline derivatives in which 1,2,3,4-tetrahydroisoquinoline, piperidine, piperazine and pyrrolidine moieties were introduced have been tested for ability to displace human [125 I]U-II. Other non-peptide molecules reported in patent applications were based on 4-aminoquinoline [58], 2-aminoquinoline and 2-aminoalkylquinolin-4-one derivatives [59] (Figure 2.7).

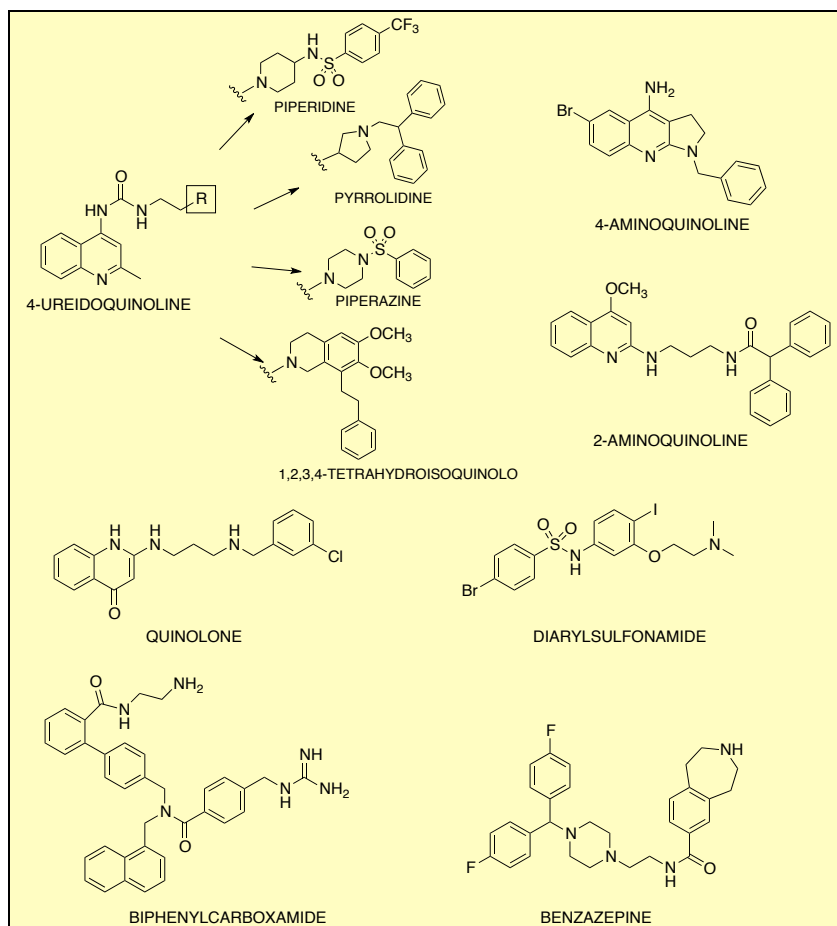


Figure 2.7. Structures of non-peptide Urotensin-II antagonists reported in the patent literature.

Researchers at GlaxoSmithKline conducted extensive biological studies leading to a series of **arylsulfonamide** derivatives identified from high-throughput screening: **SB-611812** exhibited potent binding at the rat UT receptor and was proposed as useful pharmacological tool based on its antagonist activity in rat aortic tissue and interesting pharmacokinetic properties such as high bioavailability (~100%) and half-life (~5h). The related analogs **SB-706375** and **SB-657510** [60, 61] were also potent antagonists. Substituted **diarylsulfonamides** reported in other patent applications possessed significant affinity for UT receptors.

Aminoalkoxybenzylpyrrolidine derivatives reported by GlaxoSmithKline to be identified by a HTS protocol involving *hU*-II-mediated calcium mobilization in *hUT*-expressing HEK293

cells included **SB-436811** which exhibited moderate affinity for the human UT receptor but weak rat UT binding [62].

Biphenylcarboxamide and **benzazepine** scaffolds were also reported in patent applications claiming high UT receptor antagonism [63]. In particular, most structurally different from other UT receptor antagonists, the benzazepines represent one of the most potent antagonists at the human UT receptor so far described.

3 Design of New Urotensin-II Derivatives

3.1 Leads optimization of U-II(4-11), P5U and Urantide

The aim of my Ph.D. research has been to investigate the structure-activity relationships of Urotensin-II sequences: U-II(4-11), P5U and urantide, the latter two recognized as the most potent agonist and antagonist, respectively. Optimization of lead peptides was aimed to stabilize specific conformations and to improve pharmacokinetic profiles. The latter goal was designed to surmount unfavourable properties of peptides such as low stability, poor absorption, and short half-life. Different synthetic strategies were considered to address such pharmacokinetic issues, such as incorporation of uncoded amino acids, head to tail and side-chain to side-chain cyclization, modification of peptide bonds, introduction of peptidomimetics, and termini protections and modifications. In the case of U-II(4-11), P5U and urantide, such chemical modifications were pursued to provide more potent and useful analogues. In particular, site-specific incorporation of uncoded amino acids, N-methylation of amide bonds and peptidomimetics development were examined to improve pharmacokinetic properties, to evaluate effects on conformation, and to provide structure-activity relationship information. Ideally, these studies will furnish information on the physiological and pathological pathways of this important peptide hormone.

3.1.1 Trp-constrained analogues

The main conformational difference observed in the structures of antagonists and agonists implicate the orientation of the (D/L)-Trp⁷ side chain. In particular, in models of agonists and antagonists, the (D/L)-Trp⁷ indole moiety is respectively close to the Lys⁸ side chain, or more flexible and distant from the Orn⁸ side chain. Based on these considerations, the Trp residue in position 7 was replaced with the constrained uncoded amino acids. Specifically, 1,2,3,4-tetrahydro- β' -carboline-3-carboxylic acid residue (Tpi), in both configurations was employed to replace Trp⁷ to examine conformation-activity relationships of agonists and antagonists of the UT receptor [64] (Figure 3.1).

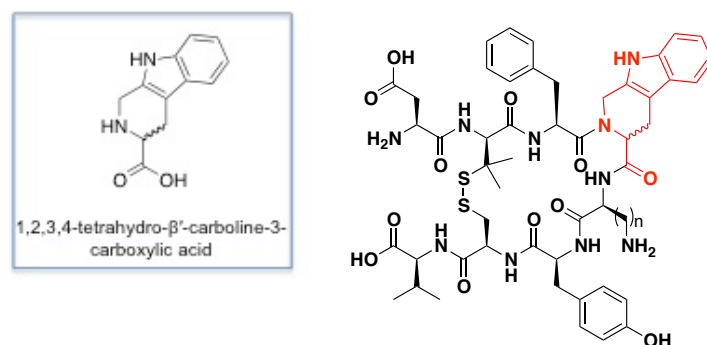


Figure 3.1. The Trp⁷ residue in P5U (n = 4) and urantide (n = 3) sequences has been replaced with the uncoded Tpi residue, 1,2,3,4-tetrahydro-β'-carboline-3-carboxylic acid.

The Tpi amino acid arises from a condensation between L-tryptophan and formaldehyde. This reaction occurs in food and it is temperature and pH dependent [65]. The replacement of the Trp⁷ with Tpi led to active analogues and solution NMR analysis gave insight on conformation-activity relationships of earlier reported urotensin ligands. Accordingly, all highly potent analogues of *h*U-II possess a type II' β-hairpin backbone conformation regardless of their agonist or antagonist activity, indicating that such a backbone conformation is necessary for the UT recognition [41,66].

The Tpi residue can only adopt either gauche (+) or gauche (−) side chain rotamer populations because the indole moiety is cyclized to the peptide backbone nitrogen [67]. Hence, the Tpi⁷ indole moiety is held away from the Lys⁸ side chain. Moreover, both L-Tpi and D-Tpi were used because L-Trp and D-Trp residues are both compatible with UT receptor binding mode. Finally, Lys/Orn replacement was shown to modulate the urotensin analogues activity because the Orn residue promotes antagonist activity [40]. Hence, four analogues **1-4** were designed (Table 3.1).

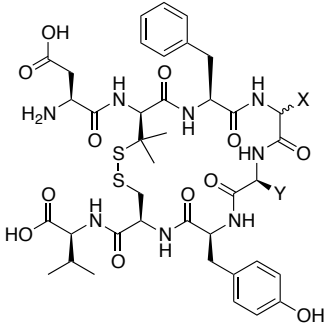
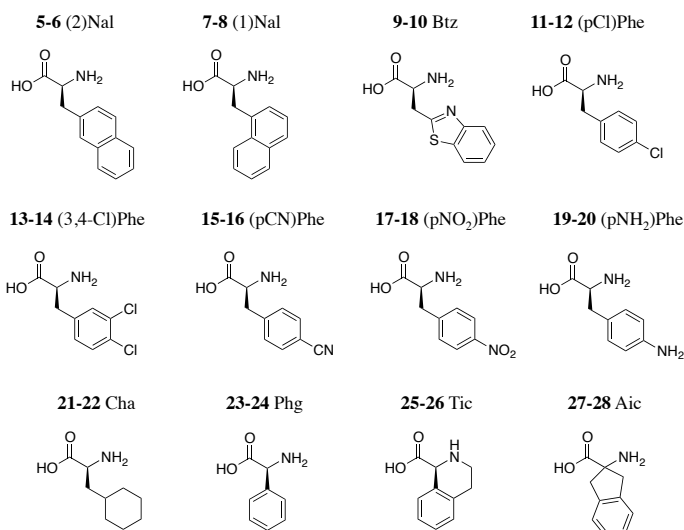
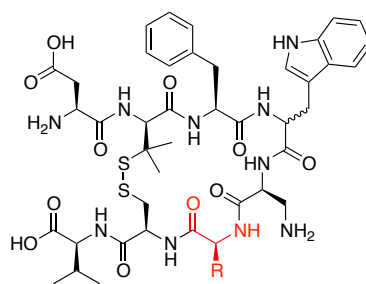
General formula: Asp-c[Pen-Phe-Xaa-Yaa-Tyr-Cys]-Val-OH	Compound	Xaa ⁷	Yaa ⁸
	1	Tpi	Lys
	2	DTpi	Lys
	3	Tpi	Orn
	4	DTpi	Orn

Table 3.1. Compounds **1-4** have been designed by insertion of (D/L)-Tpi residues in P5U and urantide sequences.

3.1.2 Tyr⁹-selective uncoded amino acids incorporation

To optimize the activity of P5U and urantide, we designed and synthesized several analogues featuring replacement of the Tyr⁹ residue with uncoded amino acids [68] to improve the potency and stability of urotensin ligands [69].

A SAR study on Tyr⁹ was prompted by recent finding that the side chain orientation of this residue influences the activity of P5U and urantide constrained analogues [64]. For this reason, the Tyr⁹ was replaced with non-coded amino acids, which were chosen in an attempt to improve the serum stability (Table 3.2). Substitutions included bulky electron-rich aromatic moieties (e.g., **5-10**), phenyl rings substituted with bulky chlorine atoms (e.g., **11-14**), and replacement of the electron donating hydroxyl group of Tyr⁹ with electron withdrawing groups, such as cyano (e.g., **15-16**) and nitro (e.g., **17-18**) groups, and with primary amino groups (e.g., **19-20**). In addition, non-aromatic residues (e.g., peptides **21-22**), as well as conformationally constrained unnatural amino acids (e.g., peptides **23-28**) were evaluated in this specific position.



Compound	Peptide Sequence
5	H-Asp-c[Pen-Phe-Trp-Lys-(2)Nal-Cys]-Val-OH
6	H-Asp-c[Pen-Phe-DTrp-Orn-(2)Nal-Cys]-Val-OH
7	H-Asp-c[Pen-Phe-Trp-Lys-(1)Nal-Cys]-Val-OH
8	H-Asp-c[Pen-Phe-DTrp-Orn-(1)Nal-Cys]-Val-OH
9	H-Asp-c[Pen-Phe-Trp-Lys-Btz-Cys]-Val-OH
10	H-Asp-c[Pen-Phe-DTrp-Orn-Btz-Cys]-Val-OH
11	H-Asp-c[Pen-Phe-Trp-Lys-(pCl)Phe-Cys]-Val-OH
12	H-Asp-c[Pen-Phe-DTrp-Orn-(pCl)Phe-Cys]-Val-OH
13	H-Asp-c[Pen-Phe-Trp-Lys-(3,4-Cl)Phe-Cys]-Val-OH
14	H-Asp-c[Pen-Phe-DTrp-Orn-(3,4-Cl)Phe-Cys]-Val-OH
15	H-Asp-c[Pen-Phe-Trp-Lys-(pCN)Phe-Cys]-Val-OH
16	H-Asp-c[Pen-Phe-DTrp-Orn-(pCN)Phe-Cys]-Val-OH
17	H-Asp-c[Pen-Phe-Trp-Lys-(pNO ₂)Phe-Cys]-Val-OH
18	H-Asp-c[Pen-Phe-DTrp-Orn-(pNO ₂)Phe-Cys]-Val-OH
19	H-Asp-c[Pen-Phe-Trp-Lys-(pNH ₂)Phe-Cys]-Val-OH
20	H-Asp-c[Pen-Phe-DTrp-Orn-(pNH ₂)Phe-Cys]-Val-OH
21	H-Asp-c[Pen-Phe-Trp-Lys-Cha-Cys]-Val-OH
22	H-Asp-c[Pen-Phe-DTrp-Orn-Cha-Cys]-Val-OH
23	H-Asp-c[Pen-Phe-Trp-Lys-Phg-Cys]-Val-OH
24	H-Asp-c[Pen-Phe-DTrp-Orn-Phg-Cys]-Val-OH
25	H-Asp-c[Pen-Phe-Trp-Lys-Tic-Cys]-Val-OH
26	H-Asp-c[Pen-Phe-DTrp-Orn-Tic-Cys]-Val-OH
27	H-Asp-c[Pen-Phe-Trp-Lys-Aic-Cys]-Val-OH
28	H-Asp-c[Pen-Phe-DTrp-Orn-Aic-Cys]-Val-OH

Table 3.2. Tyr⁹-modified series.

Novel analogues were found with improved agonist activity compared to the parent P5U and antagonist activity similar to urantide. Some new ligands showed good stability in a serum proteolytic assay, indicative of enhanced peptide bioavailability.

3.2 N-Methylation of Urotensin-II

With a minimal sequence required for the biological activity in hand, conformational analysis of the peptide is usually performed in the next step to examine SARs [70]. Active sequences may be constrained to a specific conformation to stabilize particular secondary structures and improve activity and selectivity. Conformational flexibility is usually an undesired property of a ligand for a G-protein coupled receptor. Peptides are in general flexible due to their low rotational barriers about the bond between N and C_α, determined by the Φ dihedral angle, and the bond between C_α and CO, given by the ψ dihedral angle (Figure 3.2). Such flexibility hampers peptides as drugs in a therapeutic applications, because it renders them susceptible to parasitic receptors such as proteolytic enzymes, leading to unfavorable pharmacokinetic properties such as poor oral and tissue absorption.

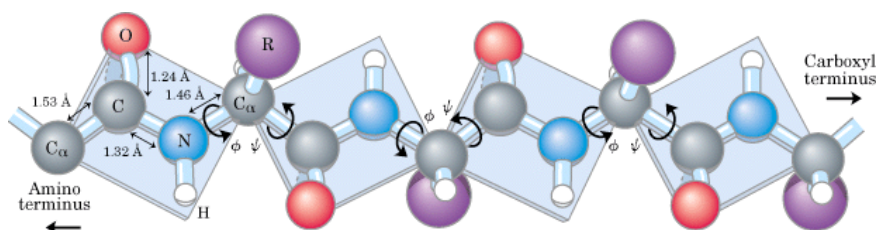


Figure 3.2. Peptide bond geometry.

Among different synthetic strategies that are available to address such pharmacokinetic issues, N-methylation of select peptide bonds has become an attractive tool for investigating conformation and biological properties. N-Methylation can increase steric hindrance between the N-methylated amide bond [71] and the adjacent amino acid side chain and modify the amide bond *cis-trans* isomer equilibrium by enhancing the population of the *cis* isomer [72].

Cyclic peptides can be strongly influenced from this kind of modification, which may disrupt secondary structure due to the long-range steric interactions caused by mono- and multiple-N-methylated amide bonds. Additionally, the replacement of hydrogen by methyl on the amide may break-up intramolecular and intermolecular hydrogen-bonds [73], essential for interaction with the receptor (Figure 3.3). Examples of N-methylated peptides occurring in nature in various microorganisms and vegetables, include cyclosporine A and omphalotin, [74] which exhibit remarkable biological and pharmacological profiles. The wide-ranging biological activity of N-methylated peptides includes antibiotic [75], antitumoral [76], and immunosuppressive [77] effects.

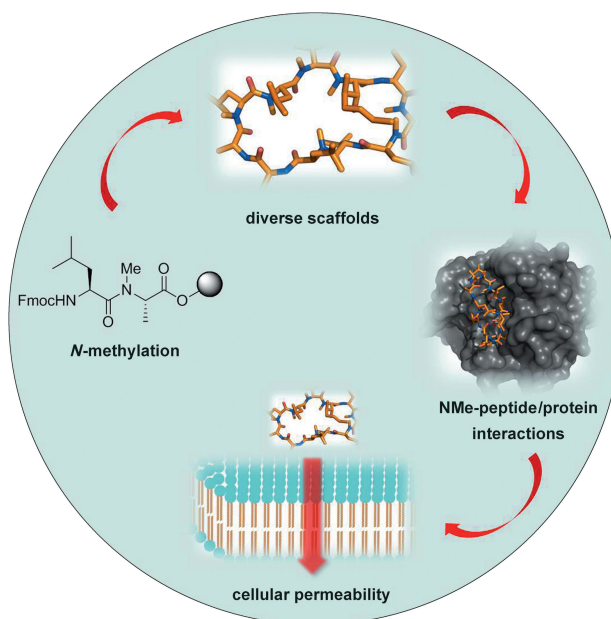


Figure 3.3. Features of N-methylation as chemical modification, and its impact upon pharmacokinetic and pharmacodynamic properties of peptides.

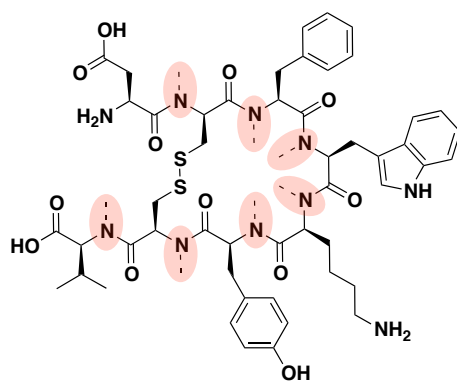
In recent years, the development of more conformationally constrained urotensin analogues has suggested investigation of the spatial orientation of amino acids belonging to the cyclic portion [41,64,66]. For example, modifications induced by penicillamine residues in P5U, urantide and other derivatives have revealed the importance of the spatial orientation of

amino acid side chains for interacting with the receptor. The introduction of a methyl group into the cyclic portion of U-II(4-11) may thus result in conformational alteration of the peptide backbone and subsequent interaction with the receptor counterpart. Application of N-methylation for modifying peptide bonds has had success in developing peptide ligands [78], improving subtype selectivity, and pharmacological properties [79], such as metabolic stability, lipophilicity, potency, and bioavailability [80]. Such N-methylation may also switch agonists to antagonists [81]. Suppression of proton-donating N-H groups capable of hydrogen bonding may also contribute to understanding of their relevance in the bioactive conformation [82]. Moreover, as mentioned above, Urotensin-II is widely expressed in several organs in human diseases, and its role is still under investigation. The prediction of biologically active conformers remains speculative and necessitates analogs to distinguish conformational requirements for agonism and antagonism, as well as for selective patho-physiological pathways involved in urotensin systems.

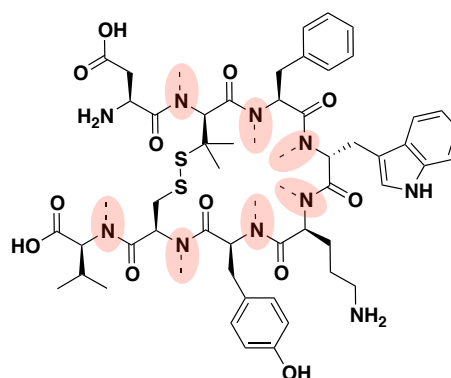
3.2.1 Mono- and multiple-N-methylated series

Mono-N-methylation has been used for years to change pharmacological properties of peptides. The introduction of a methyl group on a single amide bond into an active peptide sequence can discriminate which hydrogen bond is essential for maintaining the biological activity. Hence, the amino acids of the bioactive hexapeptide sequence of U-II(4-11) and urantide have been exchanged in a systematic manner with their corresponding N^α-methylated analogs to provide U-II derivatives. Multiple N-methylations were also considered to elucidate conformational effects imparted by steric constraints in the peptide backbone and to improve the pharmacokinetic profile of the peptides for use as drug prototypes [83].

The influence of N-methylation on the conformation of the pharmacophore Cys⁵-Phe⁶-Trp⁷-Lys⁸-Tyr⁹-Cys¹⁰ was performed on the cyclic portion of U-II(4-11) and urantide by synthesis of the following peptides:



N-methylated hU-II₍₄₋₁₁₎



N-methylated Urantide (antagonist)

29	H-Asp-c[(NMe) Cys -Phe-Trp-Lys-Tyr-Cys]-Val-OH
30	H-Asp-c[Cys-(NMe) Phe -Trp-Lys-Tyr-Cys]-Val-OH
31	H-Asp-c[Cys-Phe-(NMe) Trp -Lys-Tyr-Cys]-Val-OH
32	H-Asp-c[Cys-Phe-Trp-(NMe) Lys -Tyr-Cys]-Val-OH
33	H-Asp-c[Cys-Phe-Trp-Lys-(NMe) Tyr -Cys]-Val-OH
34	H-Asp-c[Cys-Phe-Trp-Lys-Tyr-(NMe) Cys]-Val-OH
35	H-Asp-c[Pen-Phe-(NMe) DTrp -Orn-Tyr-Cys]-Val-OH
36	H-Asp-c[Pen-Phe-DTrp-(NMe) Orn -Tyr-Cys]-Val-OH
37	H-Asp-c[Pen-Phe-DTrp-Orn-(NMe) Tyr -Cys]-Val-OH
38	H-Asp-c[Pen-Phe-DTrp-Orn-Tyr-(NMe) Cys]-Val-OH
39	H-Asp-c[(NMe) Cys -(NMe) Phe -Trp-Lys-Tyr-Cys]-Val-OH
40	H-Asp-c[(NMe) Cys -Phe-(NMe) Trp -Lys-Tyr-Cys]-Val-OH
41	H-Asp-c[(NMe) Cys -Phe-Trp-(NMe) Lys -Tyr-Cys]-Val-OH
42	H-Asp-c[(NMe) Cys -Phe-Trp-Lys-(NMe) Tyr -Cys]-Val-OH
43	H-Asp-c[(NMe) Cys -Phe-Trp-Lys-Tyr-(NMe) Cys]-Val-OH
44	H-Asp-c[Cys-(NMe) Phe -(NMe) Trp -Lys-Tyr-Cys]-Val-OH
45	H-Asp-c[Cys-(NMe) Phe -Trp-(NMe) Lys -Tyr-Cys]-Val-OH
46	H-Asp-c[Cys-(NMe) Phe -Trp-Lys-(NMe) Tyr -Cys]-Val-OH
47	H-Asp-c[Cys-(NMe) Phe -Trp-Lys-Tyr-(NMe) Cys]-Val-OH
48	H-Asp-c[Cys-Phe-(NMe) Trp -(NMe) Lys -Tyr-Cys]-Val-OH
49	H-Asp-c[Cys-Phe-(NMe) Trp -Lys-(NMe) Tyr -Cys]-Val-OH
50	H-Asp-c[Cys-Phe-(NMe) Trp -Lys-Tyr-(NMe) Cys]-Val-OH
51	H-Asp-c[Cys-Phe-Trp-(NMe) Lys -(NMe) Tyr -Cys]-Val-OH
52	H-Asp-c[Cys-Phe-Trp-(NMe) Lys -Tyr-(NMe) Cys]-Val-OH
53	H-Asp-c[Cys-Phe-Trp-Lys-(NMe) Tyr -(NMe) Cys]-Val-OH

Table 3.3. Mono- and multiple-N-Methylated series.

3.3 Aza-sulfuryl peptides mimics of urotensin-II

The biological activity and physical properties of peptides are related to their backbone geometry and side chain functionality. Attempts to modulate the activity of natural peptides by the introduction of chemical modifications represent a valid strategic approach in designing and developing new analogues.

N-Aminosulfamides are peptidomimetics in which the C_αH and the carbonyl of an amino acid residue are respectively replaced by a nitrogen atom and a sulfonyl group (Figure 3.4).

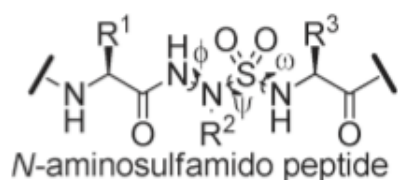


Figure 3.4. N-aminosulfamide moiety.

Examples of aza-sulfurylpeptides reported in the literature include an inhibitor of the human immunodeficiency virus-1 proteinase, in which this moiety serves effectively as a tetrahedral transition state mimic of enzyme-catalyzed amide hydrolysis [84]. Aza-sulfuryl peptide analogues combine characteristics of aza- and α -sulfonamido-peptides [85], albeit with firmer and more stable structures, potentially relevant for modification of backbone geometry. The sulfonyl group possesses a tetrahedral sulfur, which adopts ω torsion angle values around $\pm 60^\circ$ and $\pm 100^\circ$ (instead of amide *cis*-(E) and *trans*-(Z) conformations at respectively 0° and $\pm 180^\circ$) separated by a lower S-N rotational barrier ($\Delta G^\ddagger \approx 35$ kJ/mol), relative to the amide C-N ($\Delta G^\ddagger \approx 75$ kJ/mol) [86]. Furthermore, the S-N bond length is longer than the C-N, due to lack of an amide bond resonance and greater sp^3 versus sp^2 character of the sulfonamide nitrogen (Figure 3.5).

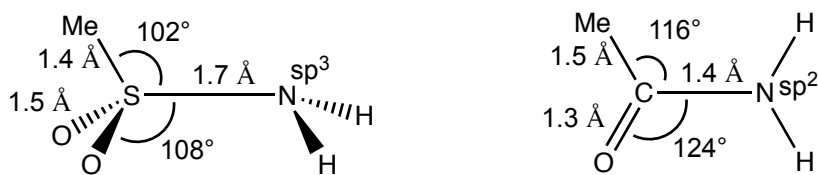


Figure 3.5. Sulfonamide and amide bond lengths and angles.

The type of structure modification generated by aza-sulfonamido residues could influence secondary structure and biological activity. Indeed, this moiety offers more inter- and intra-molecular hydrogen bond interactions and conformational distortion depending on the position of insertion. In the case of urotensin-II, aza-sulfuryl amino acids were targeted for insertion into the cyclic portion of the U-II(4-11) sequence by replacement of the Trp⁷ and Lys⁸ amino acid residues, according to observations from N-methylation studies previously reported. In fact, the N-methylation of amide bonds of Trp⁷ and Lys⁸ residues gave interesting results since the specific suppression of a proton donating N-H in these two positions led to opposite affinity versus the UT receptor. In particular, they resulted to be the most and less tolerant positions, respectively, for the introduction of methyl groups at the N^α of the amide bond. Therefore, new analogues were designed to improve hydrogen-bonding capability in positions originally located at Trp⁷ and Lys⁸ expecting different affinity at UT receptor. The conformation of such analogues could play a key role in the investigation of SAR about urotensin-II, because the aza-sulfonamide motif may generate constrained cyclic analogues. Chemoselective alkylation of an aza-sulfuryl amino acid residue provided analogues with different alkyl groups to mimics the side chains of the native ligands. Aza-sulfuryl peptide analogues were thus designed and successfully synthesized to evaluate effects produced by this modification (Figure 3.6).

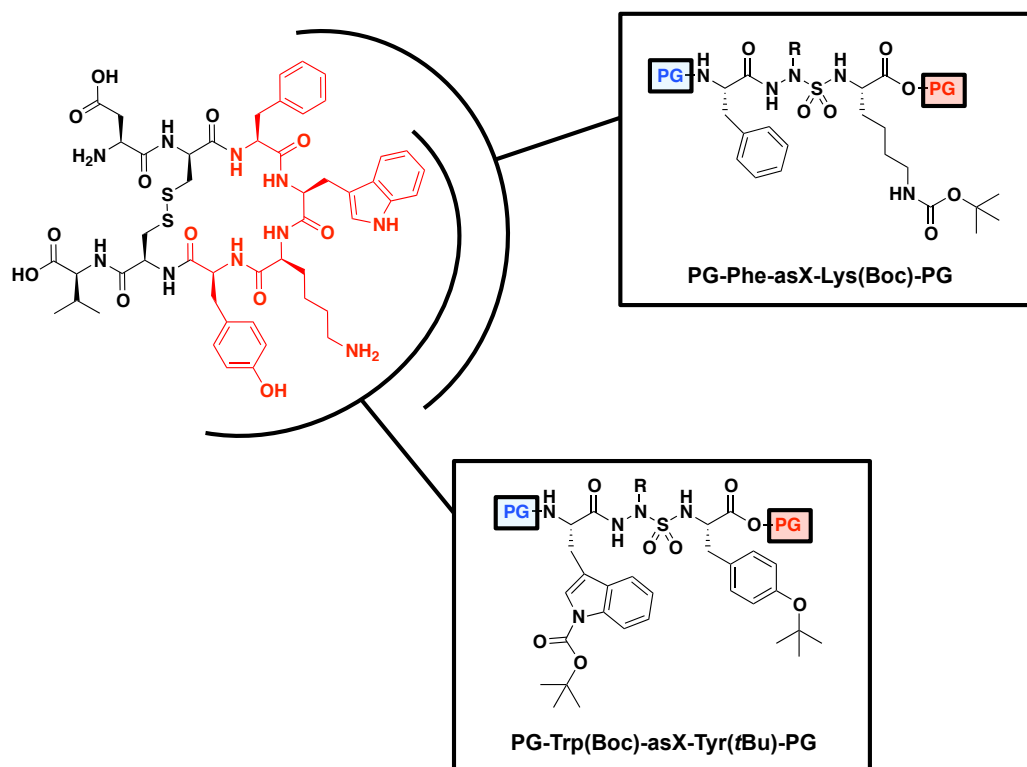


Figure 3.6. Aza-sulfuryltriptides have been designed as mimics of Trp⁷ and Lys⁸ residues, for insertion into the core sequence of U-II(4-11). Functional groups of tripeptides have to be protected by protecting groups compatible with solid phase peptide synthesis; PG: protecting group.

4 Synthetic Strategies

4.1 General method for peptide synthesis

The synthesis of *hU*-II(4-11) analogues containing uncoded amino acid replacements for Trp, Lys and Tyr at positions 7, 8 and 9 was respectively performed in a stepwise fashion on solid-phase using a Fmoc/*t*Bu strategy and Wang linker resin as solid support. The first amino acid N^α-Fmoc-Val-OH (4 equiv) was coupled to the resin in the presence of HBTU (4 equiv), HOBt (4 equiv), DIEA (8 equiv) and a catalytic amount of DMAP to facilitate ester formation in DMF for 3 h at rt. After the reaction went to completion, the resin was washed with DMF (3x) and DCM (3x), and was capped with acetic anhydride (1.2 equiv) and DIEA (2.4 equiv) in DMF for 30 min at rt to avoid potential parallel synthesis of side products. The resin was washed with DMF (3x) and DCM (3x). The N^α-Fmoc protecting group was removed from the Val residue by the treatment with piperidine (25% in DMF; 1 x 5 min and 1 x 25 min). The resin was washed with DMF (3x). A positive Kaiser ninhydrine test was observed. The following protected amino acids were added stepwise to synthesize the desired sequences for peptides **1-18**: N^α-Fmoc-Cys(Trt)-OH, N^α-Fmoc-**Zaa**-OH, (Zaa = Tyr(*t*Bu), (1')Nal, (2')Nal, Btz, (pCl)Phe, (3,4-Cl)Phe, (pCN)Phe, (pNO₂)Phe), N^α-Fmoc-**Yaa**(N^ε-Boc)-OH (Yaa: Lys, Orn), N^α-Fmoc-**Xaa**(Nⁱⁿ-Boc)-OH (Xaa: Trp, DTrp, Tpi, DTpi), N^α-Fmoc-Phe-OH, N^α-Fmoc-Pen(Trt)-OH and N^α-Fmoc-Asp(OtBu)-OH, to provide the general sequence Asp-c[Pen-Phe-**Xaa-Yaa-Zaa**-Cys]-Val-OH. Each coupling reaction was accomplished using a 4-fold excess of amino acid with HBTU (4 equiv) and HOBt (4 equiv) in the presence of DIEA (8 equiv). The peptide resin was washed with DCM (3x) and DMF (3x). The Fmoc deprotection protocol described above was repeated and the next coupling step was initiated in a stepwise manner. The Kaiser test was used as colorimetric test to confirm every coupling/deprotection step occurred in the peptide sequence elongation. Analytical HPLC and MS spectrometry monitored the achievement of linear sequences for the compounds **1-18**.

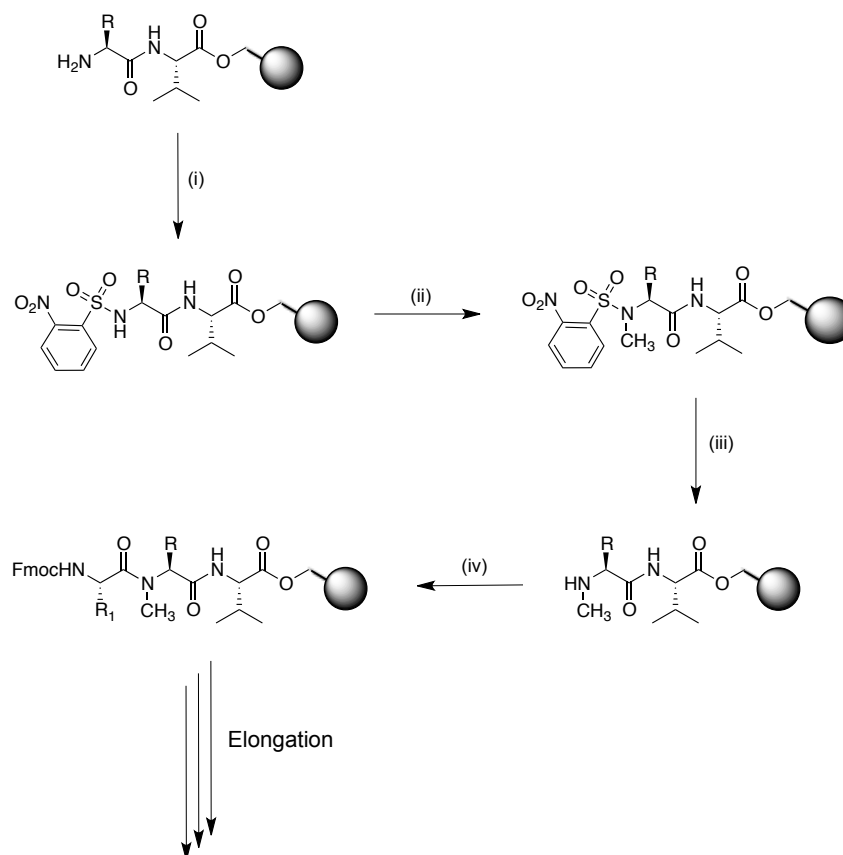
After construction of linear peptides, the S-Trt protecting groups from Pen⁵ and Cys¹⁰ were removed using 1% TFA in DCM (5 x 2 min). Release of free thiol was monitored by an Elmann's test [87]. The resin was washed with DCM (3x) and DMF (3x). Oxidation of the thiols was carried out using I₂ (10 equiv) and DIEA (5 equiv) in DCM for 30 min at rt. After reaction completion, no significant amount of linear peptide was detected by HPLC.

The N-terminal Fmoc group was removed as described above. The resin was washed with DMF (3x) and DCM (3x) and dried in vacuo. The peptide was released from the solid support and all protecting groups were cleaved using a cocktail of TFA/TIS/H₂O (95:2.5:2.5, v/v/v) for 3 h. The resin was removed by filtration. Crude peptide was recovered by precipitation from the filtrate using chilled ether to give a powder, which was purified by RP-HPLC using a semi-preparative C18-bonded silica column (Phenomenex, Jupiter 4 μ Proteo 90Å, 1.0 x 25 cm) with a gradient of MeCN and water containing 0.1% TFA (from 10 to 90% over 40 min) at a flow rate of 5.0 mL/min. The product was obtained by lyophilization of the appropriate fractions after removal of the MeCN by rotary evaporation under reduced pressure. Analytical RP-HPLC indicated >98% purity and the correct molecular ions were confirmed by LC/ESI-MS.

4.2 N-methylation on solid phase

N-methylated amino acids are commercially available, but expensive. The synthesis of a combinatorial library of N-methylated peptides has been described in the literature by several methods including the use of N-methylated amino acid building blocks prepared in solution [88] and by solid-phase methods [89]. The choice of introducing N-methylated amino acids as building blocks was dismissed in favor of a solid-phase N-methylation procedure to enhance flexibility in library design. The method employed was described by Scanlan and Miller [90], optimized by Biron *et al.* in 2006 [89], and proven compatible with many amino acids [79]. The procedure consists of three fundamental steps: i) amine protection with *o*-

nitrobenzenesulfonyl group (*o*-NBS); ii) amine alkylation and, iii) selective removal of the *o*-NBS group on solid support (Scheme 4.1).



Scheme 4.1. General N-methylation strategy on solid phase during construction of peptides. (i) *o*-NBS-Cl (4 equiv), 2,4,6-Collidine (10 equiv), NMP, 15 min; (ii) 1. DBU (3 equiv), NMP, 3 min; 2. $(\text{CH}_3)_2\text{SO}_4$ (10 equiv), NMP, 2 min; 3. Repeat 1 and 2; (iii) 2-mercaptoethanol (10 equiv), DBU (5 equiv), NMP, 2 x 5 min; (iv) Fmoc-AA-OH (4 equiv), HATU (4 equiv), HOAt (4 equiv), DIEA (8 equiv), NMP, overnight.

To introduce N-methyl groups during the peptide synthesis on solid support, the liberated primary amine was first reacted with *o*-NBS chloride and DBU in NMP as polar solvent to accelerate amine protection without any racemization. The methylation step was normally carried out with DBU and dimethylsulfate in NMP which gave alkylation of the relatively acidic sulfonamide in only 5 min. Amino acids with Trt protected side chains exhibited however loss of trityl group and low conversion to product. In these cases, a Mitsunobu procedure was used successfully [79]. Subsequently, resin treatment with mercaptoethanol and DBU removed the *o*-NBS group by way of a Meisenheimer intermediate. This reaction is

reported to be selective for N-methylated derivatives and does not occur when the protected amine is not alkylated. Couplings on N^ε-methylamino acids are known to be more challenging due to steric hindrance. For this reason, these couplings were performed with HATU and HOAt instead of HBTU and HOBt using DIEA as base in NMP, which yielded complete couplings after reaction overnight at rt. The evolution of the procedure was monitored by the observation of colorimetric tests such as Kaiser test for primary amine and *p*-chloranilin test for secondary amine, and by HPLC and ESI-MS systems.

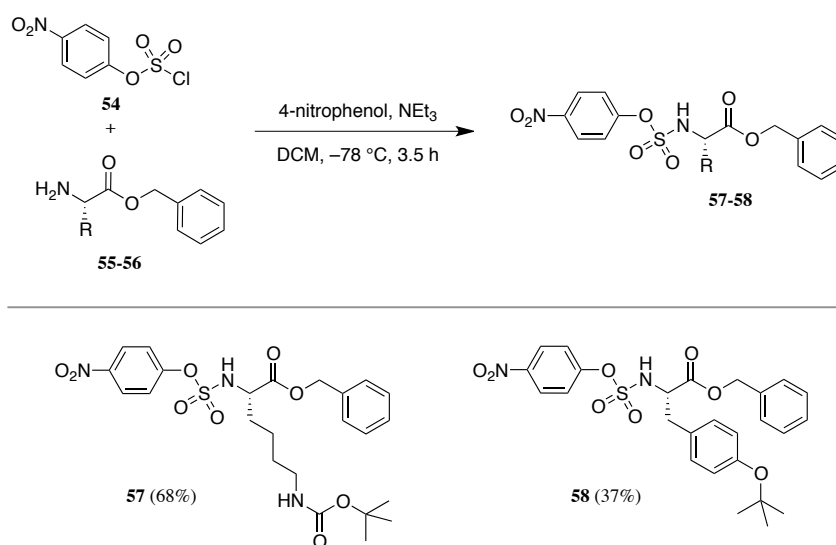
This method gave an efficient solution to synthesize libraries of N-methyl U-II(4-11) and urantide sequences possessing mono- and multiple-N-methylated analogues **29-53**.

4.3 Synthesis of protected aza-sulfuryl tripeptides

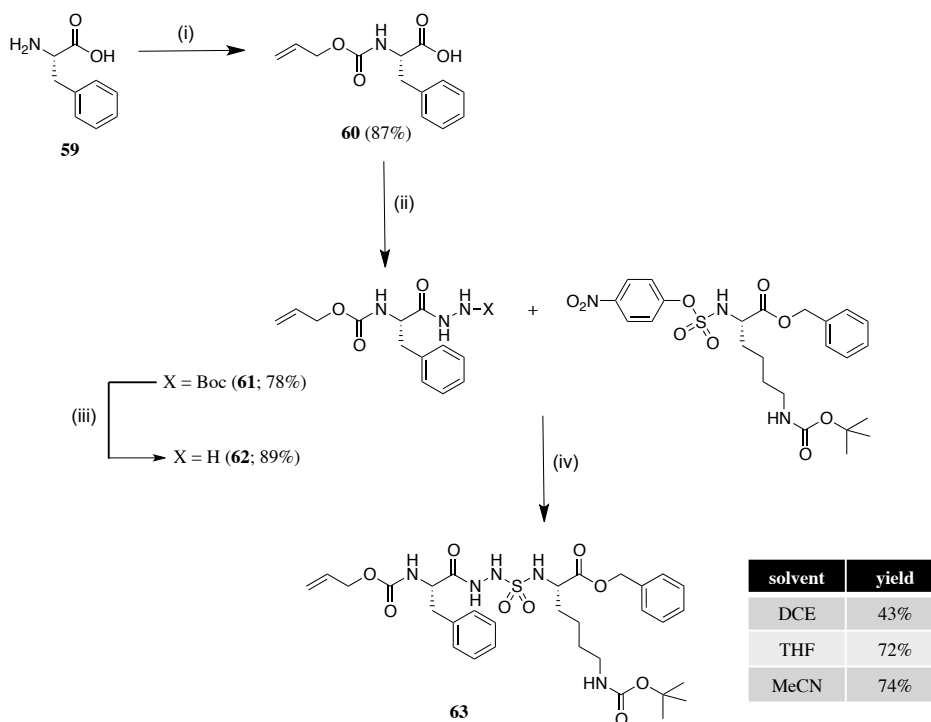
On the basis of their interesting conformational and biological properties, N-aminosulfamide analogues were designed by respective replacements of two amino acids belonging to the core sequence of the peptide U-II(4-11). Initially, aza-sulfuryl tripeptide building blocks were synthesized by modification of the approach of Turcotte *et al.* in 2012 [91] featuring chemoselective alkylation of an aza-sulfurylglycine intermediate. The choice of protecting groups was critical, because of the functionalized side chains related to the target tripeptides. The synthesis of aza-sulfonamide peptides consisted of two phases: first, the synthesis of the aza-sulfuryl tripeptide building block by solution phase reactions with protected functional groups compatible with solid phase peptide synthesis; followed by incorporation into the peptide sequence on solid support using a Fmoc/*t*Bu orthogonal protection strategy.

4-Nitrophenyl chlorosulfate **54** [106], N^ε-(alloc)-L-phenylalanine **60**, and N^ε-(alloc)-Nⁱⁿ-(Boc)-L-tryptophan **69** [107,108], all were synthesized according to literature methods. N^ε-(Alloc)-L-lysine and O-(*t*-Bu)-L-tyrosine benzyl ester **55-56** were synthesized from their corresponding Fmoc-amino acids using benzyl bromide and cesium carbonate in DMF, and free-based by treating with 20% piperidine in DMF solution.

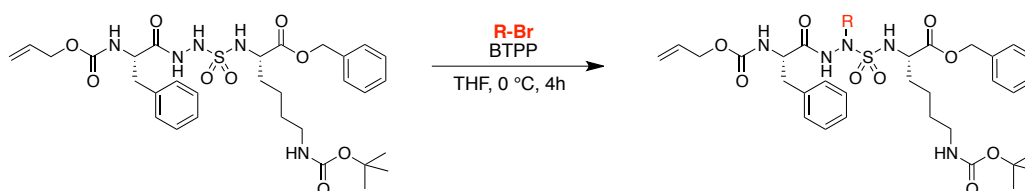
The first step for the synthesis of the building blocks **64-67** involved the reaction between 4-nitrophenyl chlorosulfate **54** and the amino esters **55-56** to give the corresponding sulfamidates **57-58** (Scheme 4.2). Two equivalents of 4-nitrophenol was necessary as an additive to avoid formation of symmetric sulfamide. Low yield of **58** was probably related to purification by column chromatography on silica gel, and trace amounts of 4-nitrophenol were detected by NMR spectroscopy.



Scheme 4.2. Synthesis of *p*-nitrophenylsulfamidate benzyl esters **57-58**.



Scheme 4.3. (i) Alloc-Cl (1.5 equiv), 1M NaOH, 3 h; (ii) 1. IBC (1.2 equiv); 2. NMM (1.5 equiv), 15 min; 3. *tert*-butyl carbazate (1 equiv), THF, 2 h, -15°C ; (iii) TFA/DCM 1:1, 1 h; (iv) Net_3 (1.1 equiv), μW , solvent, 60°C , 2.5 h.



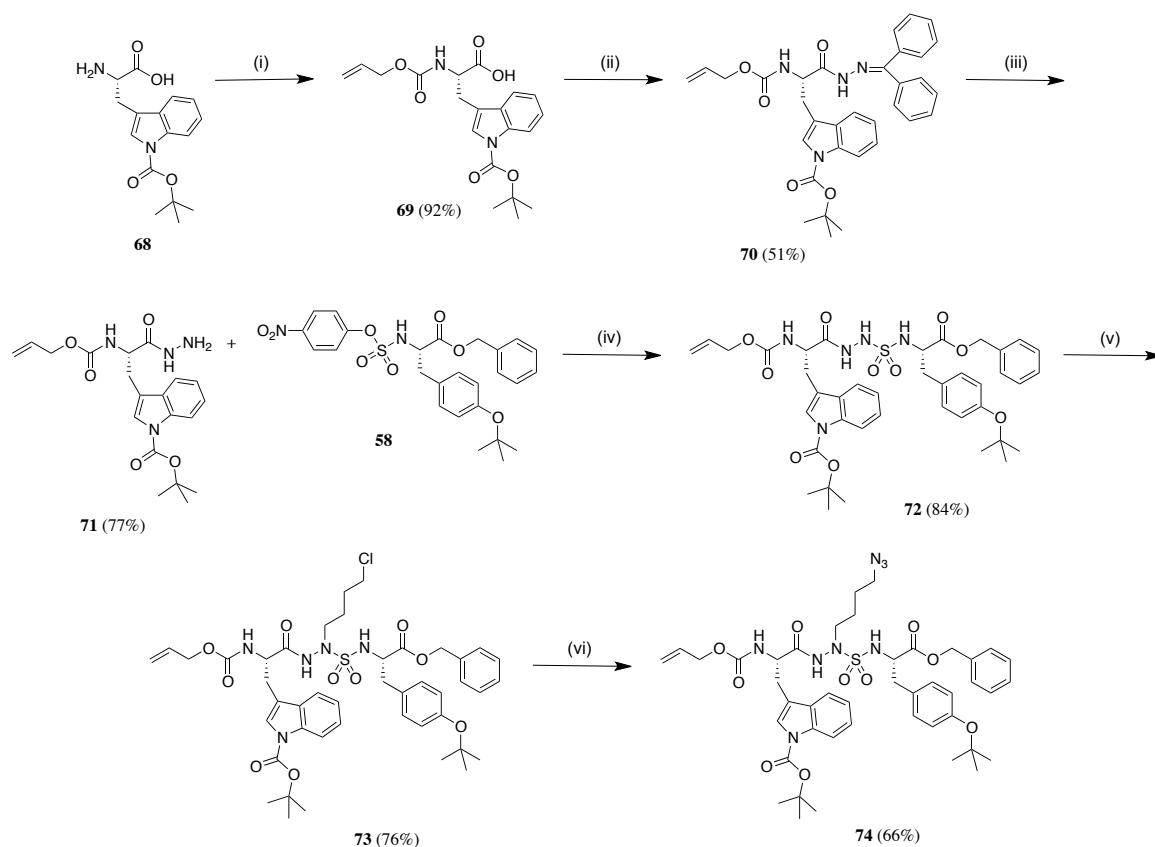
Compound	asAA	R	yield
64	Phe		68%
65	Bip		85%
66	(2)Nal		76%
67	(1)Nal		65%

Scheme 4.4. Chemoselective alkylation of the aza-sulfurylglycinyI tripeptides was used to add side-chain diversity.

N^ε-(Alloc)-L-phenylalanine hydrazide **62** was prepared starting from L-phenylalanine **59** by amine acylation with allylchloroformate, reaction with *tert*-buthylcarbazate to form the protected hydrazide, and removal of the Boc protection using a solution of 50% of TFA (Scheme 4.3). N-aminosulfamide **63** was synthesized by the reaction of sulfamidate **57** with N^ε-(Alloc)-L-phenylalanine hydrazide **62** employing microwave irradiation. Moreover, the choice of the solvent used for this reaction proved important in terms of yield due to the better absorption of microwave irradiation by solvents like MeCN (yield=74%) and THF (yield=72%) and better dissolution of the precursor in more polar solvents than DCE (yield=43%) reported in earlier protocols.

Chemoselective alkylation of the aza-sulfurylglyciny tripeptide **63** was performed by using the phosphazane base, *tert*-butylimino-tri(pyrrolidino)-phosphorane (BTPP), and different alkyl bromides to add diverse side-chains and furnish various aza-sulfuryl amino acid residues **64-67**. The risk of *bis*-alkylation was minimized by employing stoichiometric amounts of base and alkylating reagent. The position of alkylation was ascertained by NMR experiments [91].

The tryptophan hydrazide **71** was prepared by a modification of the above protocol, because the indole group of L-Trp (**68**) was already protected with Boc (Scheme 4.5). After amine acylation with allylchloroformate, the hydrazide was introduced with benzophenone protection (e.g., **70**), which could be orthogonally cleaved using hydroxylamine hydrochloride in pyridine to afford hydrazide **71**. Reaction of hydrazide **71** with sulfamidate **58** gave aza-sulfurylglyciny tripeptide **72**, which was subjected to alkylation using 1-bromo-4-chlorobutane to give chloride **73**, which was displaced with azide ion to provide a protected form of the primary amine.



Scheme 4.5. (i) Alloc-Cl (1.5 equiv), 1M NaOH, 3.5 h; (ii) 1. IBC (1 equiv); 2. NMM (1.3 equiv), 15 min; 3. Benzophenone hydrazone (1 equiv), THF, -15°C , 3 h; (iii) NH_2OH hydrochloride (5 equiv), pyridine, 60°C , overnight; (iv) Net_3 (1.1 equiv), MeCN, μW , 60°C , 2.5 h; (v) 1-bromo-4-chlorobutane (1.2 equiv), BTPP (1.2 equiv), THF, 0°C , 4.5 h; (vi) NaN_3 (3 equiv), DMF, 60°C , overnight.

Orthogonally protected building blocks **64-67** and **74** (Figure 4.1) were thus synthesized and introduced into N-aminosulfamide peptide sequences of U-II(4-11) on solid phase.

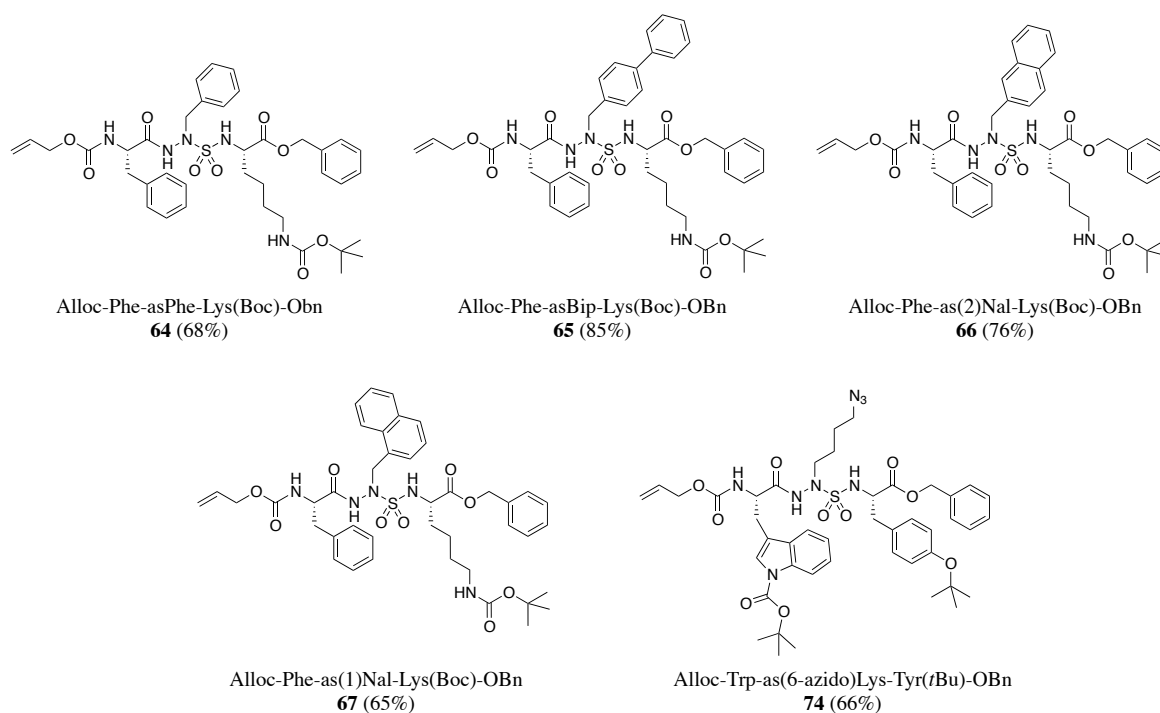
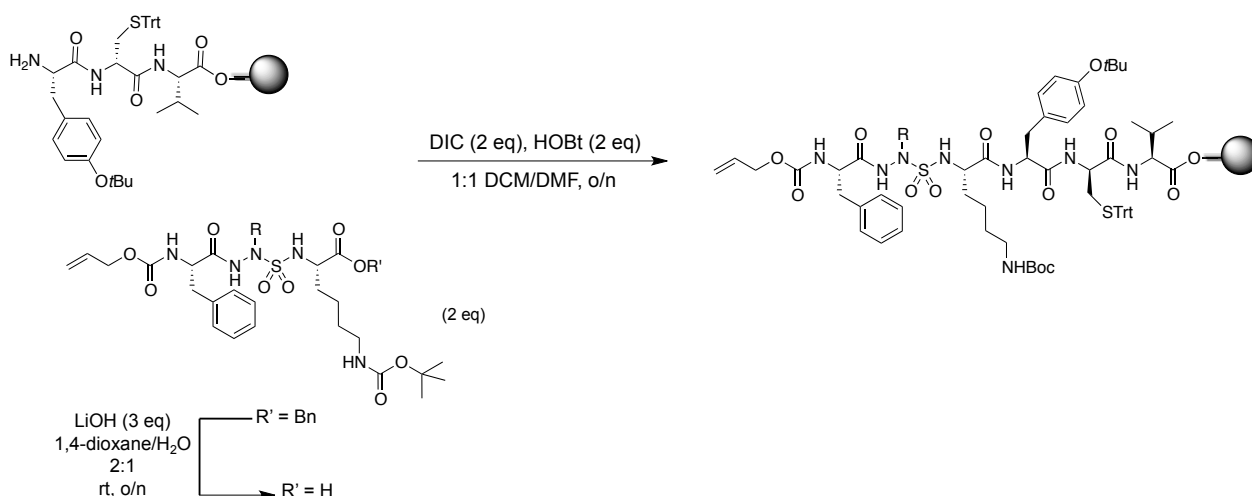


Figure 4.1. Aza-sulfurylglycinyl tripeptides **64-67** and **74** with their corresponding yields from chemoselective alkylation.

4.4 Aza-sulfuryl peptide synthesis

Aza-sulfuryl peptides were synthesized on 2-chlorotrityl chloride resin using a Fmoc/*t*Bu protocol. The resin was swollen in DCM for 30 min, agitated on a shaker with the first amino acid (1 equiv) and DIEA (1 equiv) at rt for 10 min, treated with additional DIEA (1.5 equiv), and shaken for 1 h. The loaded resin was washed with DCM (2 mL x 3) and DMF (2 mL x 3). Fmoc deprotection was performed using a 20% solution of piperidine in DMF (5 min x 1, 25 min x 1). Couplings of Fmoc amino acids (3 equiv) were performed according to general solid-phase peptide synthesis protocols using HBTU (3 equiv) and HOBt (3 equiv) as coupling reagents and DIEA (6 equiv) as base in DCM/DMF 1:1 at rt for 2 h. The resin was washed after each coupling and deprotection step with DMF (2 mL x 3) and DCM (2 mL x 3). Incorporation of the aza-sulfuryl tripeptide (1.5 equiv) into the peptide sequence was achieved using DIC (1.5 equiv) and HOBt (1.5 equiv) at rt overnight (Scheme 4.6). Complete coupling

was confirmed by LC-MS analysis of the residue from cleavage of an aliquot of resin (5 mg) by treatment with a cocktail of 45:40:2.5:2.5 TFA/DCM/TIS/H₂O at rt for 1.5 h.



Scheme 4.6. The aza-sulfuryl tripeptide building block benzyl ester was first hydrolyzed with LiOH then coupled to the primary amine of the peptide sequence on solid support.

Alloc protected aza-sulfuryl peptide resin was washed with DCM (2 ml x 3), treated with a solution of Pd(PPh₃)₄ (0.15 equiv) and NDMBA (7 equiv) in dry DCM/DMF 3:2 and agitated gently for 2 h under argon. The resin was filtered, washed with DMF (2 mL x 3), and DCM (2 mL x 3), and the deprotection procedure was repeated. The resin was filtered, washed with DMF (2 mL x 3), 0.5% solution of sodium diethylthiocarbamate in DMF (30 min x 2) and DCM (2 mL x 3). Complete removal of the Alloc group was evaluated by LC-MS of the residue from cleavage of an aliquot of resin. The peptide sequence was then completed using standard protocols. As described above, the final Fmoc group was removed, the trityl side chain protection was removed, the disulphide bridge formed and the peptide was cleaved from the solid support by treating the resin with a solution of TFA/DMSO/anisole (89:10:1, v/v/v) at rt for 3h. The resin was filtered, and washed with small amount of TFA. Evaporation of the volatiles from the combined filtrate and washings resulted in a residue which was precipitated in diethyl ether, chilled in an ice bath and centrifugated to yield a pellet which was separated

by decantation of the solution, dissolved in water, freeze-dried, and purified by HPLC to yield peptides **75-78** as white powders (Figure 4.2).

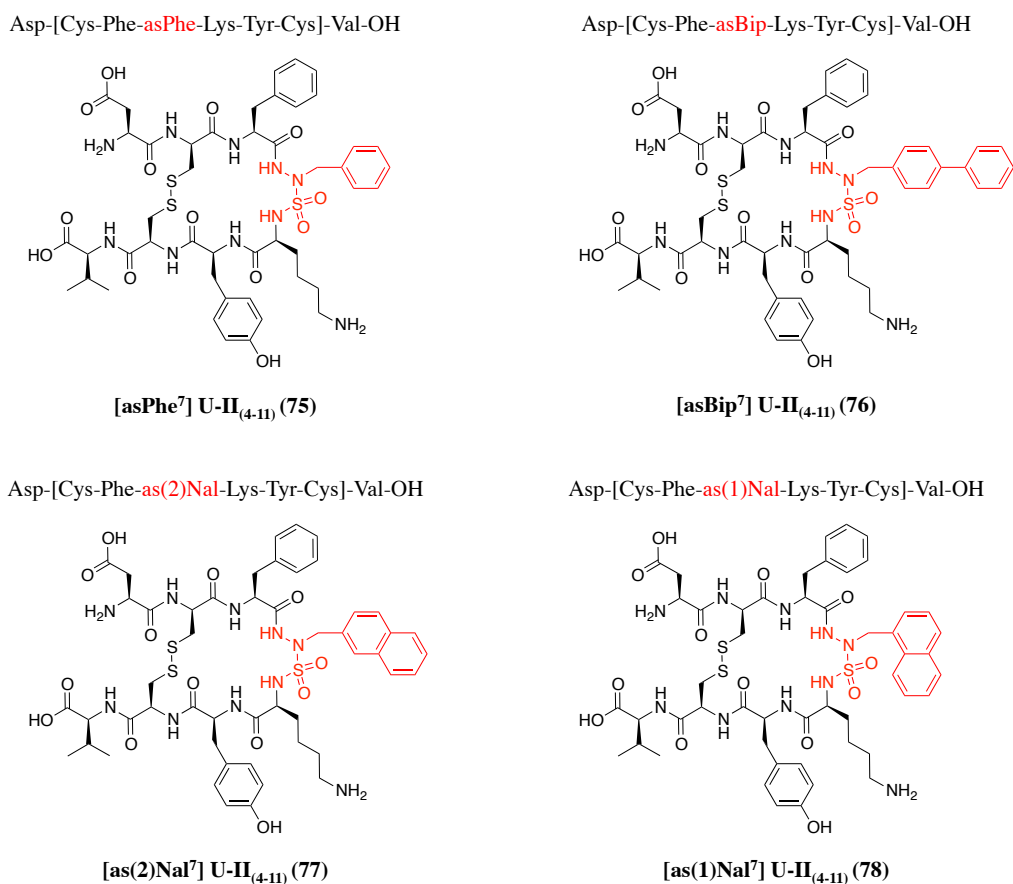


Figure 4.2. Aza-sulfuryl peptides **75-78**.

4.5 Analysis and purification of aza-sulfuryl peptides

Analytical LC-MS analyses were performed on a Gemini reverse-phase column from Phenomenex (4.6 mm x 150 mm, 5 μ m, C₁₈) or a SunFire™ reverse-phase column from Waters (2.1 mm x 50 mm, 3.5 μ m, C₁₈) with a flow rate of 0.5 mL/min using a gradient of acetonitrile (0.1% formic acid) or methanol (0.1% formic acid) in water (0.1% formic acid). Purification of aza-sulfuryl peptides was performed on a preparative column (Gemini C₁₈ column, 21.2 mm x 250 mm, particle size 5 μ m) using specified linear gradients of acetonitrile (0.1% formic acid) in water (0.1% formic acid) with a flow rate of 10.6 mL/min and UV detection at 214 nm and 254 nm.

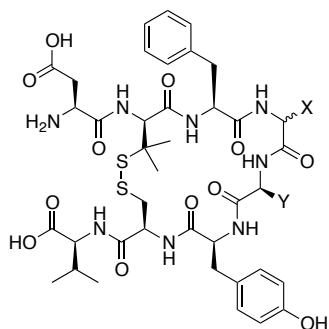
The purity of aza-sulfuryl peptides was ascertained using analytical HPLC performed on a Gemini reverse-phase column from Phenomenex (4.6 mm x 150 mm, 5 μ m, C₁₈) or a SunFireTM reverse-phase column from Waters (2.1 mm x 50 mm, 3.5 μ m, C₁₈) with a flow rate of 0.5 mL/min using gradients of acetonitrile (0.1% formic acid) or methanol (0.1% formic acid) in water (0.1% formic acid). Aza-sulfuryl peptides examined for biological activity were purified to >99%.

5 Results and Discussion

5.1 Trp-constrained analogues: results and discussion

5.1.1 Biological data

Receptor affinity at human UT receptor and biological activity (rat aorta bioassay) of the synthesized compounds are reported in Table 5.1. In the same table, P5U and Urantide activities are reported for comparison. From the data, it can be inferred that peptides **1** and **2**, carrying the Lys⁸ residue, show an agonist activity as the lead compound P5U. Compared with P5U, about 1.5 log reduction of the affinity and 2 log reduction of the activity, respectively, can be observed. Conversely, peptides **3** and **4**, carrying the Orn⁸ residue, show an antagonist activity as Urantide, resulting in 1.8 log reduction of the affinity and 2 log reduction of the activity, respectively, when compared with the urantide. Finally, the effect of the L-Tpi versus D-Tpi replacement is almost negligible both in the affinity and in the activity values (Table 5.1).



Peptide	Xaa	Yaa	pEC ₅₀	pK _B	PK _i
P5U	Trp	Lys	9.6±0.07	-	9.7±0.07
Urantide	DTrp	Orn	IN	8.3±0.09	8.3±0.04
1	Tpi	Lys	7.92±0.07	-	8.16±0.05
2	DTpi	Lys	7.68±0.07	-	8.26±0.04
3	Tpi	Orn	IN	6.30	7.61±0.04
4	DTpi	Orn	IN	6.28	7.43±0.12

Table 5.1. Receptor affinity and biological activity of P5U and urantide analogues of general formula: H-Asp-c[Pen-Phe-Xaa-Yaa-Tyr-Cys]-Val-OH. Each value in the table means \pm standard error of at least four determinations.

^apK_i: $-\log K_i$ affinity values are from [¹²⁵I]Urotensin-II binding inhibition experiments at the human uterotensin receptor.

^bpEC₅₀: $-\log EC_{50}$ and

^cpK_B ($-\log K_B$) values are from experiments in the rat thoracic aorta.

5.1.2 NMR analysis

NMR experiments were performed in collaboration with the group of Prof. Carotenuto in order to analyze conformational aspects referred to peptides **2** and **4**, which differ only for the Lys to Orn residue at position 8, although they showed different activity (agonist vs antagonist, respectively). A whole set of 1D and 2D NMR spectra in 200 mM aqueous solution of SDS were collected for compounds **2** and **4**.

Micelle solution was employed because we have reported the NMR structure of UT agonists (among which P5U) [66] and antagonist (among which Urantide) [41] in this *medium*. Complete ^1H NMR chemical shift assignments were effectively achieved for the two peptides according to the Wüthrich procedure [92] via the usual systematic application of DQF-COSY [93], TOCSY [94], and NOESY [95] experiments with the support of the XEASY software package [96]. Peptides **2** and **4** differ from P5U and urantide, respectively, only for the Trp⁷ to D-Tpi residue substitution, but they show NMR parameters different from those observed in the parent peptides.

NMR-derived constraints obtained for the analyzed peptides were used as the input data for a simulated annealing structure calculation. For each peptide, 20 calculated structures satisfying the NMR-derived constraints (violations smaller than 0.40 Å) were chosen (Figure 5.1).

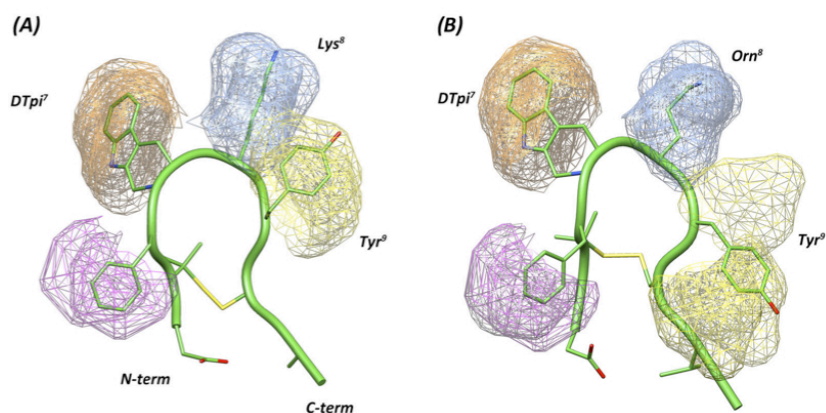


Figure 5.1. Lowest energy conformers of compound **2** (A) and compound **4** (B). Backbone is evidenced as a ribbon. Side chains of the 10 lowest energy conformers are also shown as mesh surface.

Both peptides **2** and **4** show a distorted type II' β -turn structure encompassing residues 6–9. In contrast, the N-terminal and C-terminal residues were more flexible. Considering the side chains orientation, Lys⁸ and Tyr⁹ side chains showed a large preference for g^- rotamer in peptide **2**; Orn⁸ shows also a g^- orientation in peptide **4**, whereas Tyr⁹ side chain is found both in *trans* and g^- conformations in this peptide. Therefore, Tyr⁹ phenolic ring is close to Lys⁸ in peptide **2**, and it points toward Val¹¹ in peptide **4**.

5.1.3 Discussion

In previous studies, it has been demonstrated that *hU*-II analogues, which retain high affinity for UT receptor, all possess a type II' β -hairpin backbone conformation regardless their agonist or antagonist activity, indicating that such backbone conformation is necessary for the UT recognition [41,66]. The main conformational difference observed in the structures of the antagonists and the agonists was established in different orientation of the (D/L)-Trp⁷ side chain. In particular, whereas in the agonists, the (D/L)-Trp⁷ indole moiety were found close to the Lys/Orn⁸ side chain, in the antagonists, (D/L)-Trp⁷ side chain were more flexible and further from the Lys/Orn⁸ side chain. To corroborate that hypothesis, the Trp⁷ residue was replaced with a highly constrained Trp analogue, the Tpi residue. In fact, Tpi can only possess either gauche (+) or gauche (–) side chain rotamer populations because the indole moiety is cyclized to the peptide backbone N ^{α} [65]. According to the pharmacophore model [41,66], this indole orientation should be only compatible with the antagonist conformation because the Tpi⁷ indole moiety is kept far from the Lys⁸ side chain. Moreover, both L-Tpi and D-Tpi were used because L-Trp and D-Trp residues are both compatible with UT receptor binding mode. Finally, Lys/Orn switch was shown to modulate the urotensin analogues activity because the Orn residue promotes the antagonist activity. Hence, four analogues (**1-4**) were designed as reported in Table 5.1. Biological data showed that Lys⁸ containing peptides (**1** and

2) are agonists, and peptides carrying the Orn⁸ (**3** and **4**) are antagonists. All the affinities and activities are reduced of at least one order of magnitude. Furthermore, L-Tpi versus D-Tpi replacement is almost negligible both in the affinity and activity values. The agonist activity of peptides **1** and **2** is quite unexpected because in our model, D-Tpi side chain orientation should be compatible only with an antagonist activity. Trying to understand this apparent contradiction, a conformational analysis was performed for selected peptides by solution NMR. Peptides **2** and **4**, which chemically differ only for the Lys to Orn substitution, were chosen but the activity switches from agonist to antagonist. NMR study was performed in SDS micelle solution. The use of SDS micelles to study the conformational properties of *hU*-II analogues is motivated on the basis of their interaction with a membrane receptor. For peptides acting as ligands of membrane receptors (such as G-protein-coupled receptor), the use of membrane mimetic media is suggested, hypothesizing a membrane-assisted mechanism of interactions between the peptides and their receptors [97]. According to this model, the membrane surface plays a key role in facilitating the transition of the peptide from a random coil conformation adopted in the extracellular environment to a conformation that is recognized by the receptor. The increase of the local concentration of the peptide and the reduction of the rotational and translational freedom of the neuropeptide are membrane-mediated events acting as determinant steps for the conformational transition of the peptide [98]. Indeed, micelle solutions are largely used for the conformation analysis of peptide hormones [99]. In this context, the correlation between the SDS-bound conformation of *hU*-II analogues and their biological activity succeeded [41,66,69]. Conformational analysis indicated that both the peptides **2** and **4** show a distorted type II' β -turn structure encompassing residues 6–9. Therefore, the turn structure peculiar of the active peptides P5U and urantide is kept in these derivatives. In contrast, the N-terminal and C-terminal residues of peptides **2** and **4** are highly flexible losing the short antiparallel β -sheet found in P5U and urantide. Considering the side chains orientation of pharmacophoric residues (i.e. D-Tpi⁷,

Lys⁸, and Tyr⁹) [33,34] of peptide **2**, side chains of Lys⁸ and Tyr⁹ show a large preference for *g*⁻ rotamer, hence they are spatially close, whereas indole ring of D-Tpi⁷ is locked to a *g*⁻ conformation. According to the design, the distance between D-Tpi⁷ and Lys⁸ is greater than that observed in P5U. Notably, this distance is shorter than that observed in urantide. Unexpected residual agonist activity of peptide **2** indicates that its pharmacophoric distances still fit the agonist model although not in an ideal way. Considering peptide **4**, it was designed to fulfil the antagonist pharmacophore of UT receptor blocking the side chain of Trp⁷. The distance between D-Tpi⁷ and Orn⁸ is shorter than that observed in the reference antagonist urantide and is similar to the distance observed in peptide **2**. Since these peptides are endowed with opposite activities, the distance between the positively charged nitrogen and the indole ring seems to be not relevant for the agonist/antagonist activity switching. Moreover, Tyr⁹ side chain is preferentially *trans* orientated, and consequently, phenol ring is far from Orn⁸, and the relevant pharmacophoric distance does not fit that of urantide. Tyr⁹ side chain orientation is mainly defined by an intense NOE with Val¹¹ methyl groups. To note, this NOE could not be observed in the NOESY spectrum of urantide because of signal overlapping [41]. Hence, the correct orientation of Tyr⁹ for antagonist/UT receptor interaction needs to be further investigated. Studies on urantide analogues containing tyrosine-constrained derivatives are currently in progress.

5.2 Tyr⁹-modified series

5.2.1 Biological data

Sequences, receptor binding affinity at *h*UT and biological activity (rat aorta bioassay) of the designed compounds are reported in Table 5.2. As above described, to evaluate the suitable features of the aromatic residue in position 9 and, in particular, the contribution of the phenolic group, we replaced Tyr⁹ with several aromatic uncoded amino acids, in both sequences of P5U and urantide (compounds **5-28**).

Peptide	Xaa	Yaa	R	pK _i ^b	pEC ₅₀ ^c	E _{max} ^d	pK _B ^e
<i>hU</i> -II ^f	Trp	Lys	Tyr	9.10 ±0.08	8.50±0.06	100	-
<i>hU</i> -II(4-11)	Trp	Lys	Tyr	9.60±0.07	8.437	100	-
P5U	Trp	Lys	Tyr	9.70±0.070	9.36±0.20 [§]	95±7	-
Urantide	DTrp	Orn	Tyr	8.30±0.04	-	-	8.32±0.10
5	Trp	Lys	(2')Nal	8.70±0.08	9.14±0.06 [§]	85±16	-
6	DTrp	Orn	(2')Nal	9.14±0.08	8.42±0.17	13±5 [†]	-
7	Trp	Lys	(1')Nal	9.40±0.07	8.30±0.20 [¥]	86±5	-
8	DTrp	Orn	(1')Nal	8.19±0.14	7.74±0.10 [§]	37±9 [†]	-
9	Trp	Lys	Btz	8.76±0.11	10.71±0.04 ^{¥, §}	89±16	-
10	DTrp	Orn	Btz	7.89±0.13	7.47±0.11 [§]	57±2 [†]	-
11	Trp	Lys	(pCl)Phe	8.91±0.07	9.09±0.12 [§]	85±10	-
12	DTrp	Orn	(pCl)Phe	8.98±0.05	8.57±0.18	13±3 [†]	-
13	Trp	Lys	(3,4-Cl)Phe	9.11±0.06	10.91±0.14 ^{¥, §}	102±8	-
14	DTrp	Orn	(3,4-Cl)Phe	8.65±0.09	7.89±0.17 [§]	26±7 [†]	-
15	Trp	Lys	(pCN)Phe	8.74±0.10	8.97±0.15	79±1 [†]	-
16	DTrp	Orn	(pCN)Phe	7.92±0.07	-	0.0	8.15±0.05
17	Trp	Lys	(pNO ₂)Phe	8.75±0.05	9.20±0.08 [§]	95±20	-
18	DTrp	Orn	(pNO ₂)Phe	7.77±0.08	-	0.0	8.12±0.07
19	Trp	Lys	(pNH ₂)Phe	8.57±0.08	10.040	83±10	-
20	DTrp	Orn	(pNH ₂)Phe	7.87±0.01	-	0.0	7.86
21	Trp	Lys	Cha	6.59±0.11	5.782	76±12	-
22	DTrp	Orn	Cha	7.73±0.08	8.769	79±9	-
23	Trp	Lys	Phg	7.01±0.09	6.161	68±6	-
24	DTrp	Orn	Phg	7.15±0.10	7.527	76±6	-
25	Trp	Lys	Tic	6.34±0.07	6.286	27±6	-
26	DTrp	Orn	Tic	6.05±0.08	6.698	12±5	-
27	Trp	Lys	Aic	5.62±0.06	6.234	68±15	-
28	DTrp	Orn	Aic	5.62±0.05	6.036	89±6	-

Table 5.2. Receptor affinity and biological activity of P5U and urantide analogues of geneal formula: H-Asp-c[Pen^a-Phe-Xaa-Yaa-R-Cys]-Val-OH. ^aCys in *hU*-II and *hU*-II(4-11); ^bpK_i: -log K_i; ^cpEC₅₀: -log EC₅₀; ^dpercent versus *hU*-II; ^epK_B: log(CR-1)-log[B]. Each value in the table is mean ± S.E.M. of at least 3-4 determinations. ^fFor *hU*-II, N-terminus = H-Glu-Thr-Pro-Asp. [†]p<0.05 vs. *hU*-II E_{max} (Two-tail Student's *t*-test for paired data). [¥]p<0.05 vs. P5U (ANOVA and Dunnett's post hoc test). [§]p<0.05 vs. *hU*-II (Two-tail Student's *t*-test for paired data).

First of all, we used amino acids with a bulkier aromatic group, that is, (1')Nal, (2')Nal and Btz. The substitution of the native Tyr⁹ residue in P5U by a (2')Nal residue (compound **5**), generated an analogue of similar contractile potency ($pEC_{50}=9.14\pm0.06$) and a reduced binding affinity of about 1 log unit ($pK_i=8.70\pm0.08$). Similar modification in urantide sequence produced compound **6** with improved binding affinity when compared to urantide ($pK_i=9.14\pm0.08$). Anyway, this compound retains a small residual agonist activity ($E_{max}=13\pm5\%$). Compound **7** [(1')Nal/Tyr replacement in P5U] proved an agonist less potent than P5U ($pEC_{50}=8.30\pm0.20$, $E_{max}=86\pm5\%$) although it shows a good receptor affinity ($pK_i=9.40$). The same substitution in urantide sequence, compound **8**, generated a partial agonist ($pEC_{50}=7.74\pm0.10$, $E_{max}=37\pm9\%$). Then, in compound **9**, we replaced Tyr⁹ with a residue of benzothiazolylalanine (Btz), that is, an analogue of Trp in which the indole group is replaced by a benzothiazolyl moiety which is a highly electron-rich system. Compound **9**, showed to be significantly ($p<0.05$) more potent agonist compared to P5U ($pEC_{50}=10.71\pm0.04$, $E_{max}=89\pm16\%$). In parallel, compound **10** (Btz⁹ derivative of urantide) showed an increased partial agonist activity ($E_{max}=57\pm2\%$) compared to analogues **6** and **8**.

Then, Tyr⁹ residue was replaced with some aromatic amino acids containing an isoster of phenolic group in *para* position. Replacing the Tyr⁹ residue in P5U with the amino acid (pCl)Phe led to a compound with similar activity to the parent peptide. In fact, compound **11** resulted to have a comparable potency in functional assay ($pEC_{50}=9.09\pm0.12$, $E_{max}=85\pm10\%$) albeit with a slight reduction in binding affinity at UT receptor ($pK_i=8.91\pm0.07$). Instead, compound **12** resulted in a weak partial agonist ($E_{max}=13\pm3\%$) with an improved binding affinity profile ($pK_i=8.98\pm0.05$).

Interestingly, replacing the Tyr⁹ residue with the amino acid (3,4-Cl)Phe generated the compound **13** with a high agonist activity ($pEC_{50}=10.91\pm0.14$, $p<0.05$ compared to P5U; $E_{max}=102\pm8\%$) resulting a superagonist. In fact, this compound is about 1.6 log more potent than P5U and represents the most potent peptide agonist at UT receptor discovered to date.

Compound **14**, (3,4-Cl)Phe⁹ derivative of urantide, similarly to compound **12** resulted in a partial agonist with increased efficacy compared to the last ($E_{\max}=26\pm7\%$ vs $13\pm3\%$).

Phenolic -OH group was then replaced by electron withdrawing groups in compounds **15-18**.

Compound **15**, in which Tyr⁹ was replaced with a (pCN)Phe residue resulted to be less potent as agonist compared to P5U ($pEC_{50}=8.97$, $E_{\max}=79\pm1\%$) and with a reduced binding affinity ($pK_i=8.74\pm0.10$). Interestingly, compound **16**, (pCN)Phe⁹ derivative of Urantide, showed a behaviour as an antagonist producing a parallel rightward shift of the agonist response curves without depressing the agonist E_{\max} . Schild-plot analysis was consistent with competitive antagonism and a pK_B value of 8.15 ± 0.05 was calculated comparable to that of urantide [68]. Finally, replacing the Tyr⁹ residue with the amino acid (pNO₂)Phe, led to compounds with similar activity compared to the respective parent peptides. In fact, compound **17** was shown to have agonist activity comparable to P5U ($pK_i=8.75\pm0.05$, $pEC_{50}=9.20\pm0.08$, $E_{\max}=95\pm20\%$) and compound **18** showed behaviour as an antagonist comparable to urantide producing a parallel rightward shift of the agonist response curves. Also for this compound Schild-plot analysis was consistent with competitive antagonism and a pK_B value of 8.12 ± 0.07 was calculated [68].

In compounds **19-20**, where the OH group was replaced with a primary amine group, showed interesting results. In fact, the compound **19**, analogue of P5U, showed moderate affinity for UT receptor (pK_i 8.57 ± 0.08 ; around 1 log less than that compared to the parent compound, pK_i 9.70 ± 0.07) and pEC_{50} value ($pEC_{50}=10.04$ compared to 9.34 of P5U) resulting a potent agonist. In contrast, same modification in urantide sequence led to discover to a potent antagonist although less potent when compared to the urantide ($pK_B=7.86$). The replacement with non-aromatic residue of Cha in the same position, compound **21** and **22**, has allowed to get two partial agonist analogues ($pEC_{50}=5.78$, $E_{\max}=76\pm12\%$ for compound **21**; and $pEC_{50}=8.77$, $E_{\max}=79\pm9$ for compound **22**), although compound **22** exhibited higher affinity in binding experiments ($pK_i=7.73\pm0.08$). The Phg residue in compounds **23-24** have proved to

be important in understanding the importance of the distance between peptide backbone and aromatic residue in position 9; indeed, a weak partial agonism is preserved only in compound **24** ($pEC_{50}=7.53$, $E_{max}=76\pm6\%$), albeit with less binding affinity ($pK_i=7.15\pm0.10$) compared to urantide ($pK_i=8.30\pm0.04$). Uncoded amino acids such as Tic and Aic were used to fix the position of aromatic residue and reduce conformation flexibility in specific position of cyclic portion of P5U and urantide. All analogues showed weak binding at UT receptor, at least 2 log less than parent peptides. In this last series only compound **28**, with Aic residue in replacement of Tyr in urantide sequence, is able to induce significant activity ($pEC_{50}=6.04$, $E_{max}=89\pm6\%$) but low affinity ($pK_i=5.62\pm0.05$).

5.2.2 Peptide stability

To investigate the effects of the modifications of peptides on proteolytic susceptibility, the disappearance of the intact peptides incubated in diluted serum at 37 °C was followed by RP-HPLC [100]; peptides *hU-II*(4-11), Urantide, **13**, and **16** were assayed (Figure 5.2).

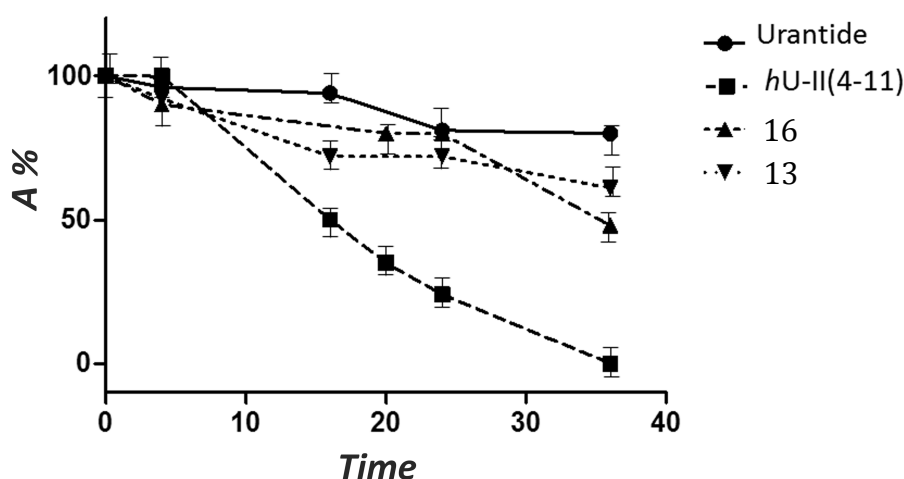


Figure 5.2. The resistance to enzyme degradation of *hU-II*(4-11), Urantide, **13** and **16** was assessed by incubation in 25% FCS for 36 h. Residual peptide quantity, expressed as the percentage of the initial amount versus time (h), was plotted. The results represent the average of three independent experiments.

Overall results, shown in Figure 5.2, display the course of degradation up to 36 h to highlight the differences in the profiles of the degraded peptides. After 16 h of treatment, *hU*-II(4-11) had a residual concentration lower than 50%, while for other compounds it is higher than 70% of the initial concentration. After 36 h, Urantide, compounds **13**, and **16** showed a residual concentration higher than 50%. Clearly, developed peptides are very stable in 25% FCS.

5.2.3 NMR analysis

NMR experiments were performed in collaboration with the group of Prof. Carotenuto. A whole set of 1D and 2D NMR spectra in 200 mM aqueous solution of SDS were collected for compounds **13**, and **16**. These peptides were chosen since **13** behaves as a superagonist compared to P5U while **16** is a potent antagonist devoid of agonist activity. SDS micelle solutions were used since they are membrane mimetic environments and are largely used for conformational studies of peptide hormones and antimicrobial peptides [99].

Complete ^1H NMR chemical shift assignments were effectively achieved for the two peptides according to the Wüthrich [92] procedure via the usual systematic application of DQF-COSY [93], TOCSY [94], and NOESY [95] experiments with the support of the XEASY software package [96]. Peptide **13** differs from P5U only for the (3,4-Cl)Phe/Tyr⁹ substitution and peptide **16** differs from Urantide only for the (pCN)Phe/Tyr⁹ substitution.

All the data obtained from NMR experiments indicated the preservation, in **13** and **16**, of the β -hairpin structure.

NMR-derived constraints obtained for the analyzed peptides were used as the input data for a simulated annealing structure calculation. For each peptide, 20 calculated structures satisfying the NMR-derived constraints (violations smaller than 0.20 Å) were chosen (Figure 5.3).

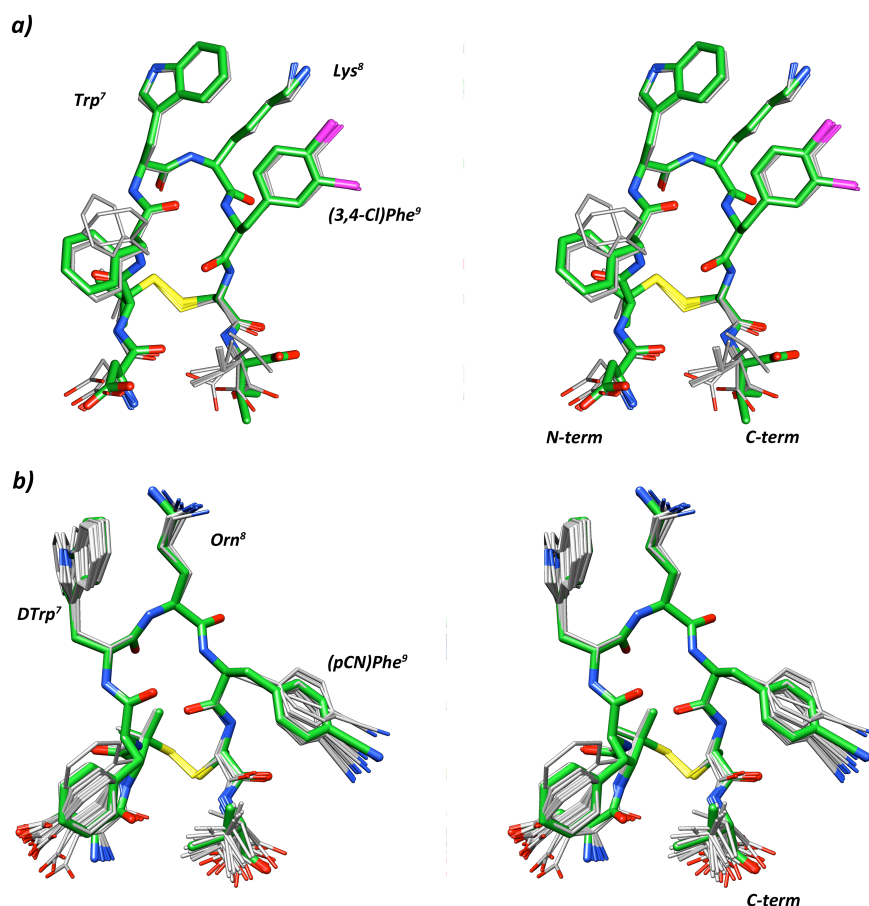


Figure 5.3. Stereoview of the superposition of the 10 lowest energy conformers of **13** (a), **16** (b). Structures were superimposed using the backbone heavy atoms of residues 5-10. Heavy atoms are shown with different colours (carbon, green; nitrogen, blue; oxygen, red; sulfur, yellow; chlorine, magenta). Hydrogen atoms are not shown for clarity.

As shown, both the peptides **13**, and **16** show a well defined type II' β -hairpin structure encompassing residue 5-10. In contrast, the N- and C-terminal residues were more flexible.

Considering the side chains orientation, Phe⁶, D-Trp⁷, and Orn⁸ χ_1 angles showed a large preference for *trans*, *trans*, and *g⁻* rotamers, respectively. In Urantide, dihedral angle χ_2 of

DTrp⁷ was about 125° or -70°. Finally, side chain of residue 9 is found preferentially in *g*⁻ and in *trans* orientation in peptide **13** and **16**, respectively.

5.2.4 Discussion

As part of the ongoing efforts in improving the potency and stability of urotensin analogues and in elucidating the knowledge about their SARs, a series of analogues of P5U and Urantide in which the Tyr⁹ residue was replaced with aromatic non-coded amino acids have been designed and synthesized. Tyr⁹ belongs to the Trp-Lys-Tyr pharmacophoric sequence of U-II, crucial for interaction with its receptor as demonstrated by earlier studies. In fact, the replacement of Trp, Lys, and Tyr cause large changes in biological activity, suggesting the importance of the side chain of these residues for binding and activation of the UT receptor [33,34,101]. In this study the phenol moiety of P5U and Urantide was replaced with bulky electron-rich aromatic moieties in compounds **5-10** or phenyl ring substituted with bulky chlorine atoms (**11-14**). Alternatively, electron donating hydroxyl group of the Tyr⁹ was replaced by withdrawing groups as cyano (**15-16**) or nitro (**17-18**). All synthesized compounds were tested for their binding affinity on *h*UT-transfected CHO cells and for their contractile activity on de-endothelialized rat aortic rings [40]. Overall, bioactivity results indicate that in the P5U derivatives the substitution of Tyr⁹ with other aromatic-based moieties is well tolerated. In fact, all these compounds gave a rat aorta contraction of, at least, 70%. These SARs are in accordance with previous results [33,48], which demonstrated that Tyr⁹ in *h*U-II or *h*U-II(4-11) can be replaced by various aromatic residues preserving most of the agonist activity, at least when the flexibility of Tyr⁹ side chain is kept [102]. The best results in the P5U derivatives were obtained replacing tyrosine with bulky Btz (**9**) or (3,4-Cl)Phe (**13**) residues significantly improving in both cases the potency of more than one log (pEC₅₀=10.71 and 10.91, respectively, p<0.05 vs. P5U) compared to P5U (pEC₅₀=9.36±0.20), and more than two logs compared to the endogenous agonist *h*U-II (pEC₅₀=8.50±0.06). The

peptide **13** is particularly notable as the most potent UT agonist discovered to date. Bulky aromatic amino acids may increase the binding affinity and the biological activity of the U-II agonists through an enhancement of the hydrophobic interactions within a putative Tyr binding pocket of UT.

Considering the Urantide derivatives, SAR studies at position 9 are unprecedented. As for P5U, also Urantide seems to tolerate aromatic substitutions at position 9; in fact, all derivatives bind to UT receptor with $pK_i \geq 7.77$. The main result obtained in this series is the finding of two antagonists (compounds **16**, and **18**). Despite a slight loss of affinity, these compounds behave as pure antagonists in the rat aorta bioassay as the parent Urantide. SAR data clearly indicate that small polar groups (pCN, pNO₂ and the original OH) are requested for pure antagonist activity. In contrast, bulky lipophilic moieties [(1')Nal, (3,4-Cl)Phe, Btz] increase the agonist activity (efficacy) of Urantide derivatives.

As widely discussed elsewhere [41], Urantide behaves as a partial agonist in a calcium mobilization assay performed in CHO cells expressing the *hUT* [102]. The same behaviour was shown by compounds **16** and **18**, i.e. pure antagonist in the aorta assay and partial agonist in a calcium mobilization assay, although with slightly higher efficacy compared to Urantide (Table 5.3).

Peptide	Ca ⁺⁺ efflux efficacy in % ^a	
	1 μ M	10 μ M
Urantide	43.3	46.2
16	61.4	61.7
18	56.5	61.2

Table 5.3. Intracellular calcium efficacy.

^aEfficacy is expressed as % of the maximum response to *hU*-II.

Nevertheless, it is well known that urantide has been used by several groups as reference antagonist compound in studies of the urotensinergic system [103,104]. These novel ligands can be useful to discriminate the partial agonism/antagonism effects at the UT receptor in different cell lines/tissues. Also, the availability of novel agonists and antagonists as pharmacological tools to investigate the urotensinergic system is very important since subtle pharmacokinetic differences can differentiate their effects *in vivo*. In this respect, stability tests were performed on peptide *hU*-II(4-11), urantide and on the novel derivatives **13** and **16**. These studies demonstrated that urantide and peptides **13**, and **16** are highly stable showing a residual concentration higher than 50% in fetal calf serum even after 36 h. The higher level of stability shown by urantide, **13** and **16** compared to *hU*-II may be tentatively ascribed to the presence of a Pen residue, which can hinder the reduction of the disulfide bridge. In contrast, comparing the serum stability of Urantide and peptide **16**, it comes out that aromatic non-coded amino acid (pCN)Phe doesn't improve peptide stability.

A conformational analysis by solution NMR of the most interesting derivatives **13** and **16** was also carried out. In previous works [41,66], it has been showed that *hU*-II analogues, which retain high affinity for UT receptor, all possess a type II' β -hairpin backbone conformation regardless their agonist or antagonist activity, indicating that such backbone conformation is necessary for the UT recognition. Indeed, such backbone conformation is observed also in the novel derivatives confirming the above outcome. The main conformational difference observed in the structures of peptide **9** (agonist activity) and peptide **12** (antagonist activity) is established in a different orientation of the (3,4-Cl)Phe or (pCN)Phe side chain, respectively. In particular, while in the agonist **9** the (3,4-Cl)Phe⁹ residue is close to the Lys⁸ side chain, in the antagonist **12** (pCN)Phe⁹ side chain is close to the Val¹¹ side chain and further from the Orn⁸ side chain. This result is in accordance with that obtained studying constrained analogues of P5U and urantide [64] and with a revision of the conformational preferences of Urantide performed using DPC micelles [105].

Preliminary results obtained for peptides **19-28** proved relevant evidences about replacement of Tyr⁹ residue with other substituents. Compounds **19-20** represented the more interesting in this series as analogues of P5U and urantide. Indeed the primary amino group in *para* position may mimic effects of the original –OH giving compounds, which are closely related to parent peptides. Compound **19** is agonist and compound **20** is a full antagonist toward UT receptor. The only non-aromatic residue Cha in analogues **21-22** does not influence significantly binding and activation and both compounds behave as partial agonist. In compounds **23-24** the distance between C_α and the aromatic ring was reduced, although agonist/antagonist activity is not discriminated and both compounds showed less affinity and partial activity at UT receptor, probably due to the lack of polar groups which may contribute to the interaction with UT receptor. Thus, the only aromatic moiety is not necessary to promise significant activity, even fixed in a specific position as evaluated for peptides **25-28**. These peptides are characterized by weak affinity, losing in great part the biological activity.

5.3 N-methylation: biological data and discussion

The N-methylation as tool to investigate the conformational and biological aspects related to urotensin-II, a series of mono and multiple N-methylated analogues have been synthesized. The amino acids included into the cyclic exapeptide sequence Cys⁵-Cys¹⁰, recognized as the pharmacophoric sequence due to the maintainance of biological activity, have been exchanged in a systematic manner giving mono- and di-methylated peptides **29-53**. Competitive binding assays with the radioligand [¹²⁵I]Urotenisin-II were performed for the peptide series **29-53** (Table 5.4).

Peptide	Sequence	pEC ₅₀	pK _D /pK _i
<i>hU-II(4-11)</i>	H-Asp-c[Cys-Phe-Trp-Lys-Tyr-Cys]-Val-OH	8.20±0.01	8.34±0.04
29	H-Asp-c[(NMe)Cys-Phe-Trp-Lys-Tyr-Cys]-Val-OH	8.26±0.03	8.53±0.08
30	H-Asp-c[Cys-(NMe)Phe-Trp-Lys-Tyr-Cys]-Val-OH	6.36±0.04	6.64±0.10
31	H-Asp-c[Cys-Phe-(NMe)Trp-Lys-Tyr-Cys]-Val-OH	8.50±0.05	8.76±0.07
32	H-Asp-c[Cys-Phe-Trp-(NMe)Lys-Tyr-Cys]-Val-OH	4.91±0.18	=5
33	H-Asp-c[Cys-Phe-Trp-Lys-(NMe)Tyr-Cys]-Val-OH	5.25±0.07	=5
34	H-Asp-c[Cys-Phe-Trp-Lys-Tyr-(NMe)Cys]-Val-OH	8.31±0.08	8.45±0.05
35	H-Asp-c[Pen-Phe-(NMe)DTrp-Orn-Tyr-Cys]-Val-OH	d.n.a.	6.71±0.04
36	H-Asp-c[Pen-Phe-DTrp-(NMe)Orn-Tyr-Cys]-Val-OH	d.n.a.	6.40±0.06
37	H-Asp-c[Pen-Phe-DTrp-Orn-(NMe)Tyr-Cys]-Val-OH	d.n.a.	5.37±0.10
38	H-Asp-c[Cys-Phe-DTrp-Orn-Tyr-(NMe)Cys]-Val-OH	d.n.a.	7.57±0.07

Peptide	Sequence	pK _D /pK _i
<i>hU-II(4-11)</i>	H-Asp-c[Cys-Phe-Trp-Lys-Tyr-Cys]-Val-OH	8.56±0.03
39	H-Asp-c[(NMe)Cys-(NMe)Phe-Trp-Lys-Tyr-Cys]-Val-OH	6.86±0.06
40	H-Asp-c[(NMe)Cys-Phe-(NMe)Trp-Lys-Tyr-Cys]-Val-OH	8.68±0.04
41	H-Asp-c[(NMe)Cys-Phe-Trp-(NMe)Lys-Tyr-Cys]-Val-OH	5.73±0.05
42	H-Asp-c[(NMe)Cys-Phe-Trp-Lys-(NMe)Tyr-Cys]-Val-OH	5.34±0.06
43	H-Asp-c[(NMe)Cys-Phe-Trp-Lys-Tyr-(NMe)Cys]-Val-OH	8.62±0.05
44	H-Asp-c[Cys-(NMe)Phe-(NMe)Trp-Lys-Tyr-Cys]-Val-OH	6.39±0.05
45	H-Asp-c[Cys-(NMe)Phe-Trp-(NMe)Lys-Tyr-Cys]-Val-OH	<5
46	H-Asp-c[Cys-(NMe)Phe-Trp-Lys-(NMe)Tyr-Cys]-Val-OH	5.93±0.06
47	H-Asp-c[Cys-(NMe)Phe-Trp-Lys-Tyr-(NMe)Cys]-Val-OH	7.53±0.06
48	H-Asp-c[Cys-Phe-(NMe)Trp-(NMe)Lys-Tyr-Cys]-Val-OH	6.09±0.06
49	H-Asp-c[Cys-Phe-(NMe)Trp-Lys-(NMe)Tyr-Cys]-Val-OH	6.07±0.28
50	H-Asp-c[Cys-Phe-(NMe)Trp-Lys-Tyr-(NMe)Cys]-Val-OH	8.96±0.04
51	H-Asp-c[Cys-Phe-Trp-(NMe)Lys-(NMe)Tyr-Cys]-Val-OH	<5
52	H-Asp-c[Cys-Phe-Trp-(NMe)Lys-Tyr-(NMe)Cys]-Val-OH	5.82±0.07
53	H-Asp-c[Cys-Phe-Trp-Lys-(NMe)Tyr-(NMe)Cys]-Val-OH	5.85±0.07

Table 5.4. Preliminary results of mono- and multiple-N-methylated derivatives.

pEC₅₀: -log EC₅₀

pK_D: -logK_D

pK_i: -logK_i

d.n.a.: data not available.

All peptides showed binding at the recombinant human UT receptor expressed on membranes obtained from stable CHO-K1 cell line, albeit with various intensity. As for the mono-methylated of U-II(4-11) (peptides **29-34**), they were also tested for their ability to induce efficacious contractions in the rat isolated thoracic aorta (Figure 5.4). In contrast, functional assays for the other compounds are still in progress.

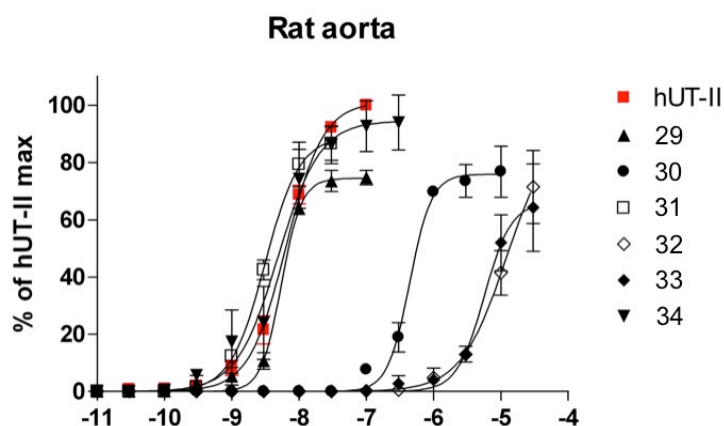


Figure 5.4. Peptides **29-34** were tested for their ability to induce efficacious contractions in the rat isolated thoracic aorta.

In the first series of peptides with the single N-methylation screen in the U-II(4-11) sequence (peptides **29-34**), it is evident that the amide bonds in positions 8 and 9, normally occupied by Lys/Orn and Tyr residues, are less tolerant versus N-methyl groups on the basis of significant decrease of binding affinity and consequently reduction of vasoconstriction on the rat thoracic aorta showed for peptide **32** and **33**. The N-Me-Tyr in position 9 gave the corresponding peptide **33**, which is already reported in literature [102]. In this study different chemical modifications occurred in position 9 of *hU-II* sequence and among these compounds N-methylated derivative is present. Thus, in agreement with Batuwangala *et al.* the single N-methylation in position 9 produced a dramatic reduction of peptide potency. For the rest of the core sequence (peptides **29**, **30**, **31** and **34**), the single N-methylation does not cause any drastic reduction in binding activity, although the conformational constriction induced by the introduction of methyl groups in the positions 5, 7 and 10 led to the more active compounds

of this series due to their ability to preserve the capability in binding and activating toward the UT receptor. In particular, peptide **31** resulted to be even more active compared to the native *h*U-II(4-11), suggesting that Trp⁷ and its side chain orientation are critical into the cyclic portion for binding mode of the peptide. This observation parallels earlier studies that have shown the primary role of Trp in position 7 which contributes significantly to the interaction between U-II/UT receptor, as well as its orientation represents important element for agonism/antagonism discrimination. The N-Me-Phe in compound **30** decreased of about 2 log both binding and efficacy values proving no relevant modification for development of more potent analogues. Also, the N-Me-Tyr in peptide **33** showed negligible potency at the UT receptor, as reported in previous works. Molecular modeling studies and NMR investigations suggested that the NH of Tyr⁹ may be involved in hydrogen bonding with the CO of Trp⁷ stabilizing a preferential conformation centered on the Trp⁷-Cys¹⁰ sequence which could predict similar observations for the other compounds, relevant for U-II activity. The methylation of Tyr⁹ might prevent the formation of such hydrogen bonding and this could be the reason of the reduced activity of this analogue. However, it can't be excluded that the introduction of a methyl group on Tyr⁹ could produce steric hindrance that prevents UT receptor binding.

On the basis of results of mono-methylated derivatives of U-II(4-11) sequence, similar observations have been formulated for mono-methylated urantide analogues, although the series is not complete and further considerations are still under discussion.

The second group of peptides are di-methylated in the exacyclic sequence of U-II(4-11), where each couple of amino acids was replaced with the corresponding N-methylated derivatives in all possible combination giving the peptides **39-53**. Examining effects on binding affinity of combined N-methylated amide bonds, some exciting results were observed. First of all it has been demonstrated that site of N-methylation combined with N-Me-Phe, N-Me-Lys or N-Me-Tyr reduced the binding at UT receptor. Instead, any combination of N-

methylated residues in positions 5, 7 and 10 (peptides **40**, **43** and **50**) led to increase in binding affinity confirming the results from mono-methylation. Indeed, the selective suppression of a proton-donating N-H group due to methyl groups introduction in positions 5, 7 and 10 occurred in both mono- and di-methylated peptides increased binding at UT receptor. According to the continuous research of urotensin analogues with more constrained motif that can stabilize a preferential conformation, the specific N-methylation upon Cys⁵, Trp⁷ and Cys¹⁰ residues may promote a type II' β -hairpin secondary structure possessed by all potent ligands so far described.

Therefore, these two series of compounds gave interesting results, which contribute to structure-activity relationship studies. Alteration of N-H of amide bonds into the peptide sequence of U-II(4-11) influences necessarily the proton-donating capability of specific sites. These effects reflect upon the potential intra- and inter- molecular hydrogen bonds that establish the bioactive conformation and, thus, the interaction with the UT receptor.

The synthesis of a third series of tri-methylated compounds has been postponed. Earlier results about mono- and di-methylated compounds are adequately in agreement each other suggesting selective positions more tolerant to methyl groups accommodation and the preference of one backbone conformation.

5.4 Aza-sulfuryl peptides: biological data

N-aminosulfamide analogues of U-II(4-11) sequence, peptides **75-78**, have been successfully synthesized featuring the synthetic strategy described above. The replacement of conventional peptide amide by aza-sulfuryl amino acid residues led to innovative urotensin analogues. Aza-sulfuryl moiety into a peptide sequence has already reported in literature revealing its capability to mimic tetrahedral transition states common in enzyme-catalyzed reactions. However, conformational features of this motif could be appropriate in stabilizing such secondary structures that improve binding affinity versus G protein-coupled receptors.

Therefore, the peptidomimetics obtained were tested for their ability to displace [125 I]U-II in the binding interaction with the UT receptor and results are shown in Table 5.5.

Compound	Sequence	[]	n	% $hU-II-^{125}I$
75	Asp-c[Cys-Phe- asPhe -Lys-Tyr-Cys]-Val-OH	1E-06	4	64,39
		1E-05	3	52,2
76	Asp-c[Cys-Phe- asBip -Lys-Tyr-Cys]-Val-OH	1E-06	4	76,8
		1E-05	d.n.a.	d.n.a.
77	Asp-c[Cys-Phe- as(2)Nal -Lys-Tyr-Cys]-Val-OH	1E-06	4	73,4
		1E-05	3	46,8
78	Asp-c[Cys-Phe- as(1)Nal -Lys-Tyr-Cys]-Val-OH	1E-06	4	60,8
		1E-05	3	25,7

Table 5.5. Binding affinity at UT receptor for compounds **75-78**.
d.n.a.: data not available.

Binding and functional assays are still in progress, in parallel with the enlargement of aza-sulfuryl peptide library, under the supervision of Prof. Lubell.

An overview of preliminary results for affinity at UT receptor is presented in Table 5.5. In general, peptides **75-78** exhibited weak binding affinity at the UT receptor, with limited capacity to displace iodinated Urotensin-II from the receptor at micromolar concentrations. The different side chains used to mimic the aromatic residue of the triptophan indole group had limited influence on affinity.

In accordance with earlier observations, the development of an aza-sulfuryl amino acid derivative as a replacement of the Trp residue in position 7 led to decreased binding affinity. In the N-methylation studies the suppression of the N-H proton at the same position gave compounds with higher affinity. Indeed, Trp⁷ is crucial for the interaction with receptor

counterpart and, hence, chemical modifications occurred in this position confirmed that the residue is tolerant versus N^ε-methyl group incorporation, whereas the potential for improved hydrogen bonding by the N-aminosulfamide moiety may reduce affinity.

Among this series, compound **78**, characterized by α -naphthyl group in replacement of indole, seems to be the most interesting in terms of affinity probably due to the similar orientation of aromatic residue with the native ligand.

This study is still under progress and proposed considerations recommend deeper investigation by enlargement of peptide library and conformational analysis, which could help to understand the importance of such modification of the urotensin peptide sequence. Preliminary results support the importance of hydrogen bond interactions and conformation for receptor interaction and biological activity. Moreover, the potential agonism/antagonism modulation of urotensin system by chemical modifications such as incorporation of aza-sulfuryl amino acids could contribute to elucidate key elements in the development of further analogues.

5.5 Future perspectives

On the basis of information obtained from N-methylation and N-aminosulfamide studies, it's evident that we need to perform a deep and detailed analysis to have a complete view about the effects induced by these modifications upon the U-II sequence. The congruence between partial results obtained for N-methylated and N-aminosulfamide derivatives described above gives way to examine in depth the apparent correlation for hydrogen-bonding modulation in specific positions of Urotensin-II sequence. Indeed, suppression of N-H proton-donating effects by alkylation with methyl group influence positively the interaction with the UT receptor when it occurs in Trp position. In contrast, improvement of hydrogen-bond interactions due to N-aminosulfamide residue in the same position led to opposite observations.

In light of the properties of aza-sulfonamido moieties, and their related possibility to facilitate inter- and intra-molecular hydrogen bonds, it could be intriguing a three-dimensional structural analysis by NMR, as well as for more interesting N-methylated compounds. It's well established that the conformation play a key role in determining biological activity since all Urotensin-II analogues possess a type II' β -hairpin secondary structure such as P5U and urantide.

For this reason, further perspectives are currently under investigation in order to accomplish structure-activity relationships study related to these new urotensin analogues and their impact in the urotensinergetic system.

6 Conclusions

In summary, new Urotensin-II analogues have been designed and developed by application of synthetic strategies available to modify peptide properties, such as incorporation of non-natural amino acids and modification of peptide bonds.

Using Trp-constrained analogues of P5U and urantide, new insight on the binding mode of agonists and antagonists at the UT receptor has been defined. In particular, Lys⁸/Orn⁸ replacement proved a key substitution for the agonist to antagonist switching. Conformationally, a type II' β -turn structure encompassing residues 6–9 was confirmed as structural element of active compounds. Considering the three-point pharmacophore model, the distance between the positively charged nitrogen and the indole ring seems to be not relevant for the agonist/antagonist activity switching. In contrast, a different orientation of the side chain of Tyr⁹ present in the analogues investigated in this study could be a factor that plays a crucial role in agonist/antagonist activity. In particular, the long distance between the phenol ring and the Orn⁸ nitrogen atom, observed in the antagonist peptide **4**, is unprecedented in earlier studies. This result needed to be examined by further studies by synthesizing additional and appropriate analogues modified in position 9. For this reason, analogues of P5U and Urantide modified at Tyr⁹ position were developed. Two of them (**9** and **13**) showed increased potency compared to the parent peptide P5U, the last being the most potent UT peptide agonist discovered to date. Two Urantide analogues (**16** and **18**) turned out to be pure antagonists in the rat aorta bioassay likewise parent urantide. Compounds **13** and **16** showed also a good stability in serum proteolytic assay, suggesting that these peptides may be stable enough to give them an additional opportunity in drug delivery. Furthermore, these novel analogues allowed improving the knowledge on structure- and conformation-activity relationships on UT receptor ligands, which can help in the design of improved compounds.

Ultimately, these novel ligands, notably the superagonist **13**, the most potent agonist discovered to date, could be useful pharmacological tools for *in vitro* and particularly *in vivo*

studies aimed at clarifying the role played by the U-II/UT system in patho-physiological conditions.

Alternatively, N-methylation studies were used to change pharmacological properties of peptides. Introduction of a methyl group on N α of amide bonds surely has an important impact on the secondary structure influencing interaction with UT receptor. Mono and multiple N-methylated analogues of U-II(4-11) and urantide, peptides **29-53**, were achieved by synthetic strategy compatible with solid support. On the basis of first mono-methylated series of peptides **29-38**, it is evident that single N-methylation occurred in Lys⁸ and Tyr⁹ positions reduces binding affinity and consequently reduction of vasoconstriction on the rat thoracic aorta. In contrast, for remaining amino acids of the core sequence, N-methylation does not cause any drastic reduction in binding activity, in fact the introduction of methyl groups in the positions 5, 7 and 10 led to the more active compounds of this series. In particular, the N-Me-Trp led to peptide **31**, which resulted to be even more active compared to the native *h*U-II(4-11), suggesting its primary role into the cyclic portion for U-II/UT receptor interaction.

Multiple N-methylation of U-II(4-11) sequence led to derivatives in which the affinity for UT receptor is mostly retained. According to observations formulated for the mono-methylated series, it has been demonstrated that site of N-methylation combined with N-Me-Phe, N-Me-Lys or N-Me-Tyr reduced the binding at UT receptor; instead, any combination of N-methylated amide bonds between residues in positions 5, 7 and 10 (peptides **40**, **43** and **50**) led to increase in binding affinity. Indeed, it has been demonstrated that specific site for N-methylation may influence binding affinity versus the UT receptor generating compounds more potent and stable due to favourable pharmacokinetic properties of N-methylated derivatives. Additionally, the conformational alteration produced by methyl groups might promote a type II' β -hairpin secondary structure, possessed by all potent Urotensin-II analogues such as P5U and urantide.

As for the aza-sulfuryl peptides, the study can't be completely evaluated since poor information about binding and functional assays doesn't allow expressing critical examinations. The aza-sulfonamide residue has been inserted into the U-II(4-11) sequence to evaluate the effects generated by this structural modification on the conformation and hydrogen bonding capability. In particular, new N-aminosulfamide analogues have been developed by the replacement of Trp⁷ with the aza-sulfuryl amino acids carrying side chains mimics of the native indole moiety.

Thus, based on the preliminary information in hand, a hypothesis has been formulated to explain the trend of N-sulfamidate derivatives. The four compounds **75-78** realized and their corresponding values related to their ability to displace [¹²⁵I]U-II in the interaction with UT receptor, suggested that introduction of aza-sulfuryl residues in this position led in principle to decrease affinity at UT receptor. However, these results are in accordance with N-methylation studies since the suppression of a proton-donating N-H in the same position gave compounds with more affinity. Indeed, Trp⁷ is crucial for the interaction with receptor counterpart and, hence, chemical modifications occurred in this position can influence biological activity. In particular, the Trp⁷ residue is tolerant versus N^α-methyl group incorporation, whereas improvement of hydrogen bonding possibility by N-aminosulfamide moiety reduces binding affinity.

7 Experimental Section

7.1 Materials and general procedures

Unless specified, 4-nitrophenyl chlorosulfate [106], as well as *N*^ε-(Alloc)-L-phenylalanine, *N*^ε-(Alloc)-*N*ⁱⁿ-(Boc)-L-tryptophan [107,108], all were synthesized according to literature methods. *N*-(Alloc)-L-lysine and O-(*t*-Bu)-L-tyrosine benzyl ester were synthesized from their corresponding Fmoc-amino acids using benzyl bromide and cesium carbonate in DMF [109], and free-based by treating with 20% piperidine in DMF solution. L-phenylalanine, allyl chloroformate, isobutyl chloroformate (IBC), *tert*-butyl carbazate, benzophenone hydrazone, 4-methylmorpholine (NMM), hydroxylamine hydrochloride, 4-nitrophenol, triethylamine, and 1,3-dimethylbarbituric acid (NDMBA), all were purchased from Aldrich and used as received. *N*ⁱⁿ-(Boc)-L-tryptophan, pyridine, 4-(bromomethyl)biphenyl, 1-(bromomethyl)naphthalene, lithium hydroxide (LiOH), all were purchased from Alfa Aesar, Acros, or Chem-Impex. Benzyl bromide was purchased from Aldrich and filtered through a small plug of silica gel prior to use. Phosphazene base (*tert*-butylimino-tri(pyrrolidino)phosphorane, BTPP), and 2-(bromomethyl)naphthalene were purchased from Fluka and used as received. Tetrakis(triphenylphosphine)palladium, was purchased from Aldrich and washed with ethanol prior to use. Anhydrous solvents [tetrahydrofuran (THF), *N,N*-dimethylformamide (DMF), acetonitrile, and dichloromethane (DCM)] were obtained by passage through a solvent-filtration system (GlassContour, Irvine, CA). Amino acids, Fmoc-Asp(OtBu), Fmoc-Cys(Trt), Fmoc-Phe, Fmoc-Lys(Boc), Fmoc-Tyr(tBu), Fmoc-Val and coupling reagents such as HBTU and HOBt, all were purchased from GL BiochemTM, and used as received. The rest of *N*^ε-Fmoc-protected amino acids, HBTU and HOBt were purchased from Inbios (Naples, Italy), and used as received. *N,N'*-Diisopropylcarbodiimide (DIC) was purchased from Aldrich and used as received. 2-Chlorotrityl chloride resin (0.65 and 0.79 mmol/g loading) were purchased from Chem-Impex, and the manufacturer's reported loading of the resin was used in the calculation of final product yields. Wang resin was purchased from Advanced ChemTech (Louisville, KY). Protected Penicillamine was

purchased from Bachem (Basel, Switzerland). Microwave irradiation was performed on a 300 MW Biotage apparatus on the high absorption level; temperature was monitored automatically. Flash chromatography [110] was on 230-400 mesh silica gel. Thin layer chromatography was performed on silica gel 60 F₂₅₄ plates from MerckTM. Melting points were made on a Gallenkamp apparatus and are uncorrected. Specific rotations, $[\alpha]_D$ values, were calculated from optical rotations measured at 20 °C in THF at the specified concentration (c in g/100 mL) and a 1-dm cell length (l) on a PerkinElmer Polarimeter 341, using the general formula: $[\alpha]_D^{20} = (100 \times \alpha)/(l \times c)$. Accurate mass measurements were performed on a LC-MSD instrument from Agilent technologies in positive electrospray ionisation (ESI) mode at the Université de Montréal Mass Spectrometry facility or by 6110 Quadrupole, Agilent Technologies. Sodium adducts $[M+Na]^+$ were used for empirical formula confirmation. ¹H NMR and ¹³C NMR spectra were recorded either on a Bruker AV300, AMX300, or AV400, and measured in CDCl₃ (7.26/77.16 ppm), acetone-d₆ (2.05/29.84 ppm), or pyridine-d₅ (7.22 ppm). Multiplicities are abbreviated: s = singlet, d = doublet, t = triplet, q = quadruplet, m = multiplet, and br = broad. Coupling constant J values are measured in Hertz (Hz) and chemical shift values in parts per million (ppm). Infrared spectra were recorded in the neat on an ATR Bruker apparatus.

7.2 Binding Experiments

All experiments were performed on membranes obtained from stable CHO-K1 cells expressing the recombinant human UT receptor (ES-440-M, lots 564-915-A and 613-577-A, Perkin Elmer, Boston, MA, USA). Assay conditions were: TRIS-buffer (20 mM, pH 7.4 at 37 °C) added with MgCl₂ (5 mM) and 0.5% BSA. Final assay volume was 0.1 ml, containing 1 or 20 µg membrane proteins depending on the lot of provided membranes. The radioligand used for competition experiments was [¹²⁵I]Urotensin-II (specific activity 2200 Ci/mmol; NEX379, Perkin Elmer) in the range 0.07–1.4 nM (as recommended by the lot of provided

membranes). Non-specific binding was determined in the presence of 1 μ M of unlabelled *hU*-II, and ranged between 10–20% of total binding. Competing ligands were tested in a wide range of concentrations (1 pM – 10 μ M). The incubation period (120 min at 37 °C) was terminated by rapid filtration through UniFilter-96 plates (Packard Instrument Company), pre-soaked for at least 2 h in BSA 0.5%, and using a MicroMate 96 Cell Harvester (Packard Instrument Company). The filters were then washed 4 times with 0.2 ml aliquots of Tris-HCl buffer (20 mM, pH 7.4, 4°C). Filters were dried and soaked in Microscint 40 (50 μ l in each well, Packard Instrument Company), and bound radioactivity was counted by a TopCount Microplate Scintillation Counter (Packard Instrument Company). Determinations were performed in duplicate. All binding data were fitted by using GraphPad Prism 4.0 in order to determine the equilibrium dissociation constant (K_d) from homologous competition experiments, the ligand concentration inhibiting the radioligand binding of the 50% (IC_{50}) from heterologous competition experiments. K_i values were calculated from IC_{50} using the Cheng-Prusoff equation ($K_i = IC_{50} / (1 + [radioligand] / K_d)$) according to the concentration and K_d of the radioligand [111]. In each experimental section one homologous competition curve to urotensin was run and the calculated K_d and the used radioligand concentration were used for the determination of ligand K_i values. The determined K_d value was 2.23 nM (1.09–3.38 nM, 95% c.l., n=5, each experiment performed in duplicate).

7.3 Intracellular calcium assay

PathHunter β -arrestin UT-CHO-K1 cells were transfected with a chimeric *Gaq-i5* G protein subunit plasmid [112] using lipofectamine (Life Technologies) and incubated overnight at 37 °C. Cells were then re-seeded in complete growth medium at 10,000 cells per well in 384-well black, clear bottom microplates and incubated overnight at 37 °C. Cells were loaded with Fluo-4 direct calcium assay reagent (Life Technologies, Paisley, UK) for 45 minutes at 37 °C

+ 15 minutes at rt in the presence of probenecid (5 mM). Compound addition and calcium mobilization were monitored on a Flex Station (Molecular Devices, Sunnyvale, CA).

7.4 Serum peptide stability

Peptide stabilities were assayed in diluted serum as previously described [113]. 25% fetal calf serum was centrifuged at 13,000 rpm for 10 min to remove lipids and the supernatant was collected and incubated at 37 °C for at least 15 min. The assay was initiated upon the addition of peptides to the serum for a final peptide concentration of 80 µM. 80 µL aliquots of the incubations were taken for the following time points: 0, 4, 16, 20, 24, 36 h. The aliquots were mixed with 40 µL of 15% trichloroacetic acid (TCA) and incubated at 2 °C for at least 15 min to precipitate serum proteins.

The supernatant was collected for each sample after centrifugation at 13,000 rpm for 10 min. These assays were performed in triplicate. Reverse phase high performance liquid chromatography (RP-HPLC) was carried out with Agilent Technologies 1200 series HPLC equipped with UV detector using a C18 column from ThermoFisher (Milan, Italy). Gradient elution was performed at 25°C (monitoring at 210 nm) in a gradient starting with buffer A (0.1 % TFA in water) and applying buffer B (0.1 % TFA in acetonitrile) from 5 to 70 % in 15 min.

7.5 Organ Bath Experiments

The experimental procedures employed in this study were approved by Institutional Animal Care and Use Committee and carried out in accordance with the legislation of Italian authorities (D.L. 116 27/01/1992), which complies with European Community guidelines (CEE Directive 86/609) for the care and use of experimental animals.

Male albino rats (Wistar strain, 275–350 g; Harlan Laboratories, UD, Italy) were euthanized by cervical dislocation, under ether anesthesia. The thoracic aorta was cleared of surrounding

tissue and excised from the aortic arch to the diaphragm. From each vessel, a helically cut strip was prepared, and then it was cut into two parallel strips. The endothelium was removed by gently rubbing the vessel intimal surface with a cotton-tip applicator; the effectiveness of this maneuver was assessed by the loss of relaxation response to acetylcholine ($1\ \mu\text{M}$) in noradrenaline ($1\ \mu\text{M}$) precontracted preparations. All preparations were placed in 5 ml organ baths filled with normal Krebs solution of the following composition (mmol/l): NaCl 119; NaHCO_3 25; KH_2PO_4 1.2; MgSO_4 1.5; CaCl_2 2.5; KCl 4.7 and glucose 11, warmed at $37\ ^\circ\text{C}$ and oxygenated with 95% O_2 , 5% CO_2 . The tissues were connected to isotonic force transducers (Ugo Basile, VA, Italy) under a constant load of 5 mN and motor activity was digitally recorded by an Octal Bridge Amplifier connected to PowerLab/8sp hardware system and analyzed using the Chart 4.2 software (ADInstruments Ltd, Oxford, UK). After 60 min equilibration, tissue responsiveness was assessed by the addition of $1\ \mu\text{M}$ noradrenaline followed by a further equilibration of 60 min.

To assess the agonist activity cumulative concentration-response curves to *hU-II* and to the agonist peptide under examination were constructed in paired aortic strips and responses obtained were normalized towards the control *hU-II* maximal contractile effect (E_{max}).

To assess the antagonist activity concentration-response curves to *hU-II* were constructed cumulatively in paired aortic strips. One strip was pretreated with vehicle (DMSO; 1-3 $\mu\text{l/ml}$) and used as a control, while the other strip was pretreated with the antagonist peptide under examination and, after a 30 min incubation period, *hU-II* was administered cumulatively to both preparations.

In each preparation only one cumulative concentration-response curve to *hU-II* was carried out and only one concentration of antagonist was tested. Concentration-response curves were analyzed by sigmoidal nonlinear regression fit using the GraphPad Prism 4.0 program (San Diego, CA, U.S.A.) to determine the molar concentration of the agonist producing the 50% (EC_{50}) of its maximal effect. Agonist activity of all compounds was expressed as pD_2 ($-\log$

EC₅₀). The antagonist potency was expressed in terms of pK_B estimated as the mean of the individual values obtained with the Gaddum equation: $pK_B = \log(CR-1) - \log[B]$ where CR is the concentration-ratio calculated from equieffective concentrations of agonist (EC₅₀) obtained in the presence and in the absence of antagonist and B is the used antagonist concentration.⁴⁵ Competitive antagonism was checked by the Schild regression analysis by plotting the estimates of $\log(CR-1)$ against $\log[B]$ to determine the slopes of linear regression: a plot with linear regression line and slope not significantly different from unity was considered as proof of competitive antagonism [111].

Results were compared for significant differences using two-tail Student's t-test for paired data or one-way analysis of variance (ANOVA) followed by Dunnett's post hoc test. A p value <0.05 was considered statistically significant.

8 Characterization

Peptide	Structure	HPLC ^a	MS (M+H)	
		<i>k'</i>	Found	Calcd
1	H-Asp-c[Pen-Phe-Tpi-Lys-Tyr-Cys]-Val-OH	5.15	1099.5	1099.38
2	H-Asp-c[Pen-Phe-DTpi-Lys-Tyr-Cys]-Val-OH	4.88	1099.3	1099.38
3	H-Asp-c[Pen-Phe-Tpi-Orn-Tyr-Cys]-Val-OH	5.03	1085.6	1085.41
4	H-Asp-c[Pen-Phe-DTpi-Orn-Tyr-Cys]-Val-OH	4.70	1085.3	1085.41
5	H-Asp-c[Pen-Phe-Trp-Lys-(2)Nal-Cys]-Val-OH	8.21	1023.41	1023.37
6	H-Asp-c[Pen-Phe-DTrp-Orn-(2)Nal-Cys]-Val-OH	8.15	1109.39	1109.34
7	H-Asp-c[Pen-Phe-Trp-Lys-(1)Nal-Cys]-Val-OH	8.31	1023.40	1023.37
8	H-Asp-c[Pen-Phe-DTrp-Orn-(1)Nal-Cys]-Val-OH	8.26	1109.34	1109.34
9	H-Asp-c[Pen-Phe-Trp-Lys-Btz-Cys]-Val-OH	7.61	1130.25	1130.24
10	H-Asp-c[Pen-Phe-DTrp-Orn-Btz-Cys]-Val-OH	7.30	1116.27	1116.21
11	H-Asp-[Pen-Phe-Trp-Lys-(pCl)Phe-Cys]-Val-OH	8.18	1107.79	1107.75
12	H-Asp-c[Pen-Phe-DTrp-Orn-(pCl)Phe-Cys]-Val-OH	8.03	1093.78	1093.73
13	H-Asp-c[Pen-Phe-Trp-Lys-(3,4-Cl)Phe-Cys]-Val-OH	8.32	1142.21	1142.20
14	H-Asp-c[Pen-Phe-DTrp-Orn-(3,4-Cl)Phe-Cys]-Val-OH	8.41	1128.19	1128.17
15	H-Asp-c[Pen-Phe-Trp-Lys-(pCN)Phe-Cys]-Val-OH	8.02	1098.31	1098.32
16	H-Asp-c[Pen-Phe-DTrp-Orn-(pCN)Phe-Cys]-Val-OH	7.90	1084.33	1084.29
17	H-Asp-c[Pen-Phe-Trp-Lys-(pNO ₂)Phe-Cys]-Val-OH	7.51	1118.32	1118.31
18	H-Asp-c[Pen-Phe-DTrp-Orn-(pNO ₂)Phe-Cys]-Val-OH	7.44	1104.30	1104.28
19	H-Asp-c[Pen-Phe-Trp-Lys-(pNH ₂)Phe-Cys]-Val-OH	7.78	1088.47	1088.32
20	H-Asp-c[Pen-Phe-DTrp-Orn-(pNH ₂)Phe -Cys]-Val-OH	7.61	1074.45	1074.29
21	H-Asp-c[Pen-Phe-Trp-Lys-Cha-Cys]-Val-OH	7.45	1079.50	1079.36
22	H-Asp-c[Pen-Phe-DTrp-Orn-Cha-Cys]-Val-OH	7.32	1065.49	1065.33
23	H-Asp-[Pen-Phe-Trp-Lys-Phg-Cys]-Val-OH	7.92	1059.44	1059.28
24	H-Asp-c[Pen-Phe-DTrp-Orn-Phg-Cys]-Val-OH	7.88	1045.42	1045.25
25	H-Asp-c[Pen-Phe-Trp-Lys-Tic-Cys]-Val-OH	8.18	1085.45	1085.30
26	H-Asp-c[Pen-Phe-DTrp-Orn-Tic-Cys]-Val-OH	8.04	1071.44	1071.27

27	H-Asp-c[Pen-Phe-Trp-Lys-Aic-Cys]-Val-OH	7.98	1085.45	1085.30
28	H-Asp-c[Pen-Phe-DTrp-Orn-Aic-Cys]-Val-OH	7.87	1071.44	1071.27

Table 8.1. Characterization data for peptides **1-28**.

^a k' = [(peptide retention time – solvent retention time)/solvent retention time].

Peptide 29: crude purity: 80%, t_R : 10.9 min (analytical HPLC, 10 to 90% acetonitrile in water (0.1% TFA) over 35 min, flow rate of 1.0 mL/min), molecular formula: $C_{51}H_{67}N_{10}O_{12}S_2$, calculated mass; 1075.44, found: 1075.9.

Peptide 30: crude purity: 62%, t_R : 10.6 min (analytical HPLC, 10 to 90% acetonitrile in water (0.1% TFA) over 35 min, flow rate of 1.0 mL/min), molecular formula: $C_{51}H_{67}N_{10}O_{12}S_2$, calculated mass; 1075.44, found: 1075.4.

Peptide 31: crude purity: 85%, t_R : 11.9 min (analytical HPLC, 10 to 90% acetonitrile in water (0.1% TFA) over 35 min, flow rate of 1.0 mL/min), molecular formula: $C_{51}H_{67}N_{10}O_{12}S_2$, calculated mass; 1075.44, found: 1075.3.

Peptide 32: crude purity: 74%, t_R : 17.9 min (analytical HPLC, 10 to 90% acetonitrile in water (0.1% TFA) over 20 min, flow rate of 1.0 mL/min), molecular formula: $C_{51}H_{67}N_{10}O_{12}S_2$, calculated mass; 1075.44, found: 1075.3.

Peptide 33: crude purity: 78%, t_R : 10.3 min (analytical HPLC, 10 to 90% acetonitrile in water (0.1% TFA) over 35 min, flow rate of 1.0 mL/min), molecular formula: $C_{51}H_{67}N_{10}O_{12}S_2$, calculated mass; 1075.44, found: 1075.4.

Peptide 34: crude purity: 67%, t_R : 11.2 min (analytical HPLC, 10 to 90% acetonitrile in water (0.1% TFA) over 35 min, flow rate of 1.0 mL/min), molecular formula: $C_{51}H_{67}N_{10}O_{12}S_2$, calculated mass; 1075.44, found: 1075.9.

Peptide 35: crude purity: 90%, t_R : 11.9 min (analytical HPLC, 10 to 90% acetonitrile in water (0.1% TFA) over 35 min, flow rate of 1.0 mL/min), molecular formula: $C_{52}H_{69}N_{10}O_{12}S_2$, calculated mass; 1089.45, found: 1088.9.

Peptide 36: crude purity: 92%, t_R : 15.8 min (analytical HPLC, 10 to 90% acetonitrile in water (0.1% TFA) over 20 min, flow rate of 1.0 mL/min), molecular formula: $C_{52}H_{69}N_{10}O_{12}S_2$, calculated mass; 1089.45, found: 1089.1.

Peptide 37: crude purity: 63%, t_R : 16.1 min (analytical HPLC, 10 to 90% acetonitrile in water (0.1% TFA) over 20 min, flow rate of 1.0 mL/min), molecular formula: $C_{52}H_{69}N_{10}O_{12}S_2$, calculated mass; 1089.45, found: 1089.0.

Peptide 38: crude purity: 74%, t_R : 14.9 min (analytical HPLC, 10 to 90% acetonitrile in water (0.1% TFA) over 20 min, flow rate of 1.0 mL/min), molecular formula: $C_{52}H_{69}N_{10}O_{12}S_2$, calculated mass; 1089.45, found: 1089.3.

Peptide 39: crude purity: 55%, t_R : 10.2 min (analytical HPLC, 10 to 90% acetonitrile in water (0.1% TFA) over 35 min, flow rate of 1.0 mL/min), molecular formula: $C_{52}H_{69}N_{10}O_{12}S_2$, calculated mass; 1089.45, found: 1089.3.

Peptide 40: crude purity: 58%, t_R : 12.2 min (analytical HPLC, 10 to 90% acetonitrile in water (0.1% TFA) over 35 min, flow rate of 1.0 mL/min), molecular formula: $C_{52}H_{69}N_{10}O_{12}S_2$, calculated mass; 1089.45, found: 1089.7.

Peptide 41: crude purity: 77%, t_R : 14.0 min (analytical HPLC, 10 to 90% acetonitrile in water (0.1% TFA) over 20 min, flow rate of 1.0 mL/min), molecular formula: $C_{52}H_{69}N_{10}O_{12}S_2$, calculated mass; 1089.45, found: 1089.1.

Peptide 42: crude purity: 56%, t_R : 15.3 min (analytical HPLC, 10 to 90% acetonitrile in water (0.1% TFA) over 35 min, flow rate of 1.0 mL/min), molecular formula: $C_{52}H_{69}N_{10}O_{12}S_2$, calculated mass; 1089.45, found: 1088.8.

Peptide 43: crude purity: 41%, t_R : 11.0 min (analytical HPLC, 10 to 90% acetonitrile in water (0.1% TFA) over 35 min, flow rate of 1.0 mL/min), molecular formula: $C_{52}H_{69}N_{10}O_{12}S_2$, calculated mass; 1089.45, found: 1089.8.

Peptide 44: crude purity: 67%, t_R : 11.0 min (analytical HPLC, 10 to 90% acetonitrile in water (0.1% TFA) over 35 min, flow rate of 1.0 mL/min), molecular formula: $C_{52}H_{69}N_{10}O_{12}S_2$, calculated mass; 1089.45, found: 1089.7.

Peptide 45: crude purity: 61%, t_R : 14.1 min (analytical HPLC, 10 to 90% acetonitrile in water (0.1% TFA) over 20 min, flow rate of 1.0 mL/min), molecular formula: $C_{52}H_{69}N_{10}O_{12}S_2$, calculated mass; 1089.45, found: 1089.2.

Peptide 46: crude purity: 80%, t_R : 9.6 min (analytical HPLC, 10 to 90% acetonitrile in water (0.1% TFA) over 35 min, flow rate of 1.0 mL/min), molecular formula: $C_{52}H_{69}N_{10}O_{12}S_2$, calculated mass; 1089.45, found: 1089.2.

Peptide 47: crude purity: 47%, t_R : 14.2 min (analytical HPLC, 10 to 90% acetonitrile in water (0.1% TFA) over 20 min, flow rate of 1.0 mL/min), molecular formula: $C_{52}H_{69}N_{10}O_{12}S_2$, calculated mass; 1089.45, found: 1089.4.

Peptide 48: crude purity: 77%, t_R : 11.0 min (analytical HPLC, 10 to 90% acetonitrile in water (0.1% TFA) over 35 min, flow rate of 1.0 mL/min), molecular formula: $C_{52}H_{69}N_{10}O_{12}S_2$, calculated mass; 1089.45, found: 1089.8.

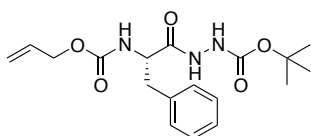
Peptide 49: crude purity: 61%, t_R : 11.4 min (analytical HPLC, 10 to 90% acetonitrile in water (0.1% TFA) over 35 min, flow rate of 1.0 mL/min), molecular formula: $C_{52}H_{69}N_{10}O_{12}S_2$, calculated mass; 1089.45, found: 1089.9.

Peptide 50: crude purity: 78%, t_R : 15.6 min (analytical HPLC, 10 to 90% acetonitrile in water (0.1% TFA) over 20 min, flow rate of 1.0 mL/min), molecular formula: $C_{52}H_{69}N_{10}O_{12}S_2$, calculated mass; 1089.45, found: 1089.1.

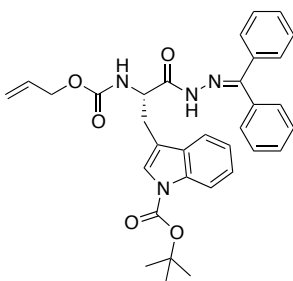
Peptide 51: crude purity: 58%, t_R : 11.6 min (analytical HPLC, 10 to 90% acetonitrile in water (0.1% TFA) over 35 min, flow rate of 1.0 mL/min), molecular formula: $C_{52}H_{69}N_{10}O_{12}S_2$, calculated mass; 1089.45, found: 1089.9.

Peptide 52: crude purity: 72%, t_R : 14.4 min (analytical HPLC, 10 to 90% acetonitrile in water (0.1% TFA) over 20 min, flow rate of 1.0 mL/min), molecular formula: $C_{52}H_{69}N_{10}O_{12}S_2$, calculated mass; 1089.45, found: 1089.2.

Peptide 53: crude purity: 46%, t_R : 13.8 min (analytical HPLC, 10 to 90% acetonitrile in water (0.1% TFA) over 20 min, flow rate of 1.0 mL/min), molecular formula: $C_{52}H_{69}N_{10}O_{12}S_2$, calculated mass; 1089.45, found: 1089.4.

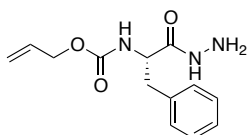


***N*-(Alloc)-*N'*-(Boc)-L-phenylalanine hydrazide (61)** *N*-(Alloc)-L-phenylalanine (4.29 g, 17.21 mmol) was dissolved in dry THF (93 mL), cooled to -15°C , treated with IBC (2.23 mL, 17.21 mmol) followed by NMM (2.37 mL, 21.51 mmol), stirred for 15 min, and treated drop-wise with a solution of *tert*-butyl carbazate in dry THF (21 mL). After stirring at -15°C for 2 h, the reaction mixture was treated with water (150 mL), transferred to a separatory funnel, and the phases were separated. The aqueous layer was extracted with EtOAc (2 x 250 mL). The combined organic phase was washed with brine, dried over MgSO_4 , filtered and evaporated under reduced pressure. The residue was purified by flash chromatography by eluting with 75:25 hexanes/EtOAc. Evaporation of the collected fractions afforded the hydrazide **61** (4.07 g; 78% yield) as white solid: R_f 0.22 (75:25 hexanes:EtOAc); mp $57-60^{\circ}\text{C}$; $[\alpha]_D^{20} -9.1^{\circ}$ (THF, c 0.96); ^1H NMR (CDCl_3 , 300 MHz) δ 1.47 (9H, s), 3.03 (1H, dd, $J = 8.0, 14.0$ Hz), 3.20 (1H, dd, $J = 6.0, 14.0$ Hz), 4.50 (2H, dd, $J = 1.4, 5.6$ Hz), 4.55 (1H, d, $J = 5.7$ Hz), 5.18 (1H, dd, $J = 1.17, 10.5$ Hz), 5.23 (1H, dd, $J = 1.17, 18.5$ Hz), 5.54 (1H, d, $J = 8.0$ Hz), 5.78-5.91 (1H, m), 6.64-6.75 (1H, br), 7.22-7.33 (5H, m), 8.28-8.39 (1H, br); ^{13}C NMR (CDCl_3 , 75 MHz) δ 170.9, 156.2, 155.3, 136.3, 132.5, 129.5, 128.8, 127.2, 118.1, 82.0, 66.2, 54.6, 38.2, 28.3; IR (neat) $\nu_{\text{max}}/\text{cm}^{-1}$ 3280, 1682, 1500, 1370, 1238, 1157, 1045; HRMS (ESI) m/z calculated for $\text{C}_{18}\text{H}_{25}\text{N}_3\text{NaO}_5$ $[\text{M}+\text{Na}]^+$ 386.1686; found 386.1691.

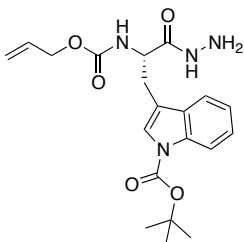


***N*-(Alloc)-*N''*-(Boc)-*N'*-(diphenylmethylene)-L-tryptophan hydrazide (70)** Employing the procedure used for the synthesis of *N*-(Alloc)-*N'*-(Boc)-L-phenylalanine (**61**), *N*-(Alloc)-*N''*-(Boc)-L-tryptophan (1.91 g, 4.92 mmol) was treated with IBC (639 μL , 4.92 mmol) and NMM (700 μL , 6.39 mmol), followed by benzophenone hydrazone (966 mg, 4.92 mmol). The residue was purified by flash chromatography by eluting with 80:20 hexanes/EtOAc to afford hydrazide **70** (1.42 g; 51% yield) as white solid: R_f 0.27 (80:20 hexanes:EtOAc); mp $68-71^{\circ}\text{C}$.

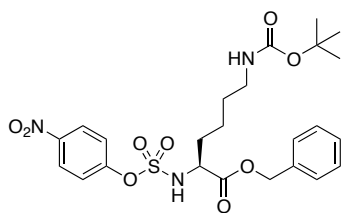
°C; $[\alpha]_D^{20}$ 46.4° (THF, *c* 1.04); ^1H NMR (CDCl_3 , 400 MHz) δ 1.61 (9H, s), 3.27-3.38 (2H, br), 4.54 (1H, d, *J* = 4.6 Hz), 4.59 (1H, d, *J* = 5.1 Hz), 5.21 (1H, d, *J* = 10.6 Hz), 5.30 (1H, d, *J* = 17.4 Hz), 5.67-5.73 (1H, br), 5.87-5.96 (1H, m), 7.02-7.62 (15H, m), 7.93-8.07 (1H, br), 8.27-8.36 (1H, br); ^{13}C NMR (CDCl_3 , 100 MHz) δ 172.8, 155.7, 152.1, 149.6, 136.3, 132.9, 131.2, 130.1, 130.0, 129.9, 129.5, 128.4, 128.3, 128.2, 127.6, 124.4, 124.3, 122.6, 119.2, 117.7, 115.5, 115.3, 83.6, 65.8, 52.0, 29.0, 28.3; IR (neat) $\nu_{\text{max}}/\text{cm}^{-1}$ 2979, 1720, 1675, 1451, 1367, 1254, 1154, 1085; HRMS (ESI) *m/z* calculated for $\text{C}_{33}\text{H}_{34}\text{N}_4\text{NaO}_5$ $[\text{M}+\text{Na}]^+$ 589.2421; found 684.2425.



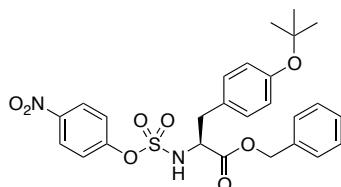
***N'*-(Alloc)-L-phenylalanine hydrazide (62)** *N'*-(Alloc)-*N'*-(Boc)-L-phenylalanine hydrazide (**61**, 1.4 g, 3.85 mmol) was dissolved in TFA/DCM (1:1, 12 mL), stirred at room temperature for 1 h, and concentrated *in vacuo*. The residue was partitioned between 5% aqueous NaHCO_3 solution (100 mL) and EtOAc (100 mL), the phases were separated, and the aqueous phase was extracted with EtOAc (100 mL x 4). The combined organic layer was dried over MgSO_4 , filtered and evaporated under reduced pressure to afford hydrazide **62** (905 mg; 89% yield): R_f 0.17 (70:30 hexanes:EtOAc); mp 131-134 °C; $[\alpha]_D^{20}$ 7.0° (THF, *c* 0.95); ^1H NMR (pyridine- d_5 , 400 MHz) δ 3.30 (1H, dd, *J* = 7.7, 13.4 Hz), 3.52 (1H, dd, *J* = 7.0, 13.4 Hz), 4.60 (1H, dd, *J* = 5.3, 13.5 Hz), 4.68 (1H, dd, *J* = 5.3, 13.7 Hz), 5.04 (1H, d, *J* = 8.0 Hz), 5.08 (1H, d, *J* = 10.4 Hz), 5.24 (1H, d, *J* = 15.9 Hz), 7.16-7.25 (5H, m), 7.36 (2H, d, *J* = 6.8 Hz), 8.96 (1H, d, *J* = 8.4 Hz); ^{13}C NMR (CDCl_3 , 100 MHz) δ 172.0, 156.1, 136.3, 132.5, 129.3, 128.8, 127.2, 118.1, 66.1, 55.1, 38.6; IR (neat) $\nu_{\text{max}}/\text{cm}^{-1}$ 3291, 1693, 1656, 1532, 1243, 1046; HRMS (ESI) *m/z* calculated for $\text{C}_{13}\text{H}_{19}\text{N}_3\text{O}_3$ $[\text{M}+\text{H}]^+$ 264.1343; found 264.1348.



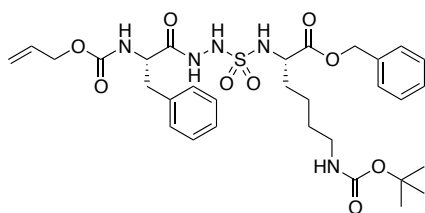
***N'*-(Alloc)-*N''*-(Boc)-L-tryptophan hydrazide (71)** *N'*-(Alloc)-*N''*-(Boc)-*N'*-(diphenylmethylene)-L-tryptophan hydrazide (1.32 g, 2.32 mmol) was dissolved in 39 mL of pyridine, treated with hydroxylamine hydrochloride (807 mg, 11.6 mmol), heated to 60 °C, and agitated with sonication overnight. The volatiles were evaporated under reduced pressure. The residue was purified by flash chromatography eluting with 98:2 DCM/MeOH to afford the hydrazide **71** (721 mg, 77% yield): R_f 0.12 (98:2 DCM:MeOH); mp 82-85 °C; $[\alpha]_D^{20}$ 7.1° (THF, *c* 1.04); ^1H NMR (CDCl_3 , 400 MHz) δ 1.66 (9H, s), 3.14 (1H, dd, *J* = 8.1, 15.0 Hz), 3.20 (1H, dd, *J* = 6.6, 14.8 Hz), 3.57-3.94 (2H, br), 4.48 (1H, dd, *J* = 7.4, 14.8 Hz), 4.55 (2H, d, *J* = 5.7 Hz), 5.21 (1H, d, *J* = 10.4 Hz), 5.27 (1H, d, *J* = 17.2 Hz), 5.42-5.64 (1H, br), 5.83-5.92 (1H, m), 7.20-7.58 (5H, m), 8.05-8.19 (1H, br); ^{13}C NMR (CDCl_3 , 100 MHz) δ 171.9, 156.0, 149.7, 135.5, 132.5, 130.2, 124.8, 124.4, 122.8, 118.9, 118.2, 115.5, 115.2, 84.0, 66.2, 53.8, 29.2, 28.3; IR (neat) $\nu_{\text{max}}/\text{cm}^{-1}$ 3290, 1726, 1452, 1367, 1252, 1154, 1085; HRMS (ESI) *m/z* calculated for $\text{C}_{20}\text{H}_{27}\text{N}_4\text{O}_5$ $[\text{M}+\text{H}]^+$ 403.1976; found 403.1976.



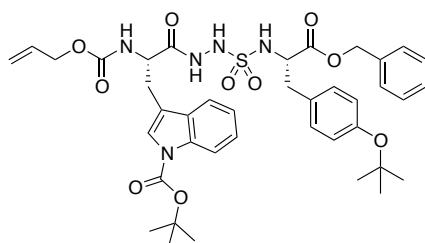
4-Nitrophenyl-N-((Boc)-L-lysine benzyl ester sulfamidate (57) Under argon, a solution of *N*-((Boc)-L-lysine benzyl ester (1.00 g, 2.97 mmol), 4-nitrophenol (1.24 g, 8.92 mmol) and triethylamine (2.49 mL, 17.83 mmol) in dry DCM (30 mL) was added drop-wise to a solution of 4-nitrophenyl chlorosulfate (1.41 g, 5.94 mmol) in dry DCM (6 mL) at -78°C . After stirring at -78°C for 2 h, the mixture was allowed to warm up to rt. The organic phase was washed with 5% citric acid solution (100 mL x 3), dried over MgSO_4 , filtered and evaporated. The residue was purified by flash chromatography eluting with 70:30 hexane/EtOAc to afford sulfamidate **57** as a pale yellow solid (1.09 g; 68% yield) contaminated with 4-nitrophenol, and used without further purification in the next step: R_f 0.28 (70:30 hexanes:EtOAc); mp $93-96^{\circ}\text{C}$; $[\alpha]_D^{20}$ 17.2° (THF, c 1.08); ^1H NMR (CDCl_3 , 400 MHz) δ 1.34-1.50 (4H, m), 1.42 (9H, s), 1.80-1.93 (2H, m), 3.07 (2H, d, $J = 6.3$ Hz), 4.25 (1H, t, $J = 5.6$ Hz), 4.49-4.59 (1H, br), 5.19 (1H, d, $J = 12.0$ Hz), 5.23 (1H, d, $J = 12.0$ Hz), 5.88-5.98 (1H, br), 7.32-7.40 (7H, m), 8.18-8.22 (2H, d, $J = 9.2$ Hz); ^{13}C NMR (CDCl_3 , 75 MHz) δ 171.2, 156.5, 154.5, 146.0, 134.9, 129.0, 128.9, 128.8, 125.6, 122.4, 79.6, 68.1, 57.0, 39.8, 32.3, 31.7, 29.6, 28.5; IR (neat) $\nu_{\text{max}}/\text{cm}^{-1}$ 3290, 1734, 1682, 1532, 1351, 1253, 1177; HRMS (ESI) m/z calculated for $\text{C}_{24}\text{H}_{31}\text{N}_3\text{NaO}_9\text{S}$ $[\text{M}+\text{Na}]^+$ 560.1673; found 560.1676.



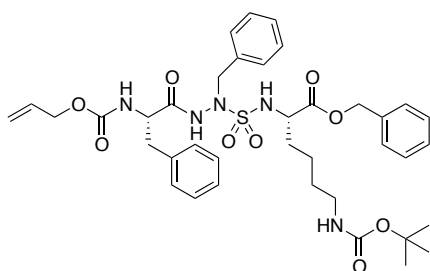
4-Nitrophenyl-O-(tert-butyl)-L-tyrosine benzyl ester sulfamidate (58) Employing the procedure for the synthesis of 4-nitrophenyl-N-((Boc)-L-lysine benzyl ester sulfamidate, *O*-(tert-butyl)-L-tyrosine benzyl ester (896 mg, 2.97 mmol), 4-nitrophenol (1.14 g, 8.22 mmol) and triethylamine (2.292 mL, 16.44 mmol) were reacted with 4-nitrophenyl chlorosulfate (1.3 g, 5.47 mmol), and sulfamidate **58** was purified by flash chromatography eluting with 80:20 hexane/EtOAc to afford sulfamidate **58** as a pale yellow solid (535 mg; 37% yield) contaminated with traces of 4-nitrophenol, that was used without further purification in the next step: R_f 0.34 (n-hexane:EtOAc 80:20); mp $112-115^{\circ}\text{C}$; $[\alpha]_D^{20}$ 4.5° (THF, c 1.02); ^1H NMR (CDCl_3 , 400 MHz) δ 1.33 (9H, s), 3.08 (1H, dd, $J = 6.0, 15.0$ Hz), 3.13 (1H, dd, $J = 5.8, 13.7$ Hz), 4.47-4.52 (1H, m), 5.14 (1H, d, $J = 11.9$ Hz), 5.18 (1H, d, $J = 11.9$ Hz), 5.47 (1H, d, $J = 8.6$ Hz), 6.85-6.96 (4H, m), 7.21-7.40 (7H, m), 8.16 (2H, d, $J = 2.1$ Hz); ^{13}C NMR (CDCl_3 , 75 MHz) δ 170.3, 155.2, 154.4, 146.1, 134.6, 130.1, 129.1, 129.0, 128.9, 128.8, 125.6, 124.4, 122.5, 78.8, 68.2, 58.1, 38.4, 29.8, 29.0; IR (neat) $\nu_{\text{max}}/\text{cm}^{-1}$ 3302, 1739, 1524, 1347, 1154; HRMS (ESI) m/z calculated for $\text{C}_{26}\text{H}_{28}\text{N}_2\text{NaO}_8\text{S}$ $[\text{M}+\text{Na}]^+$ 551.1459; found 551.1474.



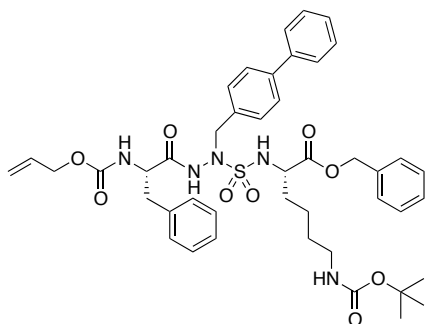
***N*-(Alloc)-L-phenylalaninyl-aza-sulfurylglycyl-*N*-(Boc)-L-lysine benzyl ester (**63**)** *N*⁶-(Alloc)-L-phenylalanine hydrazide (29 mg, 0.11 mmol) was added to a microwave vessel containing a solution of sulfamidate **57** (54 mg, 0.1 mmol) in MeCN (2.5 mL), and treated with triethylamine, at which point the solution turned yellow. The vessel was sealed and heated to 60 °C using microwave irradiation for 2.5 h. The volatiles were evaporated under reduced pressure. The residue was purified by flash chromatography eluting with 65:35 hexanes/EtOAc to afford aza-sulfurylglycyl tripeptide **63** as white solid (49 mg; 74% yield): *R*_f 0.26 (65:35 hexanes:EtOAc); mp 119-122 °C; [α]_D²⁰ 3.8° (THF, *c* 1.46); ¹H NMR (acetone-*d*₆, 400 MHz) δ 1.29-1.51 (4H, m), 1.40 (9H, s), 1.76-1.84 (2H, m), 2.98 (1H, dd, *J* = 9.6, 13.9 Hz), 3.05 (2H, dd, *J* = 6.4, 12.7 Hz), 3.20 (1H, dd, *J* = 5.1, 14.0 Hz), 4.19 (1H, q, *J* = 6.5 Hz), 4.44-4.50 (1H, m), 4.46 (2H, d, *J* = 8.8 Hz), 5.11 (1H, d, *J* = 9.2 Hz), 5.18-5.24 (1H, m), 5.21 (2H, d, *J* = 3.0 Hz), 5.79-5.90 (1H, m), 5.90-5.98 (1H, br), 6.54 (1H, d, *J* = 6.8 Hz), 6.62 (1H, d, *J* = 8.7 Hz), 7.19-7.46 (10H, m), 8.16-8.24 (1H, br), 9.36-9.44 (1H, br); ¹³C NMR (acetone-*d*₆, 100 MHz) δ 173.1, 171.6, 156.8, 156.7, 138.3, 137.0, 134.2, 130.2, 129.3, 129.2, 129.1, 129.0, 127.4, 117.3, 78.4, 67.4, 65.9, 56.9, 56.0, 40.7, 40.5, 38.5, 32.9, 28.7, 22.9; IR (neat) ν_{max} /cm⁻¹ 3294, 1746, 1684, 1524, 1458, 1327, 1249, 1158; HRMS (ESI) *m/z* calculated for C₃₁H₄₃N₅NaO₉S [M+Na]⁺ 684.2674; found 684.2678.



***N*-(Alloc)-*N*ⁱⁿ-(Boc)-L-tryptophanyl-aza-sulfurylglycyl-*O*-(*tert*-butyl)-L-tyrosine benzyl ester (**72**)** Employing the same protocol for the synthesis of *N*⁶-(Alloc)-L-phenylalaninyl-aza-sulfurylglycyl-*N*⁶-(Boc)-L-lysine benzyl ester *N*ⁱⁿ-(Alloc)-L-tryptophan hydrazide (88 mg, 0.22 mmol) was treated with the sulfamidate **58** (105 mg, 0.2 mmol) and triethylamine (31 μ L, 0.22 mmol). The volatiles were evaporated under reduced pressure and the residue was purified by flash chromatography by eluting 75:25 hexanes/EtOAc to afford aza-sulfurylglycyl tripeptide **72** as a solid (134 mg; 84% yield): *R*_f 0.22 (70:30 hexanes:EtOAc); mp 105-107 °C; [α]_D²⁰ -6.4° (THF, *c* 1.02); ¹H NMR (acetone-*d*₆, 400 MHz) δ 1.30 (9H, s), 1.65 (9H, s), 2.97 (1H, dd, *J* = 8.6, 13.2 Hz), 3.13 (2H, dd, *J* = 4.8, 13.4 Hz), 3.30 (1H, dd, *J* = 5.6, 14.8 Hz), 4.46 (2H, d, *J* = 3.9 Hz), 4.52 (1H, dd, *J* = 7.3, 13.5 Hz), 4.58 (1H, dd, *J* = 8.4, 14.1 Hz), 5.09 (1H, d, *J* = 10.4 Hz), 5.14 (1H, d, *J* = 12.4 Hz), 5.21 (2H, d, *J* = 17.6 Hz), 5.79-5.90 (1H, m), 6.48 (1H, d, *J* = 6.4 Hz), 6.68 (1H, d, *J* = 7.9 Hz), 6.85-6.92 (2H, m), 7.11-7.40 (10H, m), 7.62-7.72 (2H, m), 8.36-8.44 (1H, br), 9.53-9.62 (1H, br); ¹³C NMR (acetone-*d*₆, 100 MHz) δ 172.3, 171.8, 156.8, 155.5, 150.3, 136.7, 136.4, 134.2, 131.7, 131.4, 131.0, 130.8, 129.2, 128.9, 125.4, 125.1, 124.5, 123.3, 120.1, 117.4, 116.9, 115.9, 84.2, 78.4, 67.4, 66.0, 58.3, 54.5, 38.8, 35.2, 29.1, 28.3; IR (neat) ν_{max} /cm⁻¹ 3254, 1728, 1453, 1366, 1255, 1156, 1086; HRMS (ESI) *m/z* calculated for C₄₀H₄₉N₅NaO₁₀S [M+Na]⁺ 814.3092; found 814.3096.

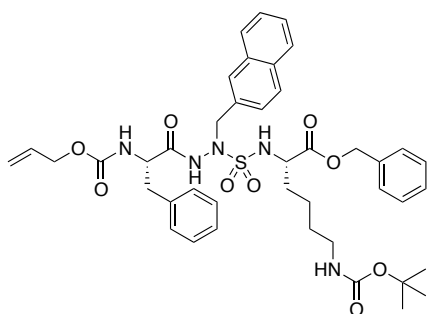


***N*-(Alloc)-L-phenylalaninyl-aza-sulfurylphenylalaninyl-*N*-(Boc)-L-lysine benzyl ester (**64**)** A 0 °C solution of aza-sulfurylglyciny tripeptide **63** (271 mg, 0.41 mmol) in THF (8 mL) was treated with BTPP (138 μ L, 0.45 mmol), stirred for 0.5 h, treated with benzyl bromide (55 μ L, 0.45 mmol) and stirred at 0 °C for 3.5 h. The volatiles were evaporated. The residue was purified by flash chromatography by eluting 65:35 hexanes/EtOAc to afford aza-sulfurylphenylalaninyl tripeptide **64** as a white solid (209 mg; 68% yield): R_f 0.37 (65:35 hexanes:EtOAc); mp 125-128 °C; $[\alpha]_D^{20}$ -4.3° (THF, c 1.77); ^1H NMR (acetone- d_6 , 400 MHz) δ 1.33-1.51 (4H, m), 1.40 (9H, s), 1.72-1.87 (2H, m), 2.78 (1H, dd, J = 10.1, 13.9 Hz), 2.94-2.98 (1H, br), 3.05 (2H, dd, J = 6.7, 12.7 Hz), 4.30-4.38 (2H, m), 4.42 (2H, d, J = 3.8 Hz), 4.49 (1H, d, J = 14.6 Hz), 4.58 (1H, d, J = 14.3 Hz), 5.10 (1H, d, J = 10.0 Hz), 5.21 (1H, d, J = 17.0 Hz), 5.21 (2H, s), 5.78-5.88 (1H, m), 5.89-5.97 (1H, br), 6.48-6.59 (1H, br), 6.81 (1H, d, J = 7.3 Hz), 7.16-7.49 (15H, m), 9.13-9.18 (1H, br); ^{13}C NMR (acetone- d_6 , 75 MHz) δ 172.9, 171.8, 156.8, 156.6, 141.1, 138.3, 137.1, 136.6, 134.2, 130.2, 130.0, 129.3, 129.1, 129.1, 129.0, 128.6, 127.4, 117.3, 78.4, 67.4, 65.9, 57.2, 57.1, 55.9, 55.2, 40.7, 38.3, 33.1, 28.7, 23.0; IR (neat) ν_{max} /cm $^{-1}$ 3320, 1685, 1601, 1506, 1436, 1392, 1238, 1163; HRMS (ESI) m/z calculated for $\text{C}_{38}\text{H}_{49}\text{N}_5\text{NaO}_9\text{S}$ $[\text{M}+\text{Na}]^+$ 774.3143; found 774.3156.

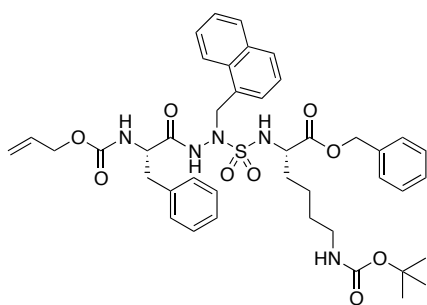


***N*-(Alloc)-L-phenylalaninyl-aza-sulfuryl-*p*-phenylphenylalaninyl-*N*-(Boc)-L-lysine benzyl ester (**65**)** Employing the protocol described for aza-sulfurylphenylalaninyl tripeptide **64**, 4-(bromomethyl)biphenyl (86 mg, 0.35 mmol) was reacted with aza-sulfurylglyciny tripeptide **63** (210 mg, 0.32 mmol). The residue was purified by flash chromatography eluting with 80:20 hexanes/EtOAc to afford aza-sulfuryl-*p*-phenylphenylalaninyl tripeptide **65** as white solid (225 mg; 85% yield): R_f 0.27 (70:30 hexanes:EtOAc); mp 121-126 °C; $[\alpha]_D^{20}$ 4.7° (THF, c 1.50); ^1H NMR (acetone- d_6 , 400 MHz) δ 1.35-1.55 (4H, m), 1.40 (9H, s), 1.74-1.88 (2H, m), 2.76-2.87 (1H, br), 2.95-3.02 (1H, br), 3.04 (2H, t, J = 5.7 Hz), 4.34-4.39 (2H, m), 4.41 (2H, d, J = 2.2 Hz), 4.54 (1H, d, J = 14.0 Hz), 4.62 (1H, d, J = 14.3 Hz), 5.08 (1H, d, J = 10.8 Hz), 5.13-5.30 (1H, br), 5.22 (2H, s), 5.77-5.87 (1H, m), 5.88-5.97 (1H, br), 6.50-6.60 (1H, br), 6.77-6.87 (1H, br), 7.16-7.66 (19H, m), 9.12-9.25 (1H, br); ^{13}C NMR (acetone- d_6 , 100 MHz) δ 172.9, 171.8, 156.8, 156.7, 141.4, 141.2, 138.2, 137.0, 135.7, 134.2, 130.6, 130.2, 129.7, 129.3, 129.1, 129.1, 129.0, 128.2, 127.7, 127.6, 127.3, 117.3, 78.4, 67.4, 65.9, 57.2, 55.9, 55.8, 55.0, 40.7, 38.3, 33.0, 28.7, 23.0; IR (neat) ν_{max} /cm $^{-1}$ 3163, 1601, 1506, 1435,

1393, 1222, 1163; HRMS (ESI) m/z calculated for $C_{44}H_{53}N_5NaO_9S$ $[M+Na]^+$ 850.3456; found 850.3448.

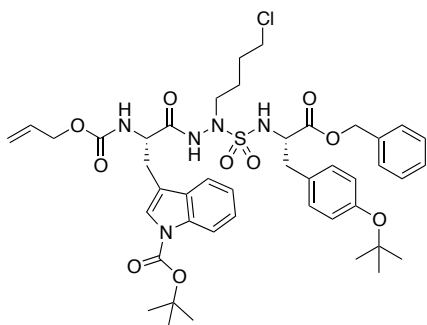


***N*-(Alloc)-L-phenylalaninyl-aza-sulfuryl-2-naphthylalaninyl-*N*-(Boc)-L-lysine benzyl ester (66)** Employing the protocol described for aza-phenylsulfurylglycyl tripeptide **64**, 2-(bromomethyl)naphthalene (90 mg, 0.41 mmol) was reacted with aza-sulfurylglycyl tripeptide (245 mg, 0.37 mmol). The residue was purified by flash chromatography by eluting n-hexane/EtOAc 90:10 to afford aza-(2)naphthylsulfurylglycyl tripeptide **66** as a white solid (224 mg; 76% yield): R_f 0.27 (80:20 hexanes:EtOAc); mp 99-101 °C; $[\alpha]_D^{20}$ 7.6° (THF, c 1.58); 1H NMR (acetone- d_6 , 400 MHz) δ 1.37-1.52 (4H, m), 1.40 (9H, s), 1.76-1.82 (2H, m), 2.78-2.82 (1H, m), 2.92-3.01 (1H, br), 3.05 (2H, dd, J = 5.9, 11.6 Hz), 4.33-4.43 (4H, m), 4.66 (1H, d, J = 14.4 Hz), 4.75 (1H, d, J = 14.4 Hz), 5.09 (1H, d, J = 10.6 Hz), 5.16-5.27 (1H, m), 5.21 (2H, s), 5.76-5.85 (1H, m), 5.87-5.96 (1H, br), 6.47-6.56 (1H, br), 6.79-6.89 (1H, br), 7.12-7.54 (13H, m), 7.84-7.90 (4H, m), 9.15-9.26 (1H, br); ^{13}C NMR (acetone- d_6 , 100 MHz) δ 172.9, 171.9, 156.8, 156.7, 138.2, 137.0, 134.2, 134.2, 134.0, 130.1, 129.3, 129.1, 129.0, 129.0, 128.8, 128.4, 127.9, 127.3, 126.8, 117.3, 78.4, 67.5, 65.9, 57.2, 55.9, 55.4, 40.7, 38.3, 30.3, 28.7, 23.0; IR (neat) ν_{max}/cm^{-1} 3259, 1744, 1682, 1520, 1454, 1346, 1249, 1162; HRMS (ESI) m/z calculated for $C_{42}H_{51}N_5NaO_9S$ $[M+Na]^+$ 824.3300; found 824.3315.

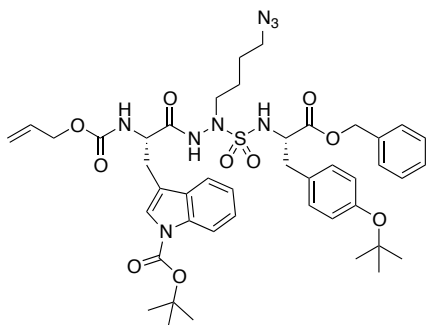


***N*-(Alloc)-L-phenylalaninyl-aza-sulfuryl-1-naphthylalaninyl-*N*-(Boc)-L-lysine benzyl ester (67)** Employing the protocol described for the synthesis of aza-sulfurylphenylalaninyl tripeptide **64**, 1-(bromomethyl)naphthalene (24 mg, 0.11 mmol) was reacted with aza-sulfurylglycyl tripeptide **63** (66 mg, 0.1 mmol). The residue was purified by flash chromatography eluting with 75:25 hexanes/EtOAc to afford aza-sulfuryl-1-naphthylalaninyl tripeptide **67** as white solid (52 mg; 65%): R_f 0.28 (75:25 hexanes:EtOAc); mp 145-147 °C; $[\alpha]_D^{20}$ -11.7° (THF, c 1.12); 1H NMR (acetone- d_6 , 400 MHz) δ 1.34-1.47 (4H, m), 1.39 (9H, s), 1.72-1.87 (2H, br), 2.69 (1H, dd, J = 10.5, 13.5 Hz), 2.81-2.95 (1H, m), 2.97-3.09 (2H, br), 4.30 (1H, m), 4.37 (1H, d, J = 6.4 Hz), 4.40 (2H, d, J = 4.6 Hz), 4.95 (1H, d, J = 13.0 Hz), 5.09 (1H, d, J = 10.5 Hz), 5.15-5.28 (2H, m), 5.20 (2H, d, J = 2.0 Hz), 5.77-5.85 (1H, m),

5.86-5.96 (1H, br), 6.38-6.52 (1H, br), 6.81-6.92 (1H, br), 7.14-7.52 (14H, m), 7.72-7.98 (2H, m), 8.24-8.38 (1H, m), 9.12-9.33 (1H, br); ^{13}C NMR (acetone- d_6 , 100 MHz) δ 172.9, 171.9, 156.7, 138.3, 137.0, 134.8, 134.2, 133.0, 131.8, 130.1, 129.7, 129.5, 129.3, 129.1, 129.0, 127.3, 127.2, 126.6, 126.0, 125.1, 117.3, 78.4, 67.4, 65.8, 57.3, 55.8, 52.6, 40.7, 38.3, 33.0, 30.3, 28.7, 23.0; IR (neat) $\nu_{\text{max}}/\text{cm}^{-1}$ 3322, 1601, 1506, 1436, 1393, 1237, 1163, 1033; HRMS (ESI) m/z calculated for $\text{C}_{42}\text{H}_{51}\text{N}_5\text{NaO}_9\text{S}$ $[\text{M}+\text{Na}]^+$ 824.3300; found 824.3310.



***N*-(Alloc)-*N*ⁱⁿ-(Boc)-L-tryptophanyl-(4-chloro-butyl)aza-sulfurylglycinylo-(*tert*-butyl)-L-tyrosine benzyl ester (**73**)** A 0 °C solution of aza-sulfurylglycinylo tripeptide **72** (225 mg, 0.28 mmol) in THF (2.5 mL) was treated with BTPP (105 μL , 0.34 mmol), stirred for 0.5 h, treated with 1-bromo-4-chlorobutane (40 μL , 0.34 mmol) and stirred at 0 °C for 4 h. The volatiles were evaporated. The residue was purified by flash chromatography by eluting 80:20 hexanes/EtOAc to afford the (4-chloro-butyl)aza-sulfurylo tripeptide **73** as a solid (189 mg; 76% yield): R_f 0.18 (80:20 hexanes:EtOAc); mp 83-85 °C; $[\alpha]_D^{20}$ -5.0° (THF, c 0.88); ^1H NMR (acetone- d_6 , 400 MHz) δ 1.30 (9H, s), 1.49-1.56 (2H, m), 1.66 (9H, s), 1.76-1.84 (2H, m), 2.97 (1H, dd, J = 8.6, 12.8 Hz), 3.10 (1H, dd, J = 5.2, 13.5 Hz), 3.14 (1H, dd, J = 8.5, 15.2 Hz), 3.28 (2H, d, J = 6.1 Hz), 3.32 (1H, d, J = 6.2 Hz), 3.52 (2H, t, J = 6.7 Hz), 4.48 (2H, d, J = 4.9 Hz), 4.51-4.58 (2H, m), 5.01 (1H, d, J = 12.4 Hz), 5.08-5.14 (2H, m), 5.22 (1H, d, J = 15.9 Hz), 5.80-5.89 (1H, m), 6.66-6.73 (1H, br), 6.77-6.84 (1H, br), 6.85-6.92 (2H, m), 7.11-7.37 (9H, m), 7.65-7.71 (2H, m), 8.09-8.18 (1H, br), 9.11-9.21 (1H, br); ^{13}C NMR (acetone- d_6 , 100 MHz) δ 172.2, 172.1, 157.0, 155.5, 150.3, 136.7, 136.3, 134.1, 131.6, 131.3, 131.0, 129.3, 129.1, 128.9, 125.5, 125.2, 124.6, 123.3, 120.1, 117.5, 116.8, 115.9, 84.3, 78.5, 67.4, 66.0, 58.7, 54.7, 50.8, 45.3, 38.7, 29.2, 28.3, 28.0, 25.0; IR (neat) $\nu_{\text{max}}/\text{cm}^{-1}$ 3280, 1727, 1453, 1366, 1255, 1155, 1087; HRMS (ESI) m/z calculated for $\text{C}_{44}\text{H}_{56}\text{ClN}_5\text{NaO}_{10}\text{S}$ $[\text{M}+\text{Na}]^+$ 904.3329; found 904.3334.



***N*-(Alloc)-*N*ⁱⁿ-(Boc)-L-tryptophanyl-(4-azidobutyl)aza-sulfurylglycinylo-(*tert*-butyl)-L-tyrosine benzyl ester (**74**)** To a solution of *N*-(Alloc)-*N*ⁱⁿ-(Boc)-L-tryptophanyl-(4-chloro-butyl)aza-sulfurylglycinylo-(*tert*-butyl)-L-tyrosine benzyl ester (**73**) (33 mg, 0.037 mmol) in

DMF (800 μ L) sodium azide (8mg, 0.11 mmol) was added and the mixture was stirred overnight at 60 °C. The product was precipitated by the addition of water (10 mL) and the aqueous phase was extracted with EtOAc (15 mL x 3). The combined organic layer was washed with brine (20 mL x 2), treated with MgSO_4 , filtered and evaporated under reduced pressure. The residue was purified by flash chromatography eluting with 75:25 hexanes/EtOAc to afford (4-azido-butyl)aza-sulfuryl tripeptide **74** as a solid (22 mg; 66% yield): R_f 0.31 (75:25 hexanes:EtOAc); mp 118-121 °C; $[\alpha]_D^{20}$ -0.65° (THF, c 0.92); ^1H NMR (acetone- d_6 , 400 MHz) δ 1.30 (9H, s), 1.42-1.49 (2H, m), 1.57-1.64 (2H, m), 1.66 (9H, s), 2.94-3.03 (1H, m), 3.10 (1H, dd, J = 5.0, 13.7 Hz), 3.14 (1H, dd, J = 8.7, 15.2 Hz), 3.23 (2H, d, J = 6.8 Hz), 3.28 (2H, dd, J = 6.2, 12.4 Hz), 3.33 (1H, dd, J = 5.8, 10.8 Hz), 4.48 (2H, d, J = 4.5 Hz), 4.54 (2H, d, J = 7.0 Hz), 5.03 (1H, t, J = 12.0 Hz), 5.09-5.16 (2H, m), 5.23 (1H, d, J = 16.2 Hz), 5.81-5.90 (1H, m), 6.63-6.73 (1H, br), 6.74-6.85 (1H, br), 6.85-6.92 (2H, m), 7.09-7.37 (9H, m), 7.62-7.74 (2H, m), 8.08-8.18 (1H, br), 9.09-9.21 (1H, br); ^{13}C NMR (acetone- d_6 , 75 MHz) δ 172.2, 172.1, 157.0, 155.5, 150.3, 136.7, 136.3, 134.2, 131.6, 131.4, 131.0, 129.2, 129.1, 128.9, 125.5, 125.2, 124.6, 123.3, 120.1, 117.4, 116.8, 115.9, 84.3, 78.5, 67.4, 66.0, 58.8, 54.7, 51.6, 51.0, 38.7, 29.2, 28.3, 28.0, 26.5, 24.8; IR (neat) $\nu_{\text{max}}/\text{cm}^{-1}$ 3282, 2096, 1727, 1452, 1366, 1255, 1155, 1087; HRMS (ESI) m/z calculated for $\text{C}_{44}\text{H}_{56}\text{N}_8\text{NaO}_{10}\text{S}$ $[\text{M}+\text{Na}]^+$ 911.3732; found 911.3742.

Peptide 75: crude purity: 43%, t_R : 10.91 min (analytical HPLC, 20 to 60% acetonitrile in water (0.1% formic acid) over 15 min + 90% acetonitrile in water (0.1% formic acid) over 5 min, flow rate of 0.5 mL/min), molecular formula: $\text{C}_{46}\text{H}_{62}\text{N}_{10}\text{O}_{13}\text{S}_3$, calculated mass; 1059.3733, found: 1059.3706.

Purity check: Gradient #1 - Purity: >99%, t_R : 14.18 min (analytical HPLC, 20 to 80% methanol in water (0.1% formic acid) over 15 min + 90% methanol in water (0.1% formic acid) over 5 min, flow rate of 0.5 mL/min; Gradient #2 - Purity: >99%, t_R : 7.68 min (analytical HPLC, 20 to 80% acetonitrile in water (0.1% formic acid) over 15 min + 90% acetonitrile in water (0.1% formic acid) over 5 min, flow rate of 0.5 mL/min.

Peptide 76: crude purity: 78%, t_R : 10.54 min (analytical HPLC, 20 to 50% acetonitrile in water (0.1% formic acid) over 15 min + 90% acetonitrile in water (0.1% formic acid) over 5 min, flow rate of 0.5 mL/min), molecular formula: $\text{C}_{52}\text{H}_{66}\text{N}_{10}\text{O}_{13}\text{S}_3$, calculated mass; 1135.4046, found: 1135.4064.

Purity check: Gradient #1 - Purity: >99%, t_R : 16.39 min (analytical HPLC, 20 to 80% methanol in water (0.1% formic acid) over 15 min + 90% methanol in water (0.1% formic

acid) over 5 min, flow rate of 0.5 mL/min; Gradient #2 - Purity: >99%, t_R : 12.45 min (analytical HPLC, 20 to 80% acetonitrile in water (0.1% formic acid) over 15 min + 90% acetonitrile in water (0.1% formic acid) over 5 min, flow rate of 0.5 mL/min.

Peptide 77: crude purity: 80% t_R : 9.39 min (analytical HPLC, 30 to 50% acetonitrile in water (0.1% formic acid) over 10 min + 90% acetonitrile in water (0.1% formic acid) over 4 min, flow rate of 0.5 mL/min), molecular formula: $C_{50}H_{64}N_{10}O_{13}S_3$, calculated mass; 1109.3889, found: 1109.3887.

Purity check: Gradient #1 - Purity: >99%, t_R : 15.54 min (analytical HPLC, 20 to 80% methanol in water (0.1% formic acid) over 15 min + 90% methanol in water (0.1% formic acid) over 5 min, flow rate of 0.5 mL/min; Gradient #2 - Purity: >99%, t_R : 10.28 min (analytical HPLC, 20 to 80% acetonitrile in water (0.1% formic acid) over 15 min + 90% acetonitrile in water (0.1% formic acid) over 5 min, flow rate of 0.5 mL/min.

Peptide 78: crude purity: 58%, t_R : 4.40 min (analytical HPLC, 20 to 60% acetonitrile in water (0.1% formic acid) over 6 min + 90% acetonitrile in water (0.1% formic acid) over 2 min, flow rate of 0.5 mL/min), molecular formula: $C_{50}H_{65}N_{10}O_{13}S_3$, calculated mass; 1109.3889, found: 1109.3879.

Purity check: Gradient #1 - Purity: >99%, t_R : 7.37 min (analytical HPLC, 20 to 60% methanol in water (0.1% formic acid) over 6 min + 90% methanol in water (0.1% formic acid) over 2 min, flow rate of 0.5 mL/min; Gradient #2 - Purity: >99%, t_R : 4.61 min (analytical HPLC, 20 to 60% acetonitrile in water (0.1% formic acid) over 6 min + 90% acetonitrile in water (0.1% formic acid) over 2 min, flow rate of 0.5 mL/min.

Acknowledgements

I would like to take this opportunity to thank all people who have contributed in different way to my Ph.D. Research.

First of all, I am deeply grateful to my advisor **Professor Paolo Grieco** for being promoter of my Ph.D. carrer and **Professor William D. Lubell** as my supervisor during my stage at the Université de Montréal. Their positive attitude and continuous support have successfully influenced the evolution of my work.

It has been an excellent opportunity and experience to meet people from several cultures and backgrounds, broadening my knowledge of the world and establishing international friendships. I would like to thank Salvatore Di Maro for his guidance and for opening my mind. I am pleased to extend my acknowledgements to many colleagues for discussions and communications, among them Stéphane Turcotte, Ali Munaim Yousif, Yésica Garca Ramos, Carine Bourguet, Arkady Khashper, Duc Ngoc Doan and all group members and students of Prof. Grieco and Prof. Lubell. I wish to express appreciation to all people who have been involved in different aspects in my research project.

I have discovered the concept of intellectual honesty and the importance of sharing ideas and being desirous of knowledge and it's my hope and purpose to keep this spirit in my future works.

10 References

- [1] Bern, H.A.; Pearson, D.; Larson, B.A.; Nishioka, R.S., Neurohormones from fish tails: the caudal neurosecretory system. I. "Urophysiology" and the caudal neurosecretory system of fishes, *Recent progress in hormone research* **1985**, 41, 533-552.
- [2] (a) Conlon, J.M.; O'Harte, F.; Smith, D.D.; Tonon, M.C.; Vaudry, H., Isolation and primary structure of urotensin II from the brain of a tetrapod, the frog *Rana ridibunda*, *Biochemical and Biophysical Research Communications* **1992**, 188, 2, 578-583. (b) Conlon, J.M.; Chartrel, N.; Leprince, J.; Charles, S.; Jean, C.; Hubert, V., A Proenkephalin A-Derived Peptide Analogous to Bovine Adrenal Peptide E From Brain: Purification, synthesis, and Behavioral Effects, *Peptides* **1996**, 17, 8, 1291-1296.
- [3] Tostivint, H.; Lihrmann, I.; Bucharles, C.; Vieau, D.; Coulouarn, Y.; Boutelet, I.; Fournier, A.; Conlon, J.M.; Vaudry, H., A Second Somatostatin Gene is Expressed in the Braine of the Frog *Rana ridibuanda*, *Annals of the New York Academy of Sciences* **1998**, 839, 1, 496-497.
- [4] Conlon, J.M.; Yano, K.; Waugh, D.; Hazon, N., Distribution and molecular forms of urotensin II and its role in cardiovascular regulation in vertebrates, *Journal of Experimental Zoology* **1996**, 275, 2-3, 226-238.
- [5] Colton, A.L., Effective Thermal Parameters for a Heterogeneous Land Surface, *Remote Sensing of Environment* **1996**, 57, 3, 143-160.
- [6] Brazeau, P.; Vale, W.; Burgus, R.; Ling, N.; Butcher, M.; Rivier, J.; Guillemin, R., Hypothalamic polypeptide that inhibits the secretion of immunoreactive pituitary growth hormone, *Science* **1973**, 179, 4068, 77-79.
- [7] (a) Ames, R.S.; Sarau, H.M.; Chambers, J.K.; Willette, R.N.; Aiyar, N.V.; Romanic, A.M.; Loudenk, C.S.; Foley, J.J.; Sauermelch, C.F.; Coatney, R.W.; Ao, Z.; Disa, J.; Holmes, S.D.; Stadel, J.M.; Martin, J.D.; Liu, W.S.; Glover, G.I.; Wilson, S.; McNulty, D.E.; Ellis, C.E.; Elshourbagy, N.A.; Shabon, U.; Trill, J.J.; Hay, D.W.; Ohlstein, E.H.; Bergsma, D.J.; Douglas, S.A., Human urotensin-II is a potent vasoconstrictor and agonist for the orphan receptor GPR14, *Nature* **1999**, 401, 282-286. (b) Nothacker, H.P.; Wang, Z.; McNeill, A.M.; Saito, Y.; Merten, S.; O'Dowd, B.; Duckles, S.P.; Civelli, O., Identification of the natural ligand of an orphan G-protein-coupled receptor involved in the regulation of vasoconstriction, *Nature Cell Biology* **1999**, 1, 6, 383-385. (c) Mori, K.; Nagao, H.; Yoshihara, Y., The olfactory bulb: coding and processing of odor molecule information, *Science* **1999**, 286, 5440, 711-715.
- [8] Douglas, S.A.; Ohlstein, E.H., Human urotensin-II, the most potent mammalian vasoconstrictor identified to date, as a therapeutic target for the management of cardiovascular disease, *Trends in cardiovascular medicine* **2000**, 10, 6, 229-237.
- [9] Maguire, J.J.; Kuc, R.E.; Davenport, A.P., Orphan-receptor ligand human urotensin II: receptor localization in human tissues and comparison of vasoconstrictor responses with endothelin-1, *British Journal of Pharmacology* **2000**, 131, 3, 441-446.
- [10] (a) Matsushita, M.; Shichiri, M.; Imai, T.; Tanaka, H.; Takasu, N.; Hirata, Y., Co-expression of urotensin-II and its receptor (GPR14) in human cardiovascular and renal tissues, *Journal of hypertension* **2001**, 19, 12, 2185-2190. (b) Maguire, J.J.; Davenport, A.P., Is urotensin-II the new endothelin?, *British Journal of Pharmacology* **2002**, 137, 5, 579-588.

(c) Zhu, Y.C.; Zhu, Y.Z.; Moore, P.K., The role of urotensin-II in cardiovascular and renal physiology and diseases, *British Journal of Pharmacology* **2006**, 148, 884–901.

[11] Susumu, S.; Zong, W.; Masashi, H.; Yoshinori, H.; Chitose, S.; Takahiro, Y.; Shinsuke, Y.; Michiko, S.; Yukio, T.; Akira, M.; Yoshitomo, O., Genetic variations at urotensin II and urotensin II receptor genes and risk of type 2 diabetes mellitus in Japanese, *Peptides* **2004**, 25, 1803–1808.

[12] Muravenko, O.V.; Gizatulin, R.Z.; Al-Amin, A.N.; Protopopov, A.I.; Kashuba, V.I.; Zelenin, A.V.; Zabarovsky, E.R., Human ALY/BEF gene Map position 17q25.3, *Chromosome Research* **2000**, 8, 6, 562.

[13] d’Emmanuele di Villa Bianca, R.; Mitidieri, E.; Fusco, F.; D’Aiuto, E.; Grieco, P.; Novellino, E.; Imbimbo, C.; Mirone, V.; Cirino, G.; Sorrentino, R., Endogenous Urotensin II Selectively Modulates Erectile Function through eNOS, *PLoS One* **2012**, 7, 2, 31019.

[14] Douglas, S. A.; H.Ohlstein, E., Human urotensin-II, the most potent mammalian vasoconstrictor identified to date, as a therapeutic target for the management of cardiovascular disease, *Trends in Cardiovascular Medicine* **2000**, 10, 229–237.

[15] Douglas, S.A.; Naselsky, D.; Ao, Z.; Disa, J.; Herold, C.L.; Lynch, F.; Aiyar, N.V., Identification and pharmacological characterization of native, functional human urotensin-II receptors in rhabdomyosarcoma cell lines, *British Journal of Pharmacology* **2004**, 142, 921–932.

[16] Vale, W.; Brazeau, P.; Grant, G.; Nussey, A.; Burgus, R.; Rivier, J.; Ling, N.; Guillemin, R., Preliminary observations on the mechanism of action of somatostatin, a hypothalamic factor inhibiting the secretion of growth hormone, *C R Acad Sci Hebd Seances Acad Sci* **1972**, 275, 2913–2916.

[17] Samson, W.; Zhang, J.; Avsian-Kretchmer, O.; Cui, K.; Yosten, G.; Klein, C.; Lyu, R.M.; Wang, Y.; Chen, X.; Yang, J.; Price, C.; Hoyda, T.; Ferguson, A.; Yuan, X.B.; Chang, J.; Hsueh, A., Neuronostatin encoded by the somatostatin gene regulates neuronal, cardiovascular, and metabolic functions, *J Biol Chem* **2008**, 283, 31949–31959.

[18] (a) Asano, T.; Aoyagi, M.; Hirakawa, K.; Ikawa, Y., Effect of endothelin-1 as growth factor on a human glioma cell line, its characteristic promotion of DNA synthesis, *J Neurooncol* **1984**, 18, 1–7. (b) Kusuhashi, M.; Yamaguchi, K.; Nagasaki, K.; Hayashi, C.; Suzuki, A.; Hori, S. *et al.*, Production of endothelin in human cancer cell lines, *Cancer Res* **1990**, 50, 3257–61. (c) Shichiri, M.; Hirata, Y.; Nakajima, T.; Ando, K.; Imai, T.; Yanagisawa, M. *et al.*, Endothelin-1 is an autocrine/paracrine growth factor for human cancer cell lines, *J Clin Invest* **1991**, 87, 1867–71. (d) Takahashi, K.; Hara, E.; Murakami, O.; Totsune, K.; Sone, M. *et al.*, Production and secretion of endothelin-1 by cultured choroid plexus carcinoma cells, *J Cardiovasc Pharmacol* **1998**, 31, S367–S9. (e) Takahashi, K.; Nakayama, M.; Shibahara, S., Production and secretion of neuropeptides by nervous system tumors, *Cancer J* **1998**, 11, 237–41. (f) Takahashi, K.; Yoshinoya, A.; Murakami, O.; Totsune, K.; Shibahara, S., Production and secretion of two vasoactive peptides adrenomedullin and endothelin-1 by cultured human adrenocortical carcinoma cells, *Peptides* **2000**, 21, 251–6. (g) Sone, M.; Takahashi, K.; Totsune, K.; Murakami, O.; Arihara, Z.; Satoh, F., *et al.*, Expression of endothelin-1 and endothelin receptors in cultured human glioblastoma cells, *J Cardiovasc Pharmacol* **2000**, 26, S390–S2.

- [19] (a) Takahashi, K.; Totsune, K.; Murakami, O.; Shibahara, S., Expression of urotensin II and urotensin II receptor mRNAs in various human tumor cell lines and secretion of urotensin II-like immunoreactivity by SW-13 adrenocortical carcinoma cells, *Peptides* **2001**, 22, 1175-9. (b) Takahashi, K.; Totsune, K.; Murakami, O.; Arihara, Z.; Noshiro, T.; Hayashi, Y. *et al.*, Expression of urotensin II and its receptor in adrenal tumors and stimulation of proliferation of cultured tumor cells by urotensin II, *Peptides* **2003**, 24, 301-6.
- [20] Grieco, P.; Franco, R.; Bozzuto, G.; Toccaceli, L.; Sgambato, A.; Marra, M., *et al.*, Urotensin II receptor predicts the clinical outcome of prostate cancer patients and is involved in the regulation of motility of prostate adenocarcinoma cells, *J Cell Biochem* **2011**, 112, 341-53.
- [21] Federico, A.; Zappavigna, S.; Romano, M.; Grieco, P.; Luca, A.; Marra, M.; Gravina, A.G.; Stiuso, P.; D'Armiento, F.P.; Vitale, G.; Tuccillo, C.; Novellino, E.; Loguercio, C.; Caraglia, M., Urotensin-II receptor is over-expressed in colon cancer cell lines and in colon carcinoma in humans, *Eur J Clin Invest* **2014**, 44, 285-94.
- [22] Ohsako, S.; Ishida, I.; Ichikawa, T.; Deguchi, T., Cloning and sequence analysis of cDNAs encoding precursors of urotensin II-alpha and -gamma, *The Journal of Neuroscience* **1986**, 6, 9, 2730-2735.
- [23] Pearson, D.; Shively, J.E.; Clark, B.R.; Geschwind, I.I.; Barkley, M.; Nishioka, R.S.; Bern, H.A., Urotensin II: a somatostatin-like peptide in the caudal neurosecretory system of fishes, *Proceedings of the National Academy of Sciences of the United States of America* **1980**, 77, 8, 5021-5024.
- [24] Douglas, A.S.; Dhanak, D.; Johns, D.G., From 'gills to pills': urotensin-II as a regulator of mammalian cardiorenal function, *Trends in Pharmacological Sciences* **2004**, 25, 76-85.
- [25] Douglas, S.A.; Naselsky, Z.; Ao *et al.*, Identification and pharmacological characterization of native, functional human urotensin-II receptors in rhabdomyosarcoma cell lines, *British Journal of Pharmacology* **2004**, 142, 6, 921-932.
- [26] Tsoukas, P.; Kane, E.; Giaid, A., Potential clinical implications of the urotensin II receptor antagonists, *Frontiers in Pharmacology* **2011**, 2, article 38.
- [27] Merlino, F.; Di Maro, S.; Yousif, A.M.; Caraglia, M.; Grieco P., Urotensin-II ligands: an overview from peptide to nonpeptide structures, *J. Amino Acids* **2013**, 2013:979016, doi: 10.1155/2013/979016.
- [28] Coy, D. H.; Rossowski, W.J.; Cheng, B.L.; Taylor, J.E., Structural requirements at the N-terminus of urotensin II octapeptides, *Peptides* **2002**, 23, 2259-2264.
- [29] McMaster, D.; Kobayashi, Y.; Rivier, J.; Lederis, K., Characterization of the biologically and antigenically important regions of urotensin II, *Proceedings of the Western Pharmacology Society* **1986**, 29, 205-208.
- [30] Grieco, P.; Carotenuto, A.; Campiglia, P.; Zampelli, E.; Patacchini, R.; Maggi, C.A.; Novellino, E.; Rovero, P., A new, potent urotensin II receptor peptide agonist containing a Pen residue at the disulfide bridge, *Journal of Medicinal Chemistry* **2002**, 45, 20, 4391-4394.

- [31] Foister, S.; Taylor, L.L.; Feng, J.J.; Chen, W.L.; Lin, A.; Cheng, F.C.; Smith, A.B.; Hirschmann, R., Design and synthesis of potent cystine-free cyclic hexapeptide agonists at the human urotensin receptor, *Organic Letters* **2006**, 8, 9, 1799-1802.
- [32] Lavecchia, A.; Cosconati, S.; Novellino, E., Architecture of the human urotensin II receptor: comparison of the binding domains of peptide and non-peptide urotensin II agonists, *Journal of Medicinal Chemistry* **2005**, 48, 7, 2480-2492.
- [33] Kinney, W.A.; Almond Jr., H.R.; Qi, J.; Smith, C.E.; Santulli, R.J.; de Garavilla, L.; Andrade-Gordon, P.; Cho, D.S.; Everson, A.M.; Feinstein, M.A.; Leung, P.A.; Maryanoff, B.E., Structure-function analysis of urotensin II and its use in the construction of a ligand-receptor working model, *Angewandte Chemie International Edition* **2002**, 41, 16, 2940-2944.
- [34] Flohr, S.; Kurz, M.; Kostenis, E.; Brkovich, A.; Fournier, A.; Klabunde, T., Identification of nonpeptidic urotensin II receptor antagonists by virtual screening based on a pharmacophore model derived from structure-activity relationships and nuclear magnetic resonance studies on urotensin II, *Journal of Medicinal Chemistry* **2002**, 45, 9, 1799-1805.
- [35] Guerrini, R.; Camarda, V.; Marzola, E.; Arduin, M.; Calò, G.; Spagnol, M.; Rizzi, A.; Salvadori, S.; Regoli, D., Structure-activity relationship study on human urotensin II, *Journal of Peptide Science* **2005**, 11, 2, 85-90.
- [36] Carotenuto, A.; Grieco, P.; Rovero, P.; Novellino, E., Urotensin-II receptor antagonists, *Current Medicinal Chemistry* **2006**, 13, 3, 267-2785.
- [37] Behm, D.J.; Herold, C.L.; Ohlstein, E.H.; Knight, S.D.; Dhanak, D.; Douglas, S.A., Pharmacological characterization of SB-710411 (Cpa-c[D-Cys-Pal-D-Trp-Lys-Val-Cys]-Cpa-amide), a novel peptidic urotensin-II receptor antagonist, *British Journal of Pharmacology* **2002**, 137, 4, 449-458.
- [38] Herold, C.L.; Behm, D.J.; Buckley, P.T.; Foley, J.J.; Wixted, W.E.; Sarau, H.M.; Douglas, S.A., The neuromedin B receptor antagonist, BIM-23127, is a potent antagonist at human and rat urotensin-II receptors, *British Journal of Pharmacology* **2003**, 139, 2, 203-207.
- [39] Herold, C.L.; Behm, D.J.; Buckley, P.T.; Foley, J.J.; Douglas, S.A., The peptidic somatostatin analogs lanreotide, BIM-23127 and BIM-23042 are urotensin-II receptor ligands, *Pharmacologist* **2002**, 44, 170-171.
- [40] Camarda, V.; Guerrini, R.; Kostenis, E.; Rizzi, A.; Calò, G.; Hattenberger, A.; Zucchini, M.; Salvadori, S.; Regoli, D., A new ligand for the urotensin II receptor, *British Journal of Pharmacology* **2002**, 137, 3, 311-314.
- [41] Grieco, P.; Carotenuto, A.; Campiglia, P.; Marinelli, L.; Lama, T.; Patacchini, R.; Santicioli, P.; Maggi, C.A.; Rovero, P.; Novellino, E., Urotensin-II receptor ligands. From agonist to antagonist activity, *Journal of Medicinal Chemistry* **2005**, 48, 23, 7290-7297.
- [42] Patacchini, R.; Santicioli, P.; Giuliani, S.; Grieco, P.; Novellino, E.; Rovero, P.; Maggi, C.A., Urantide: an ultrapotent urotensin II antagonist peptide in the rat aorta, *British Journal of Pharmacology* **2003**, 140, 7, 1155-1158.

- [43] Camarda, V.; Song, W.; Marzola, E.; Spagnol, M.; Guerrini, R.; Salvadori, S.; Regoli, D.; Thompson, J.P.; Rowbotham, D.J.; Behm, D.J.; Douglas, S.A.; Calò, G.; Lambert, D.G., Urantide mimics urotensin-II induced calcium release in cells expressing recombinant UT receptors, *European Journal of Pharmacology* **2004**, 498, 83-86.
- [44] Camarda, V.; Spagnol, M.; Song, W.; Vergura, R.; Roth, A.L.; Thompson, J.P.; Rowbotham, D.J.; Guerrini, R.; Marzola, E.; Salvadori, S.; Cavanni, P.; Regoli, D.; Douglas, S.A.; Lambert, D.G.; Calò, G., In vitro and in vivo pharmacological characterisation of the novel UT receptor ligand [Pen⁵, DTrp, Dab⁸]urotensin II(4-11)(UFP-803), *British Journal of Pharmacology* **2006**, 147, 1, 92-100.
- [45] Sugo, T.; Murakami, Y.; Shimomura, Y.; Harada, M.; Abe, M.; Ishibashi, Y.; Kitada, C.; Miyajima, N.; Suzuki, N.; Mori, M.; Fujino, M., Identification of urotensin II-related peptide as the urotensin II-immunoreactive molecule in the rat brain, *Biochemical and Biophysical Research Communications* **2003**, 310, 3, 860-868.
- [46] Jarry, M.; Diallo, M.; Lecointre, C.; Desrues, L.; Tokay, T.; Chatenet, D.; Leprince, J.; Rossi, O.; Vaudry, H.; Tonon, M.C.; Prézeau, L.; Castel, H.; Gandolfo, P., The vasoactive peptides urotensin II and urotensin II-related peptide regulate astrocyte activity through common and distinct mechanisms: involvement in cell proliferation, *Biochemical Journal* **2010**, 428, 113-124.
- [47] Prosser, H.C.G.; Leprince, J.; Vaudry, H.; Richards, A.M.; Forster, M.E.; Pemberton, C.J., Cardiovascular effects of native and non-native urotensin II and urotensin II-related peptide on rat and salmon hearts, *Peptides* **2006**, 27, 12, 3261-3268.
- [48] Chatenet, D.; Dubessy, C.; Leprince, J.; Boullaran, C.; Carlier, L.; Ségalas-Milazzo, I.; Guilhaudis, L.; Oulyadi, H.; Davoust, D.; Scalbert, E.; Pfeiffer, B.; Renard, P.; Tonon, M.C.; Lihmann, I.; Pacaud, P.; Vaudry, H., Structure-activity relationships and structural conformation of a novel urotensin II-related peptide, *Peptides* **2004**, 25, 10, 1819-1830.
- [49] Chatenet, D.; Nguyen, Q. T.; Létourneau, M.; Dupuis, J.; Fournier, A., Urocontrin, a novel UT receptor ligand with a unique pharmacological profile, *Biochemical Pharmacology* **2012**, 83, 5, 608-615.
- [50] Chatenet, D.; Létourneau, M.; Nguyen, Q.T.; Doan, N.D.; Dupuis, J.; Fournier, A., Discovery of new antagonists aimed at discriminating UII and URP-mediated biological activities: insight into UII and URP receptor activation, *British Journal of Pharmacology* **2013**, 168, 807-821.
- [51] Kenakin, T., Drug efficacy at G protein-coupled receptors, *Annu. Rev. Pharmacol. Toxicol.* **2002**, 42, 349-379.
- [52] Behm, D.J.; Stankus, G.; Doe, C.P.; Willette, R.N.; Sarau, H.M.; Foley, J.J.; Schmidt, D.B.; Nuthulaganti, P.; Fornwald, J.A.; Ames, R.S.; Lambert, D.G.; Calò, G.; Camarda, V.; Aiyar, N.V.; Douglas, S.A., The peptidic urotensin-II receptor ligand GSK248451 possesses less intrinsic activity than the low-efficacy partial agonists SB-710411 and urantide in native mammalian tissues and recombinant cell systems, *British Journal of Pharmacology* **2006**, 148, 2, 173-190.

[53] (a) Coy, D.H.; Rossowski, W.J.; Cheng, B.L.; Taylor, J.E., Highly potent heptapeptide antagonists of the vasoactive peptide urotensin II, *Abstract of papers, 225th ACS National meeting* **2003**, New Orleans, LA, United States, March 23-27. Washington, DC: American Chemical Society. (b) Aiyar, N.; Johns, D.G.; Ao, Z.; Disa, J.; Behm, D.J.; Foley, J.J.; Buckley, P.T.; Sarau, H.M.; van-der-Keyl, H.K.; Elshourbagy, N.A.; Douglas, S.A., Cloning and pharmacological characterization of the cat urotensin-II receptor (UT), *Biochemical Pharmacology* **2005**, 69, 7, 1069-1079.

[54] Croston, G.E.; Olsson, R.; Currier, E.A.; Burstein, E.S.; Weiner, D.; Nash, N.; Severance, D.; Allenmark, S.G.; Thunberg, L.; Ma, J.N.; Mohell, N.; O'Dowd, B.; Brann, M.R.; Hacksell, U., Discovery of the First Nonpeptide Agonist of the GPR14/Urotensin-II Receptor: 3-(4-Chlorophenyl)-3-(2-(dimethylamino)ethyl)isochroman-1-one (AC-7954), *Journal of Medicinal Chemistry* **2002**, 45, 23, 4950-4953.

[55] Lehmann, F.; Currier, E.A.; Olsson, R.; Hacksell, U.; Luthman, K., Isochromanone-based urotensin-II receptor agonists, *Bioorganic & Medicinal Chemistry* **2005**, 13, 8, 3057-3068.

[56] Lehmann, F.; Lake, L.; Currier, E.A.; Olsson, R.; Hacksell, U.; Luthman, K., Design, parallel synthesis and SAR of novel urotensin II receptor agonists, *European Journal of Medicinal Chemistry* **2007**, 42, 2, 276-285.

[57] Clozel, M.; Binkert, C.; Birker-Robaczewska, M.; Boukhadra, C.; Ding, S.S.; Fischli, W.; Hess, P.; Mathys, B.; Morrison, K.; Müller, C.; Müller, C.; Nayler, O.; Qiu, C.; Rey, M.; Scherz, M.W.; Velker, J.; Weller, T.; Xi, J.F.; Ziltener, P., Pharmacology of the Urotensin-II Receptor Antagonist Palosuran (ACT-058362; 1-[2-(4-Benzyl-4-hydroxy-piperidin-1-yl)-urea Sulfate Salt]: first demonstration of a pathophysiological role of the Urotensin System, *The Journal of Pharmacology and Experimental Therapeutics* **2004**, 311, 1, 204-212.

[58] Tarui, N.; Santo, T.; Mori, M.; Watanabe, H.; Takeda Chemical Industries (assignee), Quinoline derivatives as vasoactive agents exhibiting orphanreceptor GPR14 protein antagonism, PCT Int Appl., **2001**. WO2001066143

[59] Dhanak, D.; Knight, S.D.; Smithkline Beecham Corporation (assignee), Preparation of quinolones as urotensin-II receptor antagonists, PCT Int Appl., **2002**. WO2002047456

[60] Douglas, S.A.; Behm, D.J.; Aiyar, N.V.; Naselsky, D.; Disa, J.; Brooks, D.P.; Ohlstein, E.H.; Gleason, J.G.; Sarau, H.M.; Foley, J.J.; Buckley, P.T.; Schmidt, D.B.; Wixted, W.E.; Widdowson, K.; Riley, G.; Jin, J.; Gallagher, T.F.; Schmidt, S.J.; Ridgers, L.; Christmann, L.T.; Keenan, R.M.; Knight, S.D.; Dhanak, D., Nonpeptidic urotensin-II receptor antagonists I: *in vitro* pharmacological characterization of SB-706375, *British Journal of Pharmacology* **2005**, 145, 5, 620-635.

[61] Behm, D.J.; McAtee, J.J.; Dodson, J.W.; Neeb, M.J.; Fries, H.E.; Evans, C.A.; Hernandez, R. R.; Hoffman, K.D.; Harrison, S.M.; Lai, J.M.; Wu, C.; Aiyar, N.V.; Ohlstein, E.H.; Douglas, S.A., Palosuran inhibits binding to primate UT receptors in cell membranes but demonstrates differential activity in intact cells and vascular tissues, *British Journal of Pharmacology* **2008**, 155, 3, 374-386.

[62] Jin, J.; Dhanak, D.; Knight, S.D.; Widdowson, K.; Aiyar, N.; Naselsky, D.; Sarau, H.M.; Foley, J.J.; Schmidt, D.B.; Bennett, C.D.; Wang, B.; Warren, G.L.; Moore, M.L.; Keenan,

R.M.; Rivero, R.A.; Douglas, S.A., Aminoalkoxybenzyl pyrrolidines as novel human urotensin-II receptor antagonists, *Bioorganic & Medicinal Chemistry Letters* **2005**, 15, 13.

[63] Tarui, N.; Santo, T.; Watanabe, H.; Aso, K.; Miwa, T.; Takekawa, S.; Takeda Chemical Industries (assignee), Preparation of biphenylcarboxamide compounds as GPR14 antagonists or somatostatin receptor regulators, PCT Int Appl., **2002**. WO2002000606

[64] Carotenuto, A.; Auriemma, L.; Merlino, F.; Limatola, A.; Campiglia, P.; Gomez-Monterrey, I.; d'Emmanuele di Villa Bianca, R.; Brancaccio, D.; Santicioli, P.; Meini, S.; Maggi, C.A.; Novellino, E.; Grieco, P., New insight into the binding mode of peptides at urotensin-II receptor by Trp-constrained analogues of P5U and urantide, *Journal of Peptide Science* **2013**, 19, 293-300.

[65] Herraiz, T.; Ough, C.S., Chemical and technological factors determining tetrahydro-b-carboline-3-carboxylic acid content in fermented alcoholic beverages, *J. Agric. Food Chem.* **1993**, 41, 959-964.

[66] Carotenuto, A.; Grieco, P.; Campiglia, P.; Novellino, E., Rovero, P., Unraveling the active conformation of urotensin II, *Journal of Medicinal Chemistry* **2004**, 47, 7, 1652-1661.

[67] Haskell-Luevano, C.; Toth, K.; Boteju, L.; Job, C.; Castrucci, A.M.; Hadley, M.E., Hruby, V.J., b-methylation of the Phe⁷ and Trp⁹ melanotropin side chain pharmacophores affects ligand-receptor interactions and prolonged biological activity, *J. Med. Chem.* **1997**, 40, 2740-2749.

[68] Carotenuto, A.; Auriemma, L.; Merlino, F.; Yousif, A.M.; Marasco, D.; Limatola, A.; Campiglia, P.; Gomez-Monterrey, I.; Santicioli, P.; Meini, S.; Maggi, C.A.; Novellino, E.; Grieco, P., Leads optimization of P5U and urantide: discover of novel potent ligands at Urotensin-II receptor, *J. Med. Chem.* **2014** (in press).

[69] (a) Grieco, P.; Carotenuto, A.; Campiglia, P.; Gomez-Monterrey, I.; Auriemma, L.; Sala, M.; Marcozzi, C.; d'Emmanuele di Villa Bianca, R.; Brancaccio, D.; Rovero, P.; Santicioli, P.; Meini, S.; Maggi, C.A.; Novellino, E., New insight into the binding mode of peptide ligands at Urotensin-II receptor: structure-activity relationships study on P5U and Urantide, *J. Med. Chem.* **2009**, 52, 3927-3940. (b) Grieco, P.; Carotenuto, A.; Patacchini, R.; Maggi, C.A.; Novellino, E.; Rovero, P., Design, synthesis, conformational analysis, and biological studies of urotensin-II lactam analogues, *Bioorganic & Medicinal Chemistry* **2002**, 10, 3731-3739.

[70] Gurrath, M., Peptide-bonding G protein-coupled receptors: New opportunities for drug design, *Curr. Med. Chem.* **2001**, 8, 1605-1648.

[71] Piriou, F.; Lintner, K.; Femandjian, S.; Fromageot, P.; Khosla, M.C.; Smeby, R.R.; Bumpus, F.M., Amino acid side chain conformation in angiotensin II and analogs: Correlated results of circular dichroism and ¹H nuclear magnetic resonance, *Proc. Nat. Acad. Sci. USA* **1980**, 77, 82-86.

[72] Kessler, H., *Angew. Chem.* 1970, 82, 237-253; *Angew. Chem. Int. Ed. Engl.* **1970**, 9, 219-235.

- [73] Snyder, J.P., Probable unimportance of intramolecular hydrogen bonds for determining the secondary structure of cyclic hexapeptides. Roseotoxin B, *J. Am. Chem. Soc.* **1984**, 106, 2393-2400.
- [74] Hamada, Y.; Shioiri, T., Recent progress of the synthetic studies of biologically active marine cyclic peptides and depsipeptides, *Chem. Rev.* **2005**, 105, 4441-4482.
- [75] (a) Shemyakin, M.M.; Ovchinnikov, Y.A.; Ivanov, V.T.; Kiryushkin, A.A., *Tetrahedron* **1963**, 19, 581-591. (b) Bevan, K.; Davies, J.S.; Hall, M.J.; Hassall, C.H.; Morton, R.B.; Phillips, D.A.; Ogihara, Y.; Thomas, W.A., *Experientia* 1970, 26, 122-123. (c) Corbaz, R.; Ettlinger, L.; Gaumann, E.; Keller-Schierlein, W.; Kradolfer, F.; Neipp, L.; Prelog, V., *Helv. Chim. Acta* **1957**, 23, 199.
- [76] (a) Jolad, S.D.; Hoffmann, J.J.; Torrance, S.J.; Wiedhopf, R.M.; Cole, J.R.; Arora, S.K.; Bates, R.B.; Gargiulo, R.L.; Kriek, G.R., *J. Am. Chem. Soc.* **1977**, 99, 8040-8044. (b) Pettit, G.R.; Kamano, Y.; Dufresne, C.; Cerny, R.L.; Herald, C.L.; Schmidt, J.M., *J. Org. Chem.* **1989**, 54, 6005. (c) Pettit, G.R.; Kamano, Y.; Herald, C.L.; Tuinman, A.A.; Boettner, F.E.; Kizu, H.; Schimdt, J.M.; Baczynskyj, L.; Tomer, K.B.; Bontems, R.J., *J. Am. Chem. Soc.* **1987**, 109, 6883-6885.
- [77] Ruegger, A.; Kuhn, M.; Lichti, H.; Loosli, H.-R.; Huguenin, R.; Quiquerez, C.; von Wartburg, A., *Helv. Chim. Acta* **1976**, 59, 1075.
- [78] Gilon, C.; Dechantsreiter, M.A.; Burkhart, F.; Frieder, A.; Kessler, H., *Houben-Weyl Methods of Organic Chemistry*; Georg Thieme Verlag: Stuttgart, **2003**, E22c, 215-271.
- [79] Chatterjee, J.; Gilon, C.; Hoffman, A.; Kessler, H., N-methylation of peptides: a new perspective in medicinal chemistry, *Acc. Chem. Res.* **2008**, 41, 1331-1342.
- [80] Biron, E.; Chatterjee, J.; Ovadia, O.; Langenegger, D.; Brueggen, J.; Hoyer, D.; Schmid, H.A.; Jelinek, R.; Gilon, C.; Hoffman, A.; Kessler, H., *Angew. Chem., Int. Ed.* **2008**, 47, 2595-2599.
- [81] Mazur, R.H.; James, P.A.; Tyner, D.A.; Hallinan, E.A.; Sanner, J.H.; Schulze, R., *J. Med. Chem.* **1980**, 23, 758-763.
- [82] Vitoux, B.; Aubry, A.; Thong Cung, M.; Marraud, M., Conformational perturbations induced by N-methylation of model dipeptides, *J. Peptide Proteine Res.* **1986**, 27, 617-632.
- [83] Doedens, L.; Opperer, F.; Cai, M.; Beck, J.G.; Dedek, M.; Palmer, E.; Hruby, V.J.; Kessler, H., Multiple N-methylation of MT-II backbone amide bonds leads to melanocortin receptor subtype hMC1R selectivity: pharmacological and conformational studies, *J. Am. Chem. Soc.* **2010**, 132, 8115-8128.
- [84] Cheeseright, T.J.; Daenke, S.; Elmore, D.T.; Jones, J.H., *J. Chem. Soc., Perkin Trans. I* **1994**, 1953-1955.
- [85] Gilmore, W.F.; Lin, H.J., *J. Org. Chem.* **1978**, 43, 4535-4537.
- [86] Baldauf, C.; Gunther, R.; Hofmann, H.J., *THEOCHEM* **2004**, 675, 19-28.

- [87] Di Maro, S.; Pong, R.C.; Hsieh, J.T.; Ahn, J.M., Efficient solid-phase synthesis of FK228 analogues as potent antitumoral agents, *J. Med. Chem.* **2008**, 51, 6639-6641.
- [88] Biron, E.; Kessler, H., Convenient synthesis of N-methylaminoacids compatible with Fmoc solid-phase peptide synthesis, *J. Org. Chem.* **2005**, 70, 5183-5189.
- [89] Biron, E.; Chatterjee, J.; Kessler, H., Optimized selective N-methylation of peptides on solid support, *J. Pept. Sci.* **2006**, 12, 213-219.
- [90] Miller, S.; Scanlan, T.S., Site-selective N-methylation of peptides on solid support, *J. Am. Chem. Soc.* **1997**, 119, 2301-2302.
- [91] Turcotte, S.; Bouayad-Gervais, A.H.; Lubell, W.D., N-Aminosulfamide peptide mimic synthesis by alkylation of aza-sulfurylglycyl peptides, *Org. Lett.* **2012**, 14, 5, 1318-1321.
- [92] Wüthrich, K., *NMR of Proteins and Nucleic Acids*. **1986**, John Wiley & Sons, Inc: New York.
- [93] (a) Piantini, U.; Sorensen, O.W.; Ernst, R.R., Multiple quantum filters for elucidating NMR coupling network, *J. Am. Chem. Soc.* **1982**, 104, 6800-6801. (b) Marion, D.; Wüthrich, K., Application of phase sensitive two-dimensional correlated spectroscopy (COSY) for measurements of ^1H - ^1H spin-spin coupling constants in proteins, *Biochem. Biophys. Res. Commun.* **1983**, 113, 967-974.
- [94] Braunschweiler, L.; Ernst, R.R., Coherence transfer by isotropic mixing: application to proton correlation spectroscopy, *J. Magn. Reson.* **1983**, 53, 521-528.
- [95] Jenner, J.; Meyer, B.H.; Bacham, P.; Ernst, R.R., Investigation of exchange processes by two-dimensional NMR spectroscopy, *J. Chem. Phys.* **1979**, 71, 4546-4553.
- [96] Bartels, C.; Xia, T.; Billeter, M.; Güntert, P.; Wüthrich, K., The program XEASY for computer-supported NMR spectral analysis of biological macromolecules, *J. Biomol. NMR* **1995**, 6, 1-10.
- [97] Moroder, L.; Romano, R.; Guba, W.; Mierke, D.F.; Kessler, H.; Delporte, C.; Winand, J.; Christophe, J., New evidence for a membrane bound pathway in hormone receptor binding, *Biochemistry* **1993**, 32, 13551-13559.
- [98] Sargent, D.F.; Schwyzer, R., Membrane lipid phase as catalyst for peptide-receptor interactions, *Proc. Natl. Acad. Sci. USA* **1986**, 83, 5774-5778.
- [99] (a) Grieco, P.; Giusti, L.; Carotenuto, A.; Campiglia, P.; Calderone, V.; Lama, T.; Gomez-Monterrey, I.; Tartaro, G.; Mazzoni, M.R.; Novellino, E., Morphiceptin analogues containing a dipeptide mimetic structure: an investigation on the bioactive topology at the m-receptor, *J. Med. Chem.* **2005**, 48, 3153-3163. (b) D'Addona, D.; Carotenuto, A.; Novellino, E.; Piccand, V.; Reubi, J.C.; Di Cianni, A.; Gori, F.; Papini, A.M.; Ginanneschi, M., Novel sst5-selective somatostatin dicarba-analogues: synthesis and conformation-affinity relationships, *J. Med. Chem.* **2008**, 51, 512-520. (c) Di Cianni, A.; Carotenuto, A.; Brancaccio, D.; Novellino, E.; Reubi, J.C.; Beetschen, K.; Papini, A.M.; Ginanneschi, M., Novel octreotide dicarba-analogues with high affinity and different selectivity for somatostatin receptors, *J. Med. Chem.* **2010**, 53, 6188-6197. (d) Grieco, P.; Brancaccio, D.;

Novellino, E.; Hruby, V.J.; Carotenuto, A., Conformational study on cyclic melanocortin ligands and new insight into their binding mode at the MC4 receptor, *Eur. J. Med. Chem.* **2011**, 46, 3721–3733.

[100] (a) Fernandez-Lopez, S.; Kim, H.S.; Choi, E.C.; Delgado, M.; Granja, J.R.; Khasanov, A.; Kraehenbuehl, K.; Long, G.; Weinberger, D.A.; Wilcoxon, K.M.; Ghadiri, M.R., Antibacterial Agents Based on the Cyclic D,L-Alpha-Peptide Architecture, *Nature* **2001**, 412, 452-455. Erratum in: *Nature* 2001, 414, 329. (b) Chan, L.Y.; Gunasekera, S.; Henriques, S.T.; Worth, N.F.; Le, S.J.; Clark, R.J.; Campbell, J.H.; Craik, D.J.; Daly, N.L., Engineering Pro-angiogenic Peptides Using Stable, Disulfide-Rich Cyclic Scaffolds, *Blood* **2011**, 118, 6709-6717.

[101] Brkovic, A.; Hattenberger, A.; Kostenis, E.; Klabunde, T.; Flohr, S.; Kurz, M.; Bourgault, S.; Fournier, A., Functional and binding characterizations of urotensin II-related peptides in human and rat urotensin II-receptor assay, *J. Pharmacol. Exp. Ther.* **2003**, 306, 1200-1209.

[102] Batuwangala, M.; Camarda, V.; McDonald, J.; Marzola, E.; Lambert, D.G.; Ng, L.L.; Calò, G.; Regoli, D.; Trapella, C.; Guerrini, R.; Salvadori, S., Structure-activity relationship study on Tyr⁹ of urotensin-II(4-11): Identification of a partial agonist of the UT receptor, *Peptides* **2009**, 30, 1130-1136.

[103] Zhao, J.; Yu, Q.X.; Kong, W.; Gao, H.C.; Sun, B.; Xie, Y.Q.; Ren, L.Q., The Urotensin II receptor antagonist, urantide, protects against atherosclerosis in rats, *Exp. Ther. Med.* **2013**, 5, 1765-1769.

[104] (a) Chen, Z.; Xu, J.; Ye, Y.; Li, Y.; Gong, H.; Zhang, G.; Wu, J.; Jia, J.; Liu, M.; Chen, Y.; Yang, C.; Tang, Y.; Zhu, Z.; Ge, J.; Zou, Y., Urotensin II Inhibited the Proliferation of Cardiac Side Population Cells in Mice During Pressure Overload by JNK-LRP6 Signalling, *J. Cell. Mol. Med.* **2014**, doi: 10.1111/jcmm.12230. (b) Gao, S.; Oh, Y.B.; Shah, A.; Park, W.H.; Chung, M.J.; Lee, Y.H.; Kim, S.H., Urotensin II Receptor Antagonist Attenuates Monocrotaline-Induced Cardiac Hypertrophy in Rats., *Am. J. Physiol. Heart Circ. Physiol.* **2010**, 299, H1782-1789. (c) Zhang, J.Y.; Chen, Z.W.; Yao, H., Protective Effect of Urantide Against Ischemia-Reperfusion Injury via Protein Kinase C and Phosphatidylinositol 3'-kinase-Akt Pathway. *Can. J. Physiol. Pharmacol.* **2012**, 90, 637-645.

[105] Brancaccio, D.; Limatola, A.; Campiglia, P.; Gomez-Monterrey, I.; Novellino, E.; Grieco, P.; Carotenuto, A., Urantide conformation and interaction with Urotensin-II receptor, *Arch. Pharm.* **2013**, 246, 1-8.

[106] Fettes, K.J.; Howard, N.; Hickman, D.T.; Adah, S.; Player, M.R.; Torrence, P.F.; Micklefield, J., *J. Chem. Soc., Perkin Trans. 1* **2001**, 485-495.

[107] Barthel, B.L.; Rudnicki, D.L.; Kirby, T.P.; Colvin, S.M.; Burkhart, D.J.; Koch, T.H., *J. Med. Chem.* **2012**, 55, 6595-6607.

[108] Demmer, O.; Dijkgraaf, I.; Shumacher, U.; Marinelli, L.; Cosconati, S.; Gourni, E.; Wester, H.J.; Kessler, H., *J. Med. Chem.* **2011**, 54, 7648-7662.

[109] Wang, S.S.; Gisin, B.F.; Winter, D.P.; Makofske, R.; Kulesha, I.D.; Tzougraki, C.; Meienhofer, J., *J. Org. Chem.* **1977**, 42, 8, 1286-1290.

[110] Still, W.C.; Kahn, M.; Mitra, A., *J. Org. Chem.* **1978**, 43, 2923-2925.

[111] (a) Kenakin, T., , Orthosteric drug antagonism, *A Pharmacology Primer: Theory, Application, and Methods* **2006**, Second Ed. Elsevier, Academic Press, London, UK, 99-126. (b) Arunlakshana, O.; Schild, H.O., Some Quantitative Uses of Drug Antagonists, *Br. J. Pharmacol. Chemother.* **1959**, 14, 48-58. (c) Cheng, Y.; Prusoff, W.H., Relationship Between the Inhibition Constant (K_i) and the Concentration of Inhibitor which Causes 50 per Cent Inhibition (I_{50}) of an Enzymatic Reaction, *Biochem. Pharmacol.* **1973**, 22, 3099-3108.

[112] Jenkis, L.; Harries, N.; Lappin, J.E.; MacKenzie, A.E.; Neetoo-Isseljee, Z.; Southern, C.; McIver, E.G.; Nicklin, S.A.; Taylor, D.L.; Milligan, G., Antagonists of GPR35 display high species ortholog selectivity and varying modes of action, *J. Pharmacol. Exp. Ther.* **2012**, 343, 683-695.

[113] (a) Nguyen, L.T.; Chau, J.K.; Perry, N.A.; de Boer, L.; Zaat, S.A.; Vogel, H.J., Serum Stabilities of Short Tryptophan- and Arginine-Rich Antimicrobial Peptide Analogs, *PLoS One* **2010**, 5, e12684. (b) Doti, N.; Scognamiglio, P.L.; Madonna, S.; Scarponi, C.; Ruvo, M.; Perretta, G.; Albanesi, C.; Marasco, D., New Mimetic Peptides of the Kinase-Inhibitory Region (KIR) of SOCS1 through Focused Peptide Libraries, *Biochem. J.* **2012**, 443, 231-240.